Title
Cell Engineering for Neuromuscular Regeneration & Neural Reprogramming

Author
Li, LeeAnn Kai-Yin

Publication Date
2020

Peer reviewed|Thesis/dissertation

UNIVERSITY OF CALIFORNIA

Los Angeles

Cell Engineering for Neuromuscular Regeneration & Neural Reprogramming

A dissertation submitted in partial satisfaction of the

requirements for the degree Doctor of Philosophy

in Bioengineering

by

LeeAnn Kai-Yin Li

2020

ABSTRACT OF THE DISSERTATION

Cell Engineering for Neuromuscular Regeneration & Neural Reprogramming

by

LeeAnn Kai-Yin Li

Doctor of Philosophy in Bioengineering

University of California, Los Angeles, 2020

Professor Song Li, Chair

Neurological disorders are the primary cause of disability and the second leading cause of deaths worldwide, with an ever-increasing burden as populations grow and age. The peripheral nervous system (PNS) possesses great regenerative capability, but even so, no effective therapy exists for severe peripheral nerve injuries (PNIs) and underlying mechanisms are incompletely understood. Conversely, treatment for central nervous system (CNS) disease is crippled by little innate regenerative ability of the brain and inaccessibility of patient neural tissue. Direct reprogramming or transdifferentiation of adult somatic cells into neuronal fate ("induced neurons") has great potential for overcoming these barriers, but still suffers from low and variable efficiencies of conversion. My thesis harnessed principles of cell engineering, neuroengineering, and regenerative medicine to address these issues. In the PNS, we demonstrated a novel proof-of-concept that engineered synthetic neuromuscular tissue (SyNMT) can be used to guide development of and screening for stem cell therapies to treat denervation injuries. We compared neural crest stem cells (NCSCs) to bone marrow-derived mesenchymal stem cells (MSCs). Three-dimensional (3D) multicellular spheroids of NCSCs enhanced *in vitro* regenerative functions and dramatically increased *in vivo* longevity, with significant functional improvement in

rat trials that recapitulated SyNMT findings of NCSC but not MSC improvements in neuromuscular junction innervation. In the CNS, we demonstrated that 3D spheroids promoted the direct reprogramming of human fibroblasts into neurons, increasing conversion efficiency by over 67 times. Moreover, reprogramming displayed distinct spatial patterns dependent on adhesive polarity that could be rescued by dual BMP & TGF-β pathway inhibition. Overall, this work demonstrated the significant impact of engineering biophysical cues to improve regeneration and survival of neuromuscular cell therapies as well as to improve neural reprogramming, enhancing translational potential for biomedical applications.

The dissertation of LeeAnn Kai-Yin Li is approved.

April Dawn Pyle

Stephanie Kristin Seidlits

Michael Alan Teitell

Song Li, Committee Chair

University of California, Los Angeles

2020

Table of Contents

List of Figures

ACKNOWLEDGMENTS

A Ph.D. is not just a degree, but a journey – and not an individual one, at that. I would like to thank some of the many people who have helped along the way.

First and foremost, none of this would have been possible without my advisor Dr. Song Li, who provided an invaluable source of mentorship, inspiration, and feedback during my time here. He never seemed to lose his equilibrium, and discussions were imbued with a singular mix of down-to-earth practicality and big ideas. I appreciated the learning environment of guided autonomy that enabled freedom to experiment, in the literal sense, and grow. Thank you for investing in me and believing in me.

I am incredibly grateful, too, to my thesis committee. Dr. Mike Teitell has been immensely helpful since day 0 of the program when I was still interviewing at UCLA, in providing astute career guidance and empathetic advice during transitions, as a successful physician-scientist himself. Dr. April Pyle brought thoughtful questions and ideas that both connected and probed for further depth, for which my work greatly benefited. Dr. Stephanie Seidlits, a valued collaborator on the work of Chapter 3 as well, provided informed insight with an interdisciplinary perspective, and was an unfailing source of friendly energy in the department. Many thanks too to our other wonderful collaborators, Dr. Bennett Novitch, Dr. Ken Yamauchi, and Jesse Liang, who brought further dimensionality to our work.

My path to graduate school has been studded with and influenced by other remarkable scientific mentors, notably, Dr. Ian Gallicano, who saw something in me early on and enabled the first steps on my journey into research that would set the tone for the career to come; Dr. Dana Elzey, who taught me design-thinking as a way of life; Dr. James Marshall, who taught me intuition follows understanding follows persistence; and Drs. Gene Barrett and Brian Brooks, both also physician-scientists who impressed me with their combination of achievement and kindness.

To all former and current members of the Li lab, thank you for all the ways you have facilitated this work. In particular, from the early days of my joining the group, many thanks to Dr. Dong Wang for helping orient me to the gradually-unpacked lab, and an entertaining supply of cute baby stories; Dr. Jennifer Soto for teaching me fundamentals of iN work (Chapter 3) and being a model of organized lab management since; Dr. Danny Huang for teaching me how to even begin tackling NCSCs and related areas (Chapter 2), and sharing positivity and good food; Dr. Ben Hsueh for introducing me to animal surgery by elegant and patient example; and Dr. Jun Fang for teaching electrospinning, ciMCs, and creative mindset. My thanks also to Dr. Xili Ding for nerve conduit fabrication and fun bus companionship, Dr. Weikang Zhao for assisting with rat surgeries, Dr. Mahdi Hasani for SEM and invigorating idea brainstorming, and Buwei Hu for miscellaneous rat tasks. I also thank other earlier members Dr. Taya Bezhaeva and Sindy Lee, who founded our office Snack Basket with me, a herald of good things to come, and to Andy Chen for being an early fellow Ph.D. student comrade. In more recent years, I am also appreciative of input from Drs. Song Yang, Jana Zarubova, and Fei Fang; and also of Cher Zhang, my smiling desk companion. I'd like to particularly thank also my undergraduate students Natalie Olivares and Raul Davila, who have been wonderful and valuable additions, and keep me laughing at the latest pop culture. As well as all other Li lab members I have overlapped with: Drs. Xuefeng Qiu, Pingping Wang, Haoyong Yuan, George Wang, Buwei Hu, Natalie Maxwell, Izabella Samuel, Nitika Chellappa, Meagan Yuen, and Sam Roth.

I am grateful to the various others who have also generously shared science: Dr. Siavash Kurdistani; Drs. Joseph Wu and Marius Wernig (Stanford); Dr. Michael Hicks from the Pyle lab; Dr. Andrea Kasko and Dr. Sam Norris from her lab; Dr. Dino Di Carlo and lab; Dr. Brigitte

Gomperts; Dr. Tom Carmichael; Dr. Richard Wang from Dr. Stanley Nelson's lab; Dr. Tatiana Segura (Duke) and lab; the CNSI Crump Preclinical Imaging Technology Center and its staff Dr. Tove Olafsen, Dishan Abeydeera, and Dr. Jason Lee; the UCLA California Nanosystems Institute (CNSI) Advanced Light Microscopy/Spectroscopy (ALMS) Facility, particularly its staff Matt Schibler and Dr. Laurent Bentolila; the UCLA IMT Core/ Vector Core, particularly Dr. Janet Treger; and Texas A&M University Health Science Center College of Medicine. Thank you too to key staff from the Bioengineering department, Stacey Fong, Melissa Tran, Andrew Lao, and Apryll Chin.

My additional thanks to the UCLA-Caltech MSTP for giving me the opportunity to pursue my studies here in the first place, including former MSTP Co-Director Dr. Siavash Kurdistani, who was another Day 0 presence and served as my MSTP advisor for the first two years of medical school. I thank too current MSTP advisor Dr. Dave Dawson, and the other current MSTP leadership, Drs. Carlos Portera-Cailliau and Maureen Su, for any support and their service to the program. I am also grateful to MSTP staff, Susie Esquivel and Josie Alviar, for all they do for us.

I thank also mentors from med school who are reliable sources of caring advice and conversation: Drs. Margaret Stuber, Clarence Braddock, and Deborah Lehman.

I am deeply grateful to my friends: the friends made while at UCLA who have stuck with me through thick and thin, helped rejuvenate and sustain with food/climbing/chat/assorted beverage/excursions/other breaks, and get what we're going through in a way that only others who have been through this can; to our entering group of graduate engineering friends of the "Oats" family who helped ease and enliven my transition from med school into graduate school; as well as the friends outside of UCLA, who have been steady constants and grounding reminders of life before and beyond. Constrained by space here, you know who you are.

Lastly but most importantly, my boundless gratitude to my family. To my mom and dad, you each in your own way taught me to value the gifts we have been given, to think beyond the individual to the good of society, to persist and keep faith even in the face of huge obstacles, to work hard but also to enjoy life with the people who matter most. To my little sister, Angie, I got an early start on creative brainstorming in trying to find ways to keep your rambunctious self occupied, and adventures with you have shaped who I am today. To all of you, for your depth of love, support, and more throughout the years, I humbly thank you.

I have received financial support for my thesis work from the UCLA Medical Scientist Training Program (NIH NIGMS training grant GM08042). This research was also supported by grants from the UCLA Startup Fund and the Broad Stem Cell Research Center (BSCRC) Innovation Fund to Dr. Song Li.

Chapters 2 and 3 include data and text from unpublished manuscripts in preparation.

Appendix 2 reproduces an article published with Theranostics as granted under Creative Commons license.

Vita

EDUCATION

2014-Present	**University of California Los Angeles (UCLA), David Geffen School of Medicine** (DGSOM) Medical Scientist Training Program (M.D., Bioengineering Ph.D.)
2009-2013	**University of Virginia (UVA)** B.S. with Distinction, Biomedical Engineering, Minor in Engineering Business

HONORS & AWARDS

2020	**2nd Place Podium Presentation**, Annual UCLA Bioengineering Research Day
2019	**Best Poster Award**, Annual UCLA Bioengineering Research Day
2014	National Institutes of Health **Postbaccalaureate Intramural Research Award**
2013	**Raven Society** election by students and faculty to UVA's oldest and most prestigious honorary society • Recognizes high scholastic achievement, service to the University, & promise of advancement in the intellectual field
2013-14	**Awardee,** Harrison Undergraduate Research Grant, UVA (1/44 recipients)
2011	**Awardee,** Jefferson Public Citizens Grant, UVA ($25,875)
2009-13	**Rodman Scholar**, UVA Honors Engineering
2009	**Finalist,** Intel International Science & Engineering Fair (SEF); **Best of Fair Grand Prize**, Virginia State SEF

PUBLICATIONS

1. **Li, L.K.,** Olivares, N., Liang, J., Soto, J., Seidlits, S., Li, S. Spatial Promotion of Neuronal Reprogramming in Three-Dimensional Spheroids. *Manuscript in preparation.*
2. **Li, L.K.**, Olivares, N, Huang, W.C., Yamauchi, K., Hsueh, Y.Y., Ding, X, Davila, R., Zhao, W, Novitch, B, Li, S. Engineering Synthetic Neuromuscular Tissue to Guide Stem Cell Therapy. *Manuscript in preparation.*
3. Fang, J., Sia, J., Wang, P., Soto, J., **Li, L.K.**, Hsueh, Y.Y., Sun, R., Faull, K.F., Tidball, J.G., Li, S. In Vitro and In Situ Induction of Myogenic Stem Cells for Muscle Regeneration. *Nature Biomed Engr*- under revision.
4. Kalaskar, VK, Alur, RP, **Li, LK,** Thomas, JW, Sergeev, YV, Blain, D, Hufnagel, RB, Cogliati, T, Brooks, BP. High-throughput custom capture sequencing identifies novel mutations in coloboma-associated genes: Mutation in DNA binding domain of retinoic acid receptor β affects nuclear localization causing ocular coloboma. *Human Mutation*, 41(3):678-695, 2019.
5. Li, S, **Li, L.K.**, Hsueh, B. "Compositions and methods for treating peripheral nerve conditions," U.S. Provisional Pat. Ser. No. 62/875,260, filed July 17, 2019.
6. **Li, L.K.***, Wang, D.*, Dai, T., Wang, A., Li, S. Adult stem cells in vascular disease. *Theranostics*, *8*(3): 815–829, 2018. *Equal contribution
7. Stem Cell Tourism H-460.896. *American Medical Association (AMA) Policy Finder.* June, 2016.

8. **Li, LK.**, Aboubechara, J.P., Marsh, K.M., Nepomuceno, H., Moghavem, N., Yap, A. 170.017MSS Stem Cell Tourism. *American Medical Association (AMA) Medical Student Section Digest of Policy Actions*. June, 2015.
9. **Li, L.**, Larabee, S., Chen, S., Basiri, L., Yamaguchi, S., Zakaria, A., & Gallicano, G. I. Novel 5' TOP mRNAs regulated by ribosomal S6 kinase are important for cardiomyocyte development: S6 kinase suppression limits cardiac differentiation and promotes pluripotent cells toward a neural lineage. *Stem Cells and Development*, *21*(9):1538-1548, 2012.

ABSTRACTS (SINCE 2016)

Invited Podium Presentations:

1. UCLA Bioengineering Research Day Symposium, Los Angeles, CA, Feb. 2020.
2. AiChE International Stem Cell Engineering Conference, Los Angeles, CA, Dec 2018.
3. Biomedical Engineering Society (BMES) Annual Meeting, Atlanta, GA, Oct 2018.

Selected Poster Presentations:

1. International Society for Stem Cell Research (ISSCR) Conference, Los Angeles, CA, Jun. 2019.
2. UCLA Bioengineering Research Day Symposium, Los Angeles, CA, Feb. 2019.
3. UCLA Broad Stem Cell Research Center Annual Symposium Conference, Los Angeles, CA, Feb. 2019.
4. BMES Cellular and Molecular Bioengineering (CMBE) Conference, San Diego, CA, Jan 2019.
5. Micro- and Nanotechnologies in Medicine Conference, Los Angeles, CA, Jul 2018.

RESEARCH & ACADEMIC EXPERIENCE

2016-Present	**Song Li (Ph.D.) Lab** (Ph.D. Advisor), UCLA Bioengineering
2017	**Teaching Assistant**, Cell Engineering (mixed undergraduate and graduate lab course), UCLA Bioengineering
2014	**Brian Brooks (M.D., Ph.D.) Lab**, National Eye Institute, National Institutes of Health (NIH)
2012-13	**Gene Barrett (M.D., Ph.D.) Lab**, UVA Endocrinology
2008-11	**Ian Gallicano (Ph.D.) Lab**, Georgetown Medical Center Biochemistry & Molecular and Cell Biology

---

SELECT LEADERSHIP

2018-Present	**Founding Chair,** UCLA-Caltech Women in MSTP
2017-19	**Executive Board**, Bioengineering Graduate Association
2016-18	**Student Representative**, DGSOM Admissions Subcommittee
2016	**Region 1 Delegate**, American Medical Association (AMA)
2015-16	**Co-President**, UCLA AMA
2012-13	**Co-President,** Rodman Scholars, UVA

Chapter 1

Introduction

Overview

Disease survival has improved alongside advances in medical treatments and technologies, such that the endpoint of critical illness has now moved years beyond discharge. The issues of survivorship (health sequelae) and aging (organ failure, neurodegenerative disease) have shifted to the forefront issues of the day. Existing clinical standards of care like organ transplantation, tissue grafts, and blood transfusions have helped address some but not all of these issues, and are largely limited by donor supply[1,2]. The small molecule and protein drugs that transformed the face of medical care in the 20th century are similarly often insufficient for cure. The advent of tissue engineering and new methods of stem cell isolation, expansion, and reprogramming promised to herald a new shift in medical capabilities[2] (Fig. 1.1).

Nevertheless, most stem cell therapies have been plagued by *in vivo* outcomes in animals and humans that fall short in both overall and *in vitro*-predicted regenerative benefit[2–4]. Many factors contribute to this *in vitro-in vivo* discrepancy. Selection of appropriate cells and their interactions with relevant tissues are key considerations, and cell retention and survival within the body also remain major clinical barriers to their success[3–7]. 95% of cells typically migrate out of the target site within 24-48 hours, and of those remaining about 99% die by 4-6 weeks, leaving just 0.05% of the original delivery to exert effects[4]. Secretome, differentiation, and behavior of stem cells in isolation in flat, plastic dishes are far from realistic, too, as they neglect the other cell types at play as well as mechanobiological cues and the interactions and interfaces with other tissues. The cost of this prediction discrepancy is high. Animal models are financially expensive and time-consuming, and the price of failure in humans can be a patient's health[3,7–11].

Three-dimensional (3D) multicellular spheroids, a biophysical state found during

embryonic development and often used for embryonic stem cell (ESC) culture as well as neurosphere culture, in certain cells helps preserve viability, phenotype or differentiation, and function, as well as increasing protein synthesis[12–15]. Multicellular constructs and organs-on-a-chip are helping bridge the gap between single cell *in vitro* study and animal/clinical studies. These technologies have emerged as effective and promising tools to study pathology[16–18]. More complex systems may perhaps one day replace animal drug testing, as being investigated even by the U.S. Food and Drug Administration (FDA)[8,19,20]. The cancer field has been the first to harness such model systems to study cellular therapies, specifically, immunotherapy[21]. However, somewhat surprisingly, the extent of use in the stem cell field has been in the development of stem cells to create more physiologically relevant models or study of the stem cells themselves[22–27]. It has not yet been harnessed to study and predict the intrinsic therapeutic relevance of stem cell therapies.

Disorders of central nervous system (CNS) and peripheral nervous system (PNS) are pathologies prime for such exploration. Worldwide, neurological disorders are already the leading cause of disability and the second leading cause of deaths, and their global burden is only increasing with ever-growing and aging populations[28]. CNS disease is devastating due to the little, if any, capacity of the brain for regeneration to promote functional recovery, and study is hindered by the difficulty of obtaining human patient neural tissue[29]. PNS has more regenerative capacity, but even for peripheral nerve injury (PNI) there is currently no effective therapy, and much of the underlying mechanism remains unclear[30–32]. Cell reprogramming and therapies are uniquely positioned to address these critical gaps in knowledge and treatment.

Plasticity of cell fate is seen *in vivo*, even in the absence of forced transcription factor (TF) expression and exogenous chemicals that have dominated *in vitro* reprogramming thus far, suggesting that biophysical phenomena which arise naturally in development, disorder, and healing are of great physiological importance, although they are significantly less studied and

understood[7,33–35]. Mechanistic study and therapeutic engineering can mutually inform each other, and incorporating biophysical considerations may improve outcomes.

To address these challenges, my research is focused on two topics at the interface of cell engineering, neuroengineering, and regenerative medicine: (1) engineering synthetic neuromuscular tissue to guide stem cell therapy to treat denervation injuries, and (2) promoting neuronal reprogramming using three-dimensional (3D) spheroids.

PNS Regenerative Physiology

In theory, the PNS is the lower hanging fruit of the nervous systems for targeting regeneration. Muscle denervation has broad etiologies, occurring in trauma and motor neuron disease (e.g., peripheral nerve injury, amyotrophic lateral sclerosis, spinal muscular atrophy, Guillain-Barre syndrome, Charcot-Marie-Tooth disease), as well as neuropathies of diabetes and alcoholism, degenerative disk disease, pernicious anemia, and Intensive Care Unit (ICU)-acquired weakness. Peripheral nerve (PN) injury alone affects over one million worldwide a year. The resultant motor impact can contribute to consequences ranging from weakness or loss of functional independence, to respiratory failure and mortality, depending on the nerve(s) involved[30–32].

Despite the prevalence and severe implications of muscle denervation, there is currently no effective therapy, and much of the underlying mechanism remains unclear[30–32]. Prognosis varies widely depending on nature of injury or illness, delay before intervention, and patient characteristics[32,36–38]. Regain of motor function is limited in proximal nerve injury not because of failure of axonal growth, but due to the existence of an apparent period during which regenerating junction components find each other permissive for reinnervation and synapse reformation[36,37], and the progressive deterioration of nerve sheaths within the muscle itself[39]. Associated muscular deconditioning has significant negative ramifications on long-term outcomes as well[32,40]. Regeneration is thought to be supported by growth-promoting activity and signaling by the injured

nerve, Schwann cells, and target muscle[40,41]. Therapies have sought to promote a regenerative environment by addressing one or more of these issues.

PNs ordinarily are very quiescent and possess no resident stem cell population in the traditional sense. Rather, after nerve insult, within days Schwann cells dedifferentiate *en masse* to a progenitor-like state with unlimited proliferative ability from which Schwann cells with different roles and abilities may arise[42,43]. At the site of injury, inflammatory macrophages, neutrophils, and fibroblasts form a bridge between the nerve stumps. Hypoxic macrophages create a vascular endothelial growth factor (VEGF) gradient along this bridge for polarized vasculature to form. Schwann cells at the nerve injury site, which have undergone an atypical sort of epithelial-to-mesenchymal transition that promotes a migratory phenotype, then extend elongations (bands of Bungner) along the newly formed vasculature to carry regenerating axons across[42,44]. Schwann cells in the distal stump help clear debris and secrete factors, which open the blood-nerve-barrier for inflammatory cell influx to remodel the environment and provide neurotrophic support for axons[42].

Just as important as the nerve, though, is the interface of the nerve and muscle. Motor axons only innervate a single muscle, but within the muscle have many branches to innervate tens to hundreds of myofibers. Adult myofibers are innervated in their center area, at a site known as the neuromuscular junction (NMJ), by a motor neuron (MN) axon in a one-to-one ratio[44]. The NMJ itself is composed of the MN, Schwann cell, and muscle fiber[44]. Specifically, NMJ as well as other axon terminals are surrounded by a type of specialized Schwann cell known as terminal Schwann cells (tSCs) that help form, maintain, and repair synapses[42]. They modulate NMJ synaptic activity in response to synaptic transmission throughout life, though whether by proliferation or recruitment is uncertain[42]. Resident skeletal muscle stem cells, known as satellite cells, lie quiescent at the boundary of myofiber and overlying basal lamina. Although responsible for muscular regeneration after muscle injury, there is limited activation after denervation[45]. Despite the necessity of innervation for muscle health, muscle, in contrast with the motor neuron

and Schwann cell NMJ components, is thought to assist but not be essential for NMJ development[46]. This relationship, however, is understudied and the nuances unknown. Discoveries that the small number of satellite cells (~25%) that do activate after denervation occur near NMJs, and that selectively depleting the satellite cell population negatively impacts NMJ morphology and reinnervation as well as muscle atrophy, fibrosis, and force generation, suggest that there is an important role for muscle-nerve signaling as well. Myofibers are only disposable for initial reinnervation of NMJs; their presence is necessary for the completion of differentiation and maintenance of reinnervated NMJs[45].

In development, motor axons with Schwann cells in tow, notably, the opposite of regeneration, arrive as myotube formation from fusing myoblasts is occurring, and a low-transmission synapse forms within minutes of axon growth cone contact with new myotube. Over the course of around a week (in mice), nerve and muscle interact and develop and the immature synapse becomes fully-functional. It has been observed that in co-culture, uninnervated myotubes will spontaneously have dense AChR clusters, but axons organize new clusters rather than innervating those pre-specialized sites. Myotube growth occurs symmetrically at axon ends[44]. Muscle-derived organizing molecules like laminin β2 and gene expression by post-synaptic myonuclei help progressive differentiation of pre-synaptic nerve terminals[45,47].

After injury, tSCs sprout greatly and help repair the NMJ by acting as a substrate along which regenerating axons can both return to former synaptic sites and also to a lesser extent, along extended tSC processes, reach new ones[42,44]. Denervation-induced proliferation of interstitial cells and accumulation of adhesive matrix proteins (e.g., fibronectin, tenascin-C) near synapses may also help enhance or direct regrowing axons, which are further guided in reinnervation and growth cone differentiation by synaptic basal lamina which extend between pre- and post- synaptic NMJ membranes[44]. Chronically denervated skeletal muscle decreases in mass due not to cell death but protein anabolism-catabolism imbalance[45].

After axons regrow, they signal to all cells of the nerve to exit the cell cycle, and Schwann cells redifferentiate. The aftermath is visible in the increased ECM left in regenerated nerves, increase in axons due to regenerative sprouting, and three to four times increased cell density overall, of unchanged proportions, within the nerve[42].

PNI Therapy

A number of therapies have been attempted for denervation muscular atrophy. Surgical methods include nerve transection repair with end-to-end anastomosis; if such primary repair is not possible, nerve grafts, nerve conduits, nerve and nerve-muscle pedicles transfer may be considered; and in the event of lack of a distal nerve segment for anastomosis, direct nerve transplantation (neurotization) into the muscle may be performed. Only partial recovery of function after neurotization, despite regenerated NMJs within denervated muscle, have led investigators to suggest that attention should be broadened beyond that of just the nerve, though that has been the historical focus. They proposed that addition of exogenous signals like growth factors (GFs) might lead to more organized and thus productive integration[48], as such signal synthesis in non-neuronal cells simulates a “substitute target organ” area to support the nerve during regeneration[49]. The benefit, though limited, of electrical stimulation[50,51] and myofiber transfection with adeno-associated virus to upregulate GDNF[52] for muscle atrophy and reinnervation is believed to have a common mechanism of GF modulation. Bolus GF delivery is ineffective, however, thought to be due to overly simplified GF programs, and/or rapid degradation and depleted local concentrations of GFs[53]. Simply overexpressing GFs persistently is insufficient, although substantial benefits have been seen[53], and this approach is potentially detrimental to functional recovery if timeline and released concentration are not optimized[54]. Cell transplantation has advantages over synthetic manipulation of these complex and incompletely-understood paracrine programs, as they are capable not only of acting as environmentally responsive

reservoirs of physiologic levels of paracrine signals, but also additionally of integrating and inducing system responses via cell-cell contact signaling.

Research into the mechanisms behind benefits of stem cell transplantation point increasingly towards the role of paracrine modulatory trophic signals rather than direct replacement of affected cells at sites of injury[55]. Cellular therapies for denervation have more often focused on the damaged nerve itself as well. Cell therapies using adult and embryonic neural cells and muscle progenitors have some benefit for denervated muscular atrophy. Syngeneic Schwann cells improve peripheral nerve regeneration but are difficult and time-consuming to obtain in sufficient quantities[56]. Progenitors like human amniotic fluid-derived stem cells and fetal neural stem cells have been shown to help denervated muscular atrophy, though utility and efficacy have been limited thus far[57,58]. Embryonic stem cell-derived motor neurons, despite some success, are hindered by supply[59,60]. Outcomes of current treatments specifically for severe muscle injury and myopathy, including autologous muscle transplantation (surgically connecting arteries, veins, and nerves of functional donor muscle) and injection of *ex vivo* cultured muscle cells, have been limited by inadequate innervation and perfusion of the transplant, and inefficient *in vitro* muscle stem cell expansion and cell retention (whether through migration or survival), respectively[61,62].

NMJ Modeling

Methods for modeling NMJs have been developed and increasingly characterized in recent years. Various methods co-cultured on flat, unpatterned surfaces combinations of: iPSC-derived MNs with muscle[63], rat spinal cord explants of dorsal root ganglia and primary myoblasts[64], human satellite cell-derived intrafusal muscle with neuroprogenitor-derived sensory neurons[16], and human ES-cell-derived MNs under optogenetic control and human myoblast-derived skeletal muscle[65]. Compartmentalization of unpatterned culture has also been done to

create separation between MN bodies and myotubes, connected by small tunnels for axon growth[66,67].

Mechanically aligned co-cultures of myoblasts and primary motor neurons using topographical cues have reported improved myodifferentiation and NMJ functional maturation and long-term culture[68,69]. Alignment has also been achieved via myoblast suspension in hydrogel to self-assemble around anchoring structures on either end, with MNs either mixed in[70] or in a separate chamber of a microfluidic device[71]. Some of these systems were used to model disease and/or screen drugs[65,70,71]. However, they have not yet been applied for the purpose of screening cellular therapies, although they could assist in identifying specific mechanisms of clinical benefit, and also in assessing relative cell potency prior to transplantation for quality control[72].

Neural Crest Stem Cells (NCSCs)

Neural crest stem cells (NCSCs) may be a more accessible and developmentally relevant cell source for nerve-muscle regeneration. NCSCs are stem cells that can be differentiated and isolated from embryonic stem cells (ESCs), embryonic neural crest, and induced pluripotent stem cells (iPSCs) and found in low abundance in adult tissues[73–75]. They have the capacity to differentiate into cell types of all three germ layers, including peripheral neurons and Schwann cells, and maintain this multipotent potential later than any of the classical three germ layers[76–78]. Although there has been some controversy about whether NCSCs are truly homogenous and multipotent or rather are comprised of assorted fate-defined precursors, advances in lineage tracing beyond inter-species transplantation to genetically-based tracing have suggested that the first may hold true, with flexibility of differentiation potential even when taken from various tissues up to a certain point in time[42,79,80]. Regardless of the outcome of that debate, it is known the neural crest contributes to the development of a wide variety of tissues. NC-derived cells, some with demonstrated *in vitro* stem cell properties, are reported to have been found in adult tissues with

NC origins themselves such as peripheral nerves, dorsal root ganglia (mainly nociceptive afferent neurons, satellite cells), parasympathetic ganglia, enteric ganglia, dental pulp, and corneal stroma, but also non-NC-derived tissues such as bone marrow, hair follicles, the carotid body, dermis (cutaneous nerve Schwann cells, terminal glia, endoneurial fibroblasts), and adrenal medulla[80]. Altogether, NC defects cause an estimated 30% of all human congenital malformations[79]. Fleshing out their interactions with various tissues to enhance understanding of their biology and function could thus have broad implications.

Therapeutically, our lab previously showed NCSCs, transplanted not into muscle but in nerve conduits, promoted nerve regeneration and functional recovery through Schwann cell differentiation and trophic signaling[81]. Others have similarly found that boundary cap NCSCs, which can generate mature Schwann cells, can myelinate uninjured and axotomized sciatic nerves[82]. On the muscle side, although known not to be direct skeletal muscle precursors, in recent decades NCSCs have been discovered to signal to muscle during development, playing critical roles in regulating early and sustainable myogenesis as well as regulating maintenance and differentiation of the skeletal muscle progenitor pool[83,84]. NCSCs could thus be uniquely advantageous for PNI regeneration by addressing this neuromuscular interface.

Mesenchymal Stem Cells (MSCs)

MSCs are among the most abundant stem cell type in clinical trials. However, this distinction comes with a caveat: an FDA study in 2014 of submitted investigational new drug applications found negligible consistency in MSC molecular characterization[85]. A common method for obtaining MSCs involves isolation of nucleated cells from the adult bone marrow (BM) and selecting for cells that adhere and expand with fetal bovine serum[86,87]. This method is supposed to remove hematopoietic stem cells (HSCs) and nonadherent cells and leave fibroblastic MSCs[87]. It has been increasingly recognized that even if isolated from one location like BM, BM-resident

MSCs (BM-MSCs) are comprised of cells of multiple origins with composition dependent too on time of isolation. Without consistent surface markers, the abundance of effects and differentiation potential reported for “MSCs” cannot be attributed to a single cell type[88,89].

If we use this standard to screen for studies of human BM-MSCs ($CD146^+$, from long bones or iliac crest BM aspirates), we find reports affirming their ability to generate structures supporting hematopoiesis, while disproving some claims in that, *in vivo*, they are neither myogenic nor neurogenic, nor spontaneously chondrogenic[89–91]. Transplantation of these BM-MSCs into an uninjured *in vivo* environment reveal their ability to form perivascular cells that associate with blood vessel walls, with no significant impact on muscle[89]. Immunomodulation by such cells is plausible given the physiological roles of bone marrow, but cannot encompass all reported situational benefits without being contradictory, and require further understanding of regulatory MSC function in the context of the specific setting in question[90]. Given the role of neovascularization in bridging nerve gaps as well as the influx of inflammatory milieu at the nerve injury site, it is not implausible that implantation of BM-MSCs into nerve conduits in an injury model might have beneficial effects on nerve regeneration, as some have found[92]. For intramuscular transplantation for PNI, benefit with these specific BM-MSCs remains to be seen.

NCSCs and MSCs

Recent reports have found that interestingly, the neural crest and neuroepithelium supply the earliest wave of MSCs during development, which migrate to the BM with developing nerve fibers. These cells are neither Schwann nor endochondrally committed and play no role in fetal endochondrogenesis, unlike the majority of MSCs[93]. Furthermore, nonmyelinating Schwann cells have also been found in the BM[94]. Some may question then the possibility of NCSCs or NC-originating cell presence or identity within the BM-MSC population, and wonder if MSCs would then have an effect different from NCSCs. However, in the first case, not only is that subpopulation distinct from oligodendrocyte-producing pathways, but it is also a transient intermediate stage

which helps establish the bone's hematopoietic stem cell (HSC) niche[95]. That minority of MSCs progressively decreases and almost disappears postnatally[95]: Neuroectoderm-derived (nestin$^+$) MSCs form just 0.04-0.08% of nucleated bone marrow cells that typically are isolated as adult "MSCs"[93], or 0.026% of BM area[94]. Moreover, they may in fact be composed mostly of NCSCs with only a few bona fide MSCs in that population[96]. Another recent study showed that BM also contains nonmyelinating Schwann cells that occupy an even smaller separate and distinct area, just 0.004% of BM area, and ensheath sympathetic nerves there[94]. Although it is possible that such MSCs could be a portion of the human MSCs used for transplantation, they are so rare a population and so slow-dividing that their presence is, if not unlikely, negligible. If such cells were to be expanded, they could be interesting for future study.

Direct Neural Reprogramming

One of the most fundamental rules of cell biology was overturned by Shinya Yamanaka and John Gurdon's discovery that differentiated cell fate is not the bottom of an irreversible, one-way slope, but in fact capable of not only uphill back-tracking (de-differentiation) but also orthogonal conversion into other differentiated cell types (direct reprogramming, or transdifferentiation). This discovery, which was rewarded the Nobel Prize in 2012, spawned a whole new branch of regenerative medicine predicated on reconnoitering the new paths it opened and discovering key influencers of otherwise seemingly stochastic changes. Directed navigation of this field would have tremendous implications for basic biological understanding, improving accessibility to cells for disease modeling and therapeutic testing, and functionalizing knowledge for engineering improved replacement cells and tissues and/or *in situ* regeneration and healing without the cancer risks of pluripotent cell products[97–99].

The first documented cell therapy for a CNS disease occurred four decades ago, when catecholamine replacement was attempted with autologous cells of the adrenal medulla

transplanted into the striatum of Parkinson's disease (PD) patients. Any improvement was minimal. In the years since, animal and clinical trials have demonstrated that cells transplanted into the CNS are capable of participating in cell replacement, integrating into host structures, and performing physiologically relevant functions, though outcome is highly variable. Clinical trials applying stem cells, most commonly from the bone marrow, to disorders ranging from stroke, spinal cord injury, ALS, and others, have been attempted and are ongoing. Nevertheless, no clinically competitive cell therapy, with great enough clinical improvement and feasibility over existing treatments as to render risks worthwhile, yet exists for CNS disorders[72].

Direct reprogramming of neuronal fate, into "induced neurons" (iNs), has among the most extensive literature on mechanisms of reprogramming into non-pluripotency, and is thus primed for in-depth studies of transdifferentiation[97]. Like pluripotent stem cell (PSC)-derived neurons, iN technology enables generation of neurons from more easily accessible cells like skin. Unlike PSC-derived neurons, however, iNs can preserve donor epigenetic age information, and thus hold important potential for studying disorders for which age is an important factor – as is the case for the vast majority of neurological disorders[28,100].

Despite this wealth of knowledge and potential, variable efficiencies in generating iNs and incomplete comprehension of underlying mechanisms of this conversion are significant roadblocks to their application[29,98,100]. Transdifferentiation involves both disruption of the existing regulatory network (generally early on) and establishment of another. The initial generalized disruption is often mechanistically associated with cell cycle regulation, cell senescence, chromatin inactivation, and genome stability. Most commonly, transdifferentiation has involved positive or negative signaling pathway modulation or forced expression of transcription factors (TFs), which can also cause epigenetic changes. The conversion of fibroblasts to neurons by the forced expression of neural lineage transcription factors (TFs; here, *Ascl1, Brn2, Myt1l*, and *NeuroD1*, together known as BAMN) has been well established[101,102], although promising results

of transdifferentiation from other starting cell types, such as pericytes[103], peripheral blood T-cells[104], astrocytes, and other cells of neural lineage[29,105], have been published since then as well.

Like pluripotent stem cell (PSC)-derived neurons, iN technology enables generation of neurons from more easily accessible cells like skin. Unlike PSC-derived neurons, however, iNs can preserve donor epigenetic age information, and thus hold important potential for studying disorders for which age is an important factor – as is the case for the vast majority of neurological disorders[28,100]. Intriguing longer-term therapeutic potential aside, the existing though incomplete understanding of iNs prime them for in-depth studies of transdifferentiation, and place them in good stead to be a case study of fundamental mechanics of direct reprogramming[97].

TFs can indirectly synergize by binding chromatin in different ways that promote certain reprogramming outcomes[97]. The earliest iN studies identified forced expression of neural lineage TFs *Ascl1, Brn2, Myt1l*, and *NeuroD1* was enough to convert fetal and postnatal human fibroblasts into functional neurons with identities that persisted endogenously, even after exogenous stimulation of the TF transgenes was withdrawn. *Ascl1* was identified as the key "pioneer factor," with *Brn2*, *Myt1l*, and *NeuroD1* acting to promote functional maturation. Cells with immature neuronal morphologies appeared 7-10 days after BAM factor infection, and 3 weeks after BAMN had reprogrammed at 2-4% of plated cells[102]. Importantly, although TFs are sufficient to set reprogramming into motion, the completeness and specific subtype of the end product are profoundly reliant on extrinsic modulators of the process such as from the environment as well as *a priori* reprogrammability of the starting cells[97,106].

Improvement of iN conversion has been attempted with different reprogramming strategies. Small molecules have enabled reduction or elimination of ectopic gene insertion, and in some cases improved on reprogramming efficiency. They generally act first to non-specifically disrupt existing gene networks to facilitate cell fate transition (e.g., global histone deactylase inhibitor valproate [VPA], TGF-β inhibitor RepSox, GSK-3 inhibitor CHIR99021), facilitating the more specific establishment of neural lineage by other reprogramming components[99,107,108].

Application of neural-inducing factors to iN reprogramming was successfully used in implementing synergistic SMAD pathway inhibition with the activin-like kinase 5 (ALK5) inhibitor SB-431542 (SB) and noggin, which increased reprogramming efficiency several-fold over the control and over double that of GSK-3β inhibitor CHIR99021 (CHIR), which could be combined altogether to increase conversion even more[109].

Studies tracking state transitions of iNs in a variety of reprogramming protocols have found that they nonuniformly traverse transient intermediate states that express neural progenitor markers, but not always the canonical ones found in development, before arriving at a terminal differentiation[103,107,108,110]. iNs are not unique in transdifferentiation for this divergence from developmental paths[111]. Managing these intermediate states to capitalize on certain states and manage future transplantation risk is nontrivial. Still, as seen with many of the aforementioned TFs and pathway signalers, some factors that promote neural lineage in development and in other cell types like PSCs may be successfully applied for iN conversion as well[98]. Parallels and tools from differentiation may still find conversion-enhancing analogies in direct reprogramming[98,112].

A recent study discovered that mouse iPSC reprogramming is not in fact an equitable playing field where, amongst cells of a certain developmental or functional identity, chance only dictates which cells are reprogrammed[113]. Rather, a population-level look at all unrelated cell clones identifies that a subgroup of starting cells with “context-specific eliteness,” an innate fitness for reprogramming, overtakes and dominates the reprogramming niche’s bulk dynamics and composition. The elite marker there was identified as the important developmental marker Wnt1[106]. This supported similar previous findings in transdifferentiation, which identified “elite markers” unique to their reprogramming[114,115]. These discoveries lend themselves to the question of finding the markers of “elite” identity for other types of reprogramming, such as that of iN transdifferentiation, in order to engineer improved efficiency.

A Brief History of Spheroids

How do cells assemble into tissues, and tissues into organs? This has been an ageless question for biologists, and now also for the newer field of regenerative engineering. The concept of self-assembled multicellular culture originated over half a century ago in the field of development, and then germline cancer[116–118]. Early landmark studies found that dissociated embryonic gastrula cells in the right proportions would self-adhere and re-assemble *in vitro* with preferences and arrangements according to their normal morphogenetic function (ectoderm on the exterior, endoderm on the interior, and mesoderm in between), termed "cell affinities." Furthermore, aggregates created from highly differentiated tissue of later-stage embryos, transplanted back into the animal in vascularizing locations, still recreated organs of almost normal complexity[119]. "Spheroid" became the term for a free-floating aggregate of cells (though not necessarily spherical in shape), the most fundamental multicellular building block.

Neuroscientists found thereafter that such spheroids arose naturally when isolating neural cells from nervous tissue, and that culture in this form enhanced physiological responses and survival of neurons *in vitro*[120,121] as well as *in vivo* after grafting back into the brain[122]. Human neural precursors, in particular, are particularly well-suited for spheroidal culture, showing longer-term expandability than rodent neurospheres[123]. Thus "neurosphere" culture became neurobiological canon as well.

Decades later, stem cell researchers found that PSC aggregation to form three-dimensional colonies (embryoid bodies, or EBs) enhanced survival and in the absence of stem-maintaining factors facilitated differentiation into almost any cell type, including the neural lineage, and recapitulate normal development well in each of those tissue systems[124,125]. ESC-derived EBs have a large degree of self-organizing capability[126]. Human embryonic stem (ES) cells as well as embryonic carcinoma (EC) cells grown at high density without feeder layer renewal for four to seven weeks spontaneously formed multicellular aggregates above the plane of the monolayer which contained neurons and some other differentiated cell types. When early neuroectodermal

cells were removed from colonies at three weeks and replated in serum-free medium, within 24 hours they formed spheres positive for primitive neuroectoderm markers (N-CAM, nestin, vimentin, Pax-6). Replating on poly-D-lysine and laminin coated substrate enabled spheroid attachment and subsequent monolayer outgrowth of differentiated, mature neurons[127]. Similarly, inhibiting cell adhesion in ESCs by blocking E-cadherin attenuated the neurogenesis-enhancing effect of spheroid culture[125]. Cancer researchers similarly found that such self-organized clusters more closely modeled tumor response to therapy[128].

The increasing recognition that cells behaved very differently in 3D than in 2D let to increasing adoption for other cell types and applications[128,129]. Various methods have been used to form spheroids, including matrix-free approaches like suspension culture, hanging drops, and external-force-driven aggregation; matrix-based methods like hydrogels; and microfluidic strategies[130]. As often becomes the case with routine use, spheroids became largely taken for granted, and fundamental rationale for their vast impact on cells was never discovered.

The Impact of Spheroids on Cell Behavior

Development first informed the use of spheroids, but now spheroids may inform development and reprogramming. Recent years have seen a resurgence of interest in the mechanistic rationale for benefits of multicellular aggregation with the discovery that growing hESCs in a confined 2D geometry, essentially distilling the self-patterning of spheroids to a slice, could similarly recapitulate early embryonic phenomena[131]. In this study by Warmflash, *et al.*, they found that the periphery of colonies had elevated expression of pluripotency markers OCT4, SOX2, and NANOG, as well as elevated SMAD1/5/8, SMAD2/3, and β-catenin activity, known signal transducers of the BMP, Activin-Nodal, and Wnt pathways, respectively. They only saw these effects for colonies of greater than 250μm in diameter, whose peripheral zones were all the same radial distance from the colony boundary; smaller colonies homogenously expressed

markers at the peripheral levels of larger colonies. SMAD1/5/8 in the first 24 hours of BMP4 ligand application had higher expression peripherally while retaining expression in the center, but thereafter signaling formed a peripheral annulus pattern. SMAD2 nuclear expression was expressed in the mesendoderm regions, peaking at the periphery (the endoderm). Inhibition of Activin-Nodal signaling eliminated mesendodermal differentiation and was replaced by ectodermal differentiation instead, with a net effect of increased number of cells pursuing the ectodermal lineage. Similarly, BMP inhibition is essential for ectoderm formation in their system. Of note is that micropatterning recapitulates diffusion gradients to a certain extent (with the additional option of diffusion from above), but not the mechanics of spheroidal culture. Nuclei in their micropatterns appeared to possess even spacing, non-obvious alignment of orientation, and comparable nuclear shapes throughout – in direct contrast with spheroids[131]. The importance of biophysical cues in assortment of this system was highlighted later by others[132].

Another group similarly studied the growth of pluripotent hESCs on micropatterns into a complete epithelium sealed by tight junctions. Their cells aligned radially, perhaps due to the 2D nature of the colonies. Activin and BMP receptors were expressed apically (facing out) at colony edges but laterally (circumferentially, the sides) elsewhere. TGF-β receptor was laterally located as well for signal transduction. Because of this constant availability of receptors at the surface facing the medium, in contrast to interior cells which were only responsive apically when density of culture was not too high, cells at the periphery were always responsive and displayed increased ligand sensitivity. They recognized, however, that apical-basal orientation was difficult to control in such a 2D system, and grew the cells on filters to present stimuli from the top and bottom as well. Longer-term signaling reduced BMP4 signaling, and thus pSMAD1, due to negative feedback from the expression of the secreted BMP4-inhibitor NOGGIN; without NOGGIN, signaling was spatially uniform. SMAD2 was key for mesendoderm fate. Ultimately, they found that the complexity of positioning cell fates was fundamentally controlled by, first, BMP4 signaling negatively modulated by dynamic receptor localization and NOGGIN, and from that output,

signaling with Nodal. They concluded that colony cell polarity was determined by density and boundary proximity[133].

In a similar system, hiPSCs and hESCs plated onto circular micropatterned arrays uniformly expressed stem cell markers, and one day after initiating cardiac differentiation with WNT/β-catenin activator CHIR, spatial heterogeneity manifested. Center cells lost OCT4 expression. The periphery, in contrast, retained OCT4 expression as well as E-cadherin expression, and were characterized by higher cell density, cell shape distortion, and increased proliferation and consequent mesenchymal condensation. Increased cell density was found to occur as a result of increased motility of center cells, which would migrate outward to the periphery. Similar to our findings, they found peripheral cells had elongated nuclei with increased shape indices reminiscent of the apical-basal polarity of epithelial cells. They also found that smaller diameter patterns reduced WNT pathway activation and mesoderm differentiation as well as early cardiac lineage induction gene expression while increasing elongation-related gene expression. Differentiation with CHIR conversely enhanced gene expression of cell polarity and mechanotransduction pathways. In their system, peripheral cells differentiated into myofibroblasts, while center cells differentiated into cardiomyocytes[134]. Whereas they found that cell motility was a contributing factor, though, others have not found this[135].

Although such 2D micropatterned arrays are by no means identical to spheroids in behavior, analogies may perhaps be drawn. Still, 3D aggregation studies may be more illuminating. Spheroids in certain cells helps preserve viability, phenotype, and function, as well as increasing protein synthesis[12–15]. Extended culture of a somatic cell line (mouse embryonic fibroblasts) and cancer cell line (metastatic breast cancer), on micropatterns led to a pile-up aggregation due to lateral confinement that was found, in the absence of other treatments, to erase lineage characteristics and induce stemness after 10 days[136]. This was attributed to an increase in nuclear plasticity along with the reorganization of epigenetic and chromosome packing within the nucleus with time that led to the rewiring of the nuclear architecture in a manner that

primed the nucleus for reprogramming[136]. hiPSC-derived human cortical spheroids relative to monolayer cultures had upregulated synaptic transmission genes and downregulated cell cycle and cell division genes, as seen also in human fetal cortex[137]. Single endothelial cells undergo anoikis in suspension culture, but spheroid formation enables survival in the same conditions. Furthermore, these spheroids form a differentiated EC surface layer overlying unorganized central EC that then apoptose. This arrangement was independent of cell shape, which was disturbed to no effect by cytochalasin D, but rather thought to be a result of polarization[12].

In gastrulation, signaling and specific cell behavior vary widely amongst species, but the mechanics are evolutionarily conserved. Specifically, increased non-cell-autonomous deformation of cells at margins of zebrafish embryos, which ordinarily occurs by morphogenetic movement, reliably triggers β-catenin nuclear translocation to initiate maintained expression of transcription factors critical for early mesoderm. Blebbistatin (blebb), which specifically inhibits non-muscle myosin II, could interfere with this movement and stage of development and thus the β-cat translocation, but using external magnetic force on injected magnetic liposomes to externally initiate deformation could reverse this effect in blebb-treated cells[138].

During development, germ layer formation is first seen during gastrulation, a phase when self-organization acquires heightened importance. Pre-somitic mesoderm (PSM), precursors of vertebrae, establish segmental organization of the vertebral column starting in gastrulation when they acquire spatiotemporal oscillations in gene expression that guide embryonic anterior-posterior patterning[139]. Multi-cellular aggregates of dissociated PSM reassemble and collective synchronization of individual cell oscillations occurs via active Notch signaling[140]. Specifically, Notch is the stimulus for the system whose excitability threshold is dictated by YAP – notably, a mechanosensitive protein[139]. Collective synchrony was blocked by DAPT treatment[140]. PSM self-organization occurs even if starting cells are not from anterior-posterially different origins, and PSM cells adjust their oscillation rhythm in response to their new neighboring cells. The existence of pacemaker cells was ruled out, as well as any intrinsic differences in cells such as adhesion

and axial origin, and an open question of how they synchronized gene expression based on their surroundings remained[140]. It has since been found that cyclic gene oscillation period, amplitude, and phase are regulated by FGF activity as well, and cell communication and interaction is required for global synchronization[139].

The most recent discovery that compression induces dedifferentiation of adipocytes that contribute to human mammary adenocarcinoma progression highlights the clinical implications of such basic science discoveries[141]. Host pathology might similarly cause disease in engrafted cells, so understanding fundamental mechanisms driving both desirable and undesirable outcomes is of great importance[72].

Theories of Spheroid Multicellular Interactions

Fundamental to the characterization of multicellular spheroids of more than one cell type are tissue boundary theory and the principle of self-assembly. Application of thermodynamic theory first helped explain cell assortment: due to differential adhesion between motile cells, distribution would be such as would minimize surface free energy ("tissue surface tension," or TST) and maximize total work of cohesion (strongest adherence between cells)[119]. Initially thought to be mediated by the expression of different cellular surface proteins, another concept later arose that contractile "cortical tension" at the surface of individual constituent cells resulting from active actomyosin also needed to be considered[142–144]. Under the assumption that cells in aggregates had the same properties as single cells, however, these ideas would be contradictory.

More recently concordance was found *in vitro* between these two ideas by a radical concept: cell properties are not in fact roughly equivalent in aggregates and tissues, but rather, cells at the boundary change their mechanical properties from those of the bulk, a phenomenon termed "mechanical polarization"[145–147]. This response may be mediated by signaling cadherins, which reduce actomyosin contractility along cell-cell contact interfaces proportionally to the area

of this contact[148]. More quantitative concordance was found by modeling cortical tension, adhesion, and elasticity as components of a function describing a cell's mechanical energy[142]. Mechanical polarization of boundary cells would increase effective cell-cell adhesion within the tissue (mechanical energy of adhesive bonds + [the difference in cortical tension along internal and external interfaces]), and TST being proportional to this, would be predominantly defined by the larger component pertaining to boundary mechanical polarization[148,149].

Anisotropic stresses are highest at the periphery of 2D, post-confluence, circularly-confined multicellular systems, where radial gradients of cell spread area, alignment, and traction forces also peak[150]. However, it has been shown that confinement and shape anisotropy do not predict *in vivo* directionality of forces as well as asymmetric mechanical constraints, which are sensed by apical actomyosin meshwork contraction[151]. The concept of power-based self-sorting may be complementary. Cell power is a measure of a quantifiable output, for which proteins internal and external, ATP chemical energy, and system interactions beyond the cytoskeleton may all be possible inputs[144]. It says that cells of higher contractile power assemble in the core of spheroids[144]. Fibroblasts are highly contractile, and human cells have been quantified to expend 4.3±1.7 pJ/h of power in the process of self-assembly, a process which is heavily driven by cytoskeletal-mediated contraction[144], and perhaps would favor a core environment.

The recent innovation of dispersible force sensor technologies finally enabled direct mapping of internal force generation within 3D spheroids, and findings are in fact analogous to the theories originated in monolayer systems[152–155]. More specifically, spheroid physics is characterized by circumferential contraction of the peripheral layers that drives the mechanical gradients within, leading to both radial and circumferential compressive stress within the bulk[155].

Spheroids formed by aggregation displayed similar stress patterns to spheroids grown from single cells, but the nature of their formation by cellular compaction rather than gradual proliferation results in certain phenomena. In spheroids formed by centrifugation-driven aggregation, the peripheral region (a few cell layers thick) has distinct mechanical polarization,

and contraction there with a circumferential tension on the order of 10s of Pascals. This circumferential contraction, reflected in cytoskeletal staining and organized actin filaments, found on the periphery drives profiles of significantly-larger (kilopascals) compressive stress in the radial and circumferential directions within the bulk[155]. Circumferential contraction compacts peripheral cells faster, creating a gradient in cell density that is densest at the edge, and decreases as one moves inward[155]. Finite element simulations showed that, like cells in 2D sheets[156], these mechanical patterns could not be driven by proliferation[155]. The increased contractility of peripheral cells are reflected in greater phosphorylated myosin and organized actin filaments, which coincide with mechanosensitive pathway activation. Compressive stresses peak just inside the peripheral region[155].

On the other hand, spheroids formed of endothelial cells (ECs) arrange into a differentiated EC surface layer overlying unorganized central EC as a result of polarization, independently of cell shape and cytoskeletal inhibition[12]. Similarly, planar cell polarity (PCP) is a hallmark of epithelial tissues, for which apicobasal orientation is a critical component of function[157]. Anisotropic cortical tension on epithelial cells within the epidermal sheet aligns their polarization and is closely associated with adhesion between neighboring cells and basally to the basement membrane[157]. It is possible that adhesive polarity conditions of spheroid surface cells may find analogies with epithelial biology, and the respective contribution of cortical tension versus adhesion polarity to different effects on cells is of interest to identify.

Extracellular matrix (ECM) interactions with cells are one of the cornerstones of tissue engineering, and its manipulation has long been used for effective study of developmental dynamics. Variables such as stiffness, which incorporates cell adhesion and contraction; composition; and spatiotemporal modification are all important influences on cell behavior as well as organoid assembly[158]. Once a spheroid is placed in an adhesive, albeit still 3D, environment, this containment is effectively destroyed. Cells begin migrating, tractional forces reverse direction, and cell-borne stresses initially become tensile rather than compressive. This can be understood

by considering the loosely related model of a freely growing sheet of cells. At any given position, Newton's laws dictate that the accumulated traction (the sum of traction stresses perpendicular to the peripheral edge, from the edge up to that point) are equal and opposite to the local intercellular (junctions) and intracellular (cytoskeleton) stresses propagated in the sheet. Closer to the center of sheets, stresses in the cell sheet are of greater significance than traction. Altogether, the sheet is globally under tensile stress, which serves to enable its migration[156]. Multicellular aggregates embedded in migrating-enabling 3D ECM are modeled by different models of collective dynamics, in which behavior is no longer dictated by intercellular interaction, but by environmental remodeling[159].

Cell Signaling and Polarity

The TGF-β/Activin and BMP pathways play key roles in reprogramming as well as neurogenesis of hPSCs and iNs[109,131,133,160,161]. The synergy has been attributed to several mechanisms. Activin and its associated TGF-β pathway promotes the mesodermal lineage, and TGF-β is a cytokine commonly used to induce and maintain the mesenchymal state. Their inhibition destabilizes networks to facilitate differentiation as well as mesenchymal-to-epithelial transition (MET)[109,161]. Inhibition of this TGF-β/Activin/Lefty pathway via inhibition of the ALK4/5/7 receptors enhances neural induction[161]. BMP, in turn, promotes the endodermal lineage, and its inhibition both represses endogenous BMP as well as BMP responses. Naturally occurring BMP inhibitory factors like noggin, chordin, and follistatin are key inducers of neural fate[161]. PSC neural conversion requires the synergy of combined pathway inhibition rather than either alone[161].

There are known existing avenues that connect cell polarity to differential BMP and TGF-β response, both of which are key pathways in cell and neural reprogramming[109,131,133,160,161]. Cells with apicobasal polarity respond to increased cell density by re-distributing TGF-β receptors from their apical to their basolateral sides in order to prevent response to apical stimulation, selectively

impacting TGF-β stimulation of SMAD nuclear accumulation, but not TAZ responses, which remain spatially uniform[162]. This was speculated as a possible mechanism by which polarized tissues could respond to internal TGF-β ligand, while enabling paracrine signaling to other tissues via apically-secreted TGF-β without unintended autocrine effects[163]. Although fibroblasts are not considered polar cells, neurons are. It is unknown whether neurons utilize this mechanism.

The BMP-SMAD pathway similarly is stimulated by an actin-associated protein (angiomotin, or AMOT) that is only present on the apical side of polarized cells, and subject to apical internalization in response to BMP stimulation[164]. AMOT generally regulates cell proliferation, migration, and tight junction maintenance[164], as well as neuron dendritic spine maturation, and its expression increases in hPSC neural differentiation[165]. In 2D hESC circular micropatterns, in many ways analogous to a slice of a spheroid, colony cell polarity and differential response to BMP based on positioning could be dictated by cell density and proximity to the periphery. There, the complexity of positioning cell fates was fundamentally controlled by, first, BMP4 signaling negatively modulated by dynamic receptor localization and NOGGIN (the same mechanism acted on by our K02288), and from that output, signaling with Nodal (the same pathway acted on by our A83-01)[133].

References

1. Needham, D. M., Feldman, D. R. & Kho, M. E. The Functional Costs of ICU Survivorship. *Am. J. Respir. Crit. Care Med.* **183**, 962–964 (2011).
2. Daley, G. Q. The promise and perils of stem cell therapeutics. *Cell Stem Cell* **10**, 740–749 (2012).
3. Blau, H. M. & Daley, G. Q. Stem Cells in the Treatment of Disease. *N. Engl. J. Med.* **380**, 1748–1760 (2019).
4. Nguyen, P. K., Neofytou, E., Rhee, J.-W. & Wu, J. C. Potential Strategies to Address the Major Clinical Barriers Facing Stem Cell Regenerative Therapy for Cardiovascular Disease. *JAMA Cardiol.* **1**, 953 (2016).
5. Hill, E., Boontheekul, T. & Mooney, D. J. Regulating activation of transplanted cells controls tissue regeneration. *Proc. Natl. Acad. Sci. U. S. A.* **103**, 2494–9 (2006).
6. Ho, S. S., Murphy, K. C., Binder, B. Y. K., Vissers, C. B. & Leach, J. K. Increased Survival and Function of Mesenchymal Stem Cell Spheroids Entrapped in Instructive Alginate Hydrogels. *Stem Cells Transl. Med.* **5**, 773–781 (2016).
7. Madl, C. M., Heilshorn, S. C. & Blau, H. M. Bioengineering strategies to accelerate stem cell therapeutics. *Nature* **557**, 335–342 (2018).
8. Park, S. E., Georgescu, A. & Huh, D. Organoids-on-a-chip. *Science* **364**, 960–965 (2019).
9. Chen, C. S., Mrksich, M., Huang, S., Whitesides, G. M. & Ingber, D. E. Geometric control of cell life and death. *Science* **276**, 1425–8 (1997).
10. Duffy, R. M., Sun, Y. & Feinberg, A. W. Understanding the Role of ECM Protein Composition and Geometric Micropatterning for Engineering Human Skeletal Muscle. *Ann. Biomed. Eng.* **44**, 2076–2089 (2016).
11. Downing, T. L. *et al.* Biophysical regulation of epigenetic state and cell reprogramming. *Nat. Mater.* **12**, 1154–1162 (2013).

12. Korff, T. & Augustin, H. G. Integration of endothelial cells in multicellular spheroids prevents apoptosis and induces differentiation. *J. Cell Biol.* **143**, 1341–52 (1998).

13. Jiang, B. *et al.* Spheroidal formation preserves human stem cells for prolonged time under ambient conditions for facile storage and transportation. *Biomaterials* **133**, 275–286 (2017).

14. Wobma, H. M., Liu, D. & Vunjak-Novakovic, G. Paracrine Effects of Mesenchymal Stromal Cells Cultured in Three-Dimensional Settings on Tissue Repair. *ACS Biomater. Sci. Eng.* (2017). doi:10.1021/acsbiomaterials.7b00005

15. Sart, S., Tomasi, R. F.-X., Amselem, G. & Baroud, C. N. Multiscale cytometry and regulation of 3D cell cultures on a chip. *Nat. Commun.* **8**, 469 (2017).

16. Guo, X. *et al.* Tissue engineering the mechanosensory circuit of the stretch reflex arc with human stem cells: Sensory neuron innervation of intrafusal muscle fibers. *Biomaterials* **122**, 179–187 (2017).

17. Bhatia, S. N. & Ingber, D. E. Microfluidic organs-on-chips. *Nature Biotechnology* **32**, 760–772 (2014).

18. Pitsalidis, C. *et al.* Transistor in a tube: A route to three-dimensional bioelectronics. *Sci. Adv.* **4**, eaat4253 (2018).

19. Ronaldson-Bouchard, K. & Vunjak-Novakovic, G. Organs-on-a-Chip: A Fast Track for Engineered Human Tissues in Drug Development. *Cell Stem Cell* **22**, 310–324 (2018).

20. FDA. FDA Researchers to Evaluate 'Organs-on-Chips' Technology | FDA. *CFSAN Constituent Updates* (2017). Available at: https://www.fda.gov/food/cfsan-constituent-updates/fda-researchers-evaluate-organs-chips-technology. (Accessed: 16th March 2020)

21. Pavesi, A. *et al.* A 3D microfluidic model for preclinical evaluation of TCR-engineered T cells against solid tumors. *JCI insight* **2**, (2017).

22. Ingber, D. E. Developmentally inspired human 'organs on chips'. *Dev.* **145**, (2018).

23. Ertl, P., Sticker, D., Charwat, V., Kasper, C. & Lepperdinger, G. Lab-on-a-chip technologies for stem cell analysis. *Trends in Biotechnology* **32**, 245–253 (2014).

24. Titmarsh, D. M., Chen, H., Glass, N. R. & Cooper-White, J. J. Concise Review: Microfluidic Technology Platforms: Poised to Accelerate Development and Translation of Stem Cell-Derived Therapies. *Stem Cells Transl. Med.* **3**, 81–90 (2014).

25. Di Giorgio, F. P., Boulting, G. L., Bobrowicz, S. & Eggan, K. C. Human Embryonic Stem Cell-Derived Motor Neurons Are Sensitive to the Toxic Effect of Glial Cells Carrying an ALS-Causing Mutation. *Cell Stem Cell* **3**, 637–648 (2008).

26. Marchetto, M. C. N. *et al.* Non-Cell-Autonomous Effect of Human SOD1G37R Astrocytes on Motor Neurons Derived from Human Embryonic Stem Cells. *Cell Stem Cell* **3**, 649–657 (2008).

27. Lee, G. *et al.* Modelling pathogenesis and treatment of familial dysautonomia using patient-specific iPSCs. *Nature* **461**, 402–406 (2009).

28. Feigin, V. L. *et al.* Global, regional, and national burden of neurological disorders, 1990–2016: a systematic analysis for the Global Burden of Disease Study 2016. *Lancet Neurol.* **18**, 459–480 (2019).

29. Vignoles, R., Lentini, C., d'Orange, M. & Heinrich, C. Direct Lineage Reprogramming for Brain Repair: Breakthroughs and Challenges. *Trends in Molecular Medicine* **25**, 897–914 (2019).

30. Bongers, K. S. *et al.* Skeletal muscle denervation causes skeletal muscle atrophy through a pathway that involves both Gadd45a and HDAC4. *Am. J. Physiol. - Endocrinol. Metab.* **305**, E907–E915 (2013).

31. Tang, H. *et al.* mTORC1 Promotes Denervation-Induced Muscle Atrophy Through a Mechanism Involving the Activation of FoxO and E3 Ubiquitin Ligases. *Sci. Signal.* **7**, ra18–ra18 (2014).

32. Kress, J. P. & Hall, J. B. ICU-Acquired Weakness and Recovery from Critical Illness. *N.*

Engl. J. Med. **370**, 1626–1635 (2014).

33. Howard, J., Grill, S. W. & Bois, J. S. Turing's next steps: The mechanochemical basis of morphogenesis. *Nature Reviews Molecular Cell Biology* **12**, 400–406 (2011).
34. Song, Y., Soto, J., Chen, B., Yang, L. & Li, S. Cell engineering: Biophysical regulation of the nucleus. *Biomaterials* **234**, 119743 (2020).
35. Ingber, D. E. Mechanical control of tissue growth: Function follows form. *Proceedings of the National Academy of Sciences of the United States of America* **102**, 11571–11572 (2005).
36. Ma, C. H. E. *et al.* Accelerating axonal growth promotes motor recovery after peripheral nerve injury in mice. *J. Clin. Invest.* **121**, 4332–4347 (2011).
37. Scheib, J. & Höke, A. Advances in peripheral nerve regeneration. *Nat. Rev. Neurol.* **9**, nrneurol.2013.227 (2013).
38. Herridge, M. S. *et al.* One-Year Outcomes in Survivors of the Acute Respiratory Distress Syndrome. *N. Engl. J. Med.* **348**, 683–693 (2003).
39. Fu, S. Y. & Gordon, T. Contributing factors to poor functional recovery after delayed nerve repair: prolonged axotomy. *J. Neurosci.* **15**, 3876–3885 (1995).
40. Scheib, J. & Höke, A. Advances in peripheral nerve regeneration. *Nat. Rev. Neurol.* **9**, nrneurol.2013.227 (2013).
41. Arnold, A. S. *et al.* Morphological and functional remodelling of the neuromuscular junction by skeletal muscle PGC-1Î±. *Nat. Commun.* **5**, 1–11 (2014).
42. Stierli, S., Imperatore, V. & Lloyd, A. C. Schwann cell plasticity-roles in tissue homeostasis, regeneration, and disease. *Glia* **67**, 2203–2215 (2019).
43. Mathon, N. F., Malcolm, D. S., Harrisingh, M. C., Cheng, L. & Lloyd, A. C. Lack of replicative senescence in normal rodent glia. *Science (80-.).* **291**, 872–875 (2001).
44. Sanes, J. R. & Lichtman, J. W. DEVELOPMENT OF THE VERTEBRATE NEUROMUSCULAR JUNCTION. *Annu. Rev. Neurosci.* **22**, 389–442 (1999).

45. Liu, W., Wei-LaPierre, L., Klose, A., Dirksen, R. T. & Chakkalakal, J. V. Inducible depletion of adult skeletal muscle stem cells impairs the regeneration of neuromuscular junctions. *Elife* **4**, e09221 (2015).

46. Escher, P. *et al.* Neuroscience: Synapses form in skeletal muscles lacking neuregulin receptors. *Science (80-.).* **308**, 1920–1923 (2005).

47. Fox, M. A. *et al.* Distinct Target-Derived Signals Organize Formation, Maturation, and Maintenance of Motor Nerve Terminals. *Cell* **129**, 179–193 (2007).

48. Kang, S.-B., Olson, J. L., Atala, A. & Yoo, J. J. Functional recovery of completely denervated muscle: implications for innervation of tissue-engineered muscle. *Tissue Eng. Part A* **18**, 1912–20 (2012).

49. Heumann, R., Korsching, S., Bandtlow, C. & Thoenen, H. Changes of nerve growth factor synthesis in nonneuronal cells in response to sciatic nerve transection. *J. Cell Biol.* **104**, 1623–1631 (1987).

50. Willand, M. P. *et al.* Electrical muscle stimulation elevates intramuscular BDNF and GDNF mRNA following peripheral nerve injury and repair in rats. *Neuroscience* **334**, 93–104 (2016).

51. Zhao, C., Veltri, K., Li, S., Bain, J. R. & Fahnestock, M. NGF, BDNF, NT-3, and GDNF mRNA Expression in Rat Skeletal Muscle following Denervation and Sensory Protection. *J. Neurotrauma* **21**, 1468–1478 (2004).

52. Wang, L.-J. *et al.* Neuroprotective Effects of Glial Cell Line-Derived Neurotrophic Factor Mediated by an Adeno-Associated Virus Vector in a Transgenic Animal Model of Amyotrophic Lateral Sclerosis. *J. Neurosci.* **22**, 6920–6928 (2002).

53. Borselli, C. *et al.* Functional muscle regeneration with combined delivery of angiogenesis and myogenesis factors. *Proc. Natl. Acad. Sci. U. S. A.* **107**, 3287–92 (2010).

54. Hoyng, S. A. *et al.* A comparative morphological, electrophysiological and functional analysis of axon regeneration through peripheral nerve autografts genetically modified to

overexpress BDNF, CNTF, GDNF, NGF, NT3 or VEGF. *Exp. Neurol.* **261**, 578–593 (2014).

55. Bollini, S., Gentili, C., Tasso, R. & Cancedda, R. The Regenerative Role of the Fetal and Adult Stem Cell Secretome. *J. Clin. Med.* **2**, 302 (2013).

56. Guenard, V., Kleitman, N., Morrissey, T. K., Bunge, R. P. & Aebischer, P. Syngeneic Schwann cells derived from adult nerves seeded in semipermeable guidance channels enhance peripheral nerve regeneration. *J. Neurosci.* **12**, 3310–3320 (1992).

57. Chen, C.-J. *et al.* Improved Neurological Outcome by Intramuscular Injection of Human Amniotic Fluid Derived Stem Cells in a Muscle Denervation Model. *PLoS One* **10**, e0124624 (2015).

58. Gu, S. *et al.* Application of fetal neural stem cells transplantation in delaying denervated muscle atrophy in rats with peripheral nerve injury. *Microsurgery* **30**, 266–274 (2010).

59. Bryson, J. B. *et al.* Optical control of muscle function by transplantation of stem cell-derived motor neurons in mice. *Science* **344**, 94–7 (2014).

60. Yohn, D. C., Miles, G. B., Rafuse, V. F. & Brownstone, R. M. Transplanted mouse embryonic stem-cell-derived motoneurons form functional motor units and reduce muscle atrophy. *J. Neurosci.* **28**, 12409–18 (2008).

61. Bursac, N., Juhas, M. & Rando, T. A. Synergizing Engineering and Biology to Treat and Model Skeletal Muscle Injury and Disease. *Annu. Rev. Biomed. Eng.* **17**, 217–242 (2015).

62. Kwee, B. J. & Mooney, D. J. Biomaterials for skeletal muscle tissue engineering. *Curr. Opin. Biotechnol.* **47**, 16–22 (2017).

63. Umbach, J. A., Adams, K. L., Gundersen, C. B. & Novitch, B. G. Functional neuromuscular junctions formed by embryonic stem cell-derived motor neurons. *PLoS One* **7**, (2012).

64. Vilmont, V., Cadot, B., Ouanounou, G. & Gomes, E. R. A system for studying mechanisms of neuromuscular junction development and maintenance. *Dev.* **143**, 2464–

2477 (2016).

65. Steinbeck, J. A. *et al.* Functional Connectivity under Optogenetic Control Allows Modeling of Human Neuromuscular Disease. *Cell Stem Cell* **18**, 134–143 (2016).

66. Santhanam, N. *et al.* Stem cell derived phenotypic human neuromuscular junction model for dose response evaluation of therapeutics. *Biomaterials* **166**, 64–78 (2018).

67. Cisterna, B. A. *et al.* Active acetylcholine receptors prevent the atrophy of skeletal muscles and favor reinnervation. *Nat. Commun.* **11**, 1–13 (2020).

68. Happe, C. L., Tenerelli, K. P., Gromova, A. K., Kolb, F. & Engler, A. J. Mechanically patterned neuromuscular junctions-in-a-dish have improved functional maturation. *Mol. Biol. Cell* **28**, 1950–1958 (2017).

69. Luo, B. *et al.* Electrospun nanofibers facilitate better alignment, differentiation, and long-term culture in an: In vitro model of the neuromuscular junction (NMJ). *Biomater. Sci.* **6**, 3262–3272 (2018).

70. Bakooshli, M. A. *et al.* A 3d culture model of innervated human skeletal muscle enables studies of the adult neuromuscular junction. *Elife* **8**, (2019).

71. Osaki, T., Uzel, S. G. M. & Kamm, R. D. Microphysiological 3D model of amyotrophic lateral sclerosis (ALS) from human iPS-derived muscle cells and optogenetic motor neurons. *Sci. Adv.* **4**, eaat5847 (2018).

72. Lindvall, O. Why is it taking so long to develop clinically competitive stem cell therapies for CNS disorders? *Cell Stem Cell* **10**, 660–662 (2012).

73. Henderson, C. E. *et al.* GDNF: a potent survival factor for motoneurons present in peripheral nerve and muscle. *Science (80-.).* **266**, 1062–1064 (1994).

74. Li, R. *et al.* Single injection of a novel nerve growth factor coacervate improves structural and functional regeneration after sciatic nerve injury in adult rats. *Exp. Neurol.* **288**, 1–10 (2017).

75. Fu, S. Y. & Gordon, T. The cellular and molecular basis of peripheral nerve regeneration.

Mol. Neurobiol. **14**, 67–116 (1997).

76. Hoppler, S. & Wheeler, G. N. DEVELOPMENTAL BIOLOGY. It's about time for neural crest. *Science* **348**, 1316–7 (2015).

77. Buitrago-Delgado, E., Nordin, K., Rao, A., Geary, L. & LaBonne, C. NEURODEVELOPMENT. Shared regulatory programs suggest retention of blastula-stage potential in neural crest cells. *Science* **348**, 1332–5 (2015).

78. Mandalos, N. P. & Remboutsika, E. Sox2: To crest or not to crest? *Semin. Cell Dev. Biol.* **63**, 43–49 (2017).

79. Zurkirchen, L. & Sommer, L. Quo vadis: tracing the fate of neural crest cells. *Current Opinion in Neurobiology* **47**, 16–23 (2017).

80. Dupin, E., Calloni, G. W., Coelho-Aguiar, J. M. & Le Douarin, N. M. The issue of the multipotency of the neural crest cells. *Developmental Biology* **444**, S47–S59 (2018).

81. Huang, C.-W. *et al.* The Differentiation Stage of Transplanted Stem Cells Modulates Nerve Regeneration. *Sci. Rep.* (2017).

82. Aquino, J. B. *et al.* In vitro and in vivo differentiation of boundary cap neural crest stem cells into mature Schwann cells. *Exp. Neurol.* **198**, 438–449 (2006).

83. Ho, A. T. V. *et al.* Neural Crest Cell Lineage Restricts Skeletal Muscle Progenitor Cell Differentiation through Neuregulin1-ErbB3 Signaling. *Dev. Cell* **21**, 273–287 (2011).

84. Rios, A. C., Serralbo, O., Salgado, D. & Marcelle, C. Neural crest regulates myogenesis through the transient activation of NOTCH. *Nature* **473**, 532–535 (2011).

85. Mendicino, M., Bailey, A. M., Wonnacott, K., Puri, R. K. & Bauer, S. R. MSC-based product characterization for clinical trials: An FDA perspective. *Cell Stem Cell* **14**, 141–145 (2014).

86. Colter, D. C., Sekiya, I. & Prockop, D. J. Identification of a subpopulation of rapidly self-renewing and multipotential adult stem cells in colonies of human marrow stromal cells. *Proc. Natl. Acad. Sci. U. S. A.* **98**, 7841–7845 (2001).

87. Pittenger, M. F. *et al.* Multilineage potential of adult human mesenchymal stem cells. *Science (80-.).* **284**, 143–147 (1999).

88. Sipp, D., Robey, P. G. & Turner, L. Clear up this stem-cell mess. *Nature* **561**, 455–457 (2018).

89. Sacchetti, B. *et al.* No identical 'mesenchymal stem cells' at different times and sites: Human committed progenitors of distinct origin and differentiation potential are incorporated as adventitial cells in microvessels. *Stem Cell Reports* **6**, 897–913 (2016).

90. Bianco, P. *et al.* The meaning, the sense and the significance: Translating the science of mesenchymal stem cells into medicine. *Nature Medicine* **19**, 35–42 (2013).

91. Bianco, P., Robey, P. G. & Simmons, P. J. Mesenchymal Stem Cells: Revisiting History, Concepts, and Assays. *Cell Stem Cell* **2**, 313–319 (2008).

92. Ladak, A., Olson, J., Tredget, E. E. & Gordon, T. Differentiation of mesenchymal stem cells to support peripheral nerve regeneration in a rat model. *Exp. Neurol.* **228**, 242–252 (2011).

93. Méndez-Ferrer, S. *et al.* Mesenchymal and haematopoietic stem cells form a unique bone marrow niche. *Nature* **466**, 829–834 (2010).

94. Yamazaki, S. *et al.* Nonmyelinating schwann cells maintain hematopoietic stem cell hibernation in the bone marrow niche. *Cell* **147**, 1146–1158 (2011).

95. Takashima, Y. *et al.* Neuroepithelial Cells Supply an Initial Transient Wave of MSC Differentiation. *Cell* **129**, 1377–1388 (2007).

96. Wislet-Gendebien, S. *et al.* Mesenchymal stem cells and neural crest stem cells from adult bone marrow: Characterization of their surprising similarities and differences. *Cell. Mol. Life Sci.* **69**, 2593–2608 (2012).

97. Aydin, B. & Mazzoni, E. O. Cell Reprogramming: The Many Roads to Success. *Annu. Rev. Cell Dev. Biol.* **35**, 433–452 (2019).

98. Amamoto, R. & Arlotta, P. Development-inspired reprogramming of the mammalian

central nervous system. *Science* **343**, (2014).

99. Brumbaugh, J., Stefano, B. Di & Hochedlinger, K. Reprogramming: Identifying the mechanisms that safeguard cell identity. *Development (Cambridge)* **146**, (2019).
100. Herdy, J. *et al.* Chemical modulation of transcriptionally enriched signaling pathways to optimize the conversion of fibroblasts into neurons. *Elife* **8**, (2019).
101. Vierbuchen, T. *et al.* Direct conversion of fibroblasts to functional neurons by defined factors. *Nature* **463**, 1035–1041 (2010).
102. Pang, Z. P. *et al.* Induction of human neuronal cells by defined transcription factors. *Nature* **476**, 220–223 (2011).
103. Karow, M. *et al.* Direct pericyte-to-neuron reprogramming via unfolding of a neural stem cell-like program. *Nat. Neurosci.* **21**, 932–940 (2018).
104. Tanabe, K. *et al.* Transdifferentiation of human adult peripheral blood T cells into neurons. *Proc. Natl. Acad. Sci. U. S. A.* **115**, 6470–6475 (2018).
105. Zhang, L. *et al.* Small Molecules Efficiently Reprogram Human Astroglial Cells into Functional Neurons. *Cell Stem Cell* **17**, 735–747 (2015).
106. Shakiba, N. *et al.* Cell competition during reprogramming gives rise to dominant clones. *Science (80-.).* **364**, (2019).
107. Li, X. *et al.* Small-Molecule-Driven Direct Reprogramming of Mouse Fibroblasts into Functional Neurons. *Cell Stem Cell* **17**, 195–203 (2015).
108. Hu, W. *et al.* Direct Conversion of Normal and Alzheimer's Disease Human Fibroblasts into Neuronal Cells by Small Molecules. *Cell Stem Cell* **17**, 204–212 (2015).
109. Ladewig, J. *et al.* Small molecules enable highly efficient neuronal conversion of human fibroblasts. *Nat. Methods* **9**, 575–578 (2012).
110. Treutlein, B. *et al.* Dissecting direct reprogramming from fibroblast to neuron using single-cell RNA-seq. *Nature* **534**, 391–395 (2016).
111. Zhou, Q., Brown, J., Kanarek, A., Rajagopal, J. & Melton, D. A. In vivo reprogramming of

adult pancreatic exocrine cells to β-cells. *Nature* **455**, 627–632 (2008).

112. Masserdotti, G., Gascón, S. & Götz, M. Direct neuronal reprogramming: Learning from and for development. *Development (Cambridge)* **143**, 2494–2510 (2016).
113. Hanna, J. *et al.* Direct cell reprogramming is a stochastic process amenable to acceleration. *Nature* **462**, 595–601 (2009).
114. Biddy, B. A. *et al.* Single-cell mapping of lineage and identity in direct reprogramming. *Nature* **564**, 219–224 (2018).
115. Francesconi, M. *et al.* Single cell RNA-seq identifies the origins of heterogeneity in efficient cell transdifferentiation and reprogramming. *Elife* **8**, (2019).
116. Holtfreter, J. A study of the mechanics of gastrulation. *J. Exp. Zool.* **95**, 171–212 (1944).
117. Moscona, A. Cell suspensions from organ rudiments of chick embryos. *Exp. Cell Res.* **3**, 535–539 (1952).
118. Pierce, G. B., Dixon, F. J. & Verney, E. Testicular teratomas. I. Demonstration of teratogenesis by metamorphosis of multipotential Cells. *Cancer* **12**, 573–583 (1959).
119. Steinberg, M. S. Mechanism of tissue reconstruction by dissociated cells, II: Time-course of events. *Science (80-.).* **137**, 762–763 (1962).
120. Seeds, N. W. Biochemical differentiation in reaggregating brain cell culture. *Proc. Natl. Acad. Sci. U. S. A.* **68**, 1858–1861 (1971).
121. Honegger, P. & Richelson, E. Biochemical differentiation of aggregating cell cultures of different fetal rat brain regions. *Brain Res.* **133**, 329–339 (1977).
122. Strecker, R. E., Miao, R. & Loring, J. F. *Survival and function of aggregate cultures of rat fetal dopamine neurons grafted in a rat model of Parkinson's disease*. *Exp Brain Res* **76**, (1989).
123. Svendsen, C. N., Caldwell, M. A. & Ostenfeld, T. Human Neural Stem Cells: Isolation, Expansion and Transplantation. *Brain Pathol.* **9**, 499–513 (1999).
124. Keller, G. Embryonic stem cell differentiation: Emergence of a new era in biology and

medicine. *Genes and Development* **19**, 1129–1155 (2005).

125. Watanabe, K. *et al.* Directed differentiation of telencephalic precursors from embryonic stem cells. *Nat. Neurosci.* **8**, 288–296 (2005).

126. ten Berge, D. *et al.* Wnt Signaling Mediates Self-Organization and Axis Formation in Embryoid Bodies. *Cell Stem Cell* **3**, 508–518 (2008).

127. Reubinoff, B. E., Pera, M. F., Fong, C. Y., Trounson, A. & Bongso, A. Embryonic stem cell lines from human blastocysts: Somatic differentiation in vitro. *Nat. Biotechnol.* **18**, 399–404 (2000).

128. Abbott, A. Biology's new dimension. *Nature* **424**, 870–872 (2003).

129. Mueller-Klieser, W. Three-dimensional cell cultures: from molecular mechanisms to clinical applications. *Am. J. Physiol. Physiol.* **273**, C1109–C1123 (1997).

130. Cui, X., Hartanto, Y. & Zhang, H. Advances in multicellular spheroids formation. *J. R. Soc. Interface* **14**, (2017).

131. Warmflash, A., Sorre, B., Etoc, F., Siggia, E. D. & BrivanIou, A. H. A method to recapitulate early embryonic spatial patterning in human embryonic stem cells. *Nat. Methods* **11**, 847–854 (2014).

132. Xue, X. *et al.* Mechanics-guided embryonic patterning of neuroectoderm tissue from human pluripotent stem cells. *Nat. Mater.* **17**, 633–641 (2018).

133. Etoc, F. *et al.* A Balance between Secreted Inhibitors and Edge Sensing Controls Gastruloid Self-Organization. *Dev. Cell* **39**, 302–315 (2016).

134. Ma, Z. *et al.* Self-organizing human cardiac microchambers mediated by geometric confinement. *Nat. Commun.* **6**, 1–10 (2015).

135. Pas, S. P. The rise of three-dimensional human brain cultures. *Nature* **553**, 437–445 (2018).

136. Roy, B. *et al.* Laterally confined growth of cells induces nuclear reprogramming in the absence of exogenous biochemical factors. *Proc. Natl. Acad. Sci. U. S. A.* **115**, E4741–

E4750 (2018).

137. Pasca, A. M. *et al.* Functional cortical neurons and astrocytes from human pluripotent stem cells in 3D culture. *Nat. Methods* **12**, 671–678 (2015).

138. Brunet, T. *et al.* Evolutionary conservation of early mesoderm specification by mechanotransduction in Bilateria. *Nat. Commun.* **4**, 1–15 (2013).

139. Diaz-Cuadros, M. *et al.* In vitro characterization of the human segmentation clock. *Nature* **580**, 113–118 (2020).

140. Tsiairis, C. D. & Aulehla, A. Self-Organization of Embryonic Genetic Oscillators into Spatiotemporal Wave Patterns. *Cell* **164**, 656–667 (2016).

141. Li, Y. *et al.* Compression-induced dedifferentiation of adipocytes promotes tumor progression. *Sci. Adv.* **6**, eaax5611 (2020).

142. Maître, J. L. *et al.* Adhesion functions in cell sorting by mechanically coupling the cortices of adhering cells. *Science (80-.).* **338**, 253–256 (2012).

143. Brodland, G. W. The Differential Interfacial Tension Hypothesis (DITH): A comprehensive theory for the self-rearrangement of embryonic cells and tissues. *J. Biomech. Eng.* **124**, 188–197 (2002).

144. Youssef, J., Nurse, A. K., Freund, L. B. & Morgan, J. R. Quantification of the forces driving self-assembly of three-dimensional microtissues. *Proc. Natl. Acad. Sci. U. S. A.* **108**, 6993–6998 (2011).

145. Maruthamuthu, V., Sabass, B., Schwarz, U. S. & Gardel, M. L. Cell-ECM traction force modulates endogenous tension at cell-cell contacts. *Proc. Natl. Acad. Sci. U. S. A.* **108**, 4708–4713 (2011).

146. Mertz, A. F. *et al.* Scaling of traction forces with the size of cohesive cell colonies. *Phys. Rev. Lett.* **108**, (2012).

147. Krens, S. F. G., Möllmert, S. & Heisenberg, C. P. Enveloping cell-layer differentiation at the surface of zebrafish germ-layer tissue explants. *Proceedings of the National Academy*

of Sciences of the United States of America **108**, E9–E10 (2011).

148. Amack, J. D. & Manning, M. L. Knowing the boundaries: Extending the differential adhesion hypothesis in embryonic cell sorting. *Science* **338**, 212–215 (2012).

149. Manning, M. L., Foty, R. A., Steinberg, M. S. & Schoetz, E. M. Coaction of intercellular adhesion and cortical tension specifies tissue surface tension. *Proc. Natl. Acad. Sci. U. S. A.* **107**, 12517–12522 (2010).

150. Goldblatt, Z. E. *et al.* Heterogeneity Profoundly Alters Emergent Stress Fields in Constrained Multicellular Systems. *Biophys. J.* **118**, 15–25 (2019).

151. Chanet, S. *et al.* Actomyosin meshwork mechanosensing enables tissue shape to orient cell force. *Nat. Commun.* **8**, 1–13 (2017).

152. Campàs, O. *et al.* Quantifying cell-generated mechanical forces within living embryonic tissues. *Nat. Methods* **11**, 183–189 (2014).

153. Dolega, M. E. *et al.* Cell-like pressure sensors reveal increase of mechanical stress towards the core of multicellular spheroids under compression. *Nat. Commun.* **8**, 1–9 (2017).

154. Mohagheghian, E. *et al.* Quantifying compressive forces between living cell layers and within tissues using elastic round microgels. *Nat. Commun.* **9**, 1–14 (2018).

155. Lee, W. *et al.* Dispersible hydrogel force sensors reveal patterns of solid mechanical stress in multicellular spheroid cultures. *Nat. Commun.* **10**, 1–14 (2019).

156. Trepat, X. *et al.* Physical forces during collective cell migration. *Nat. Phys.* **5**, 426–430 (2009).

157. Luxenburg, C. *et al.* Wdr1-mediated cell shape dynamics and cortical tension are essential for epidermal planar cell polarity. *Nat. Cell Biol.* **17**, 592–604 (2015).

158. Takebe, T. & Wells, J. M. Organoids by design. *Science* **364**, 956–959 (2019).

159. Kim, J. *et al.* Geometric Dependence of 3D Collective Cancer Invasion. *Biophys. J.* **118**, 1177–1182 (2020).

160. Birey, F. *et al.* Assembly of functionally integrated human forebrain spheroids. *Nature* **545**, 54–59 (2017).

161. Chambers, S. M. *et al.* Highly efficient neural conversion of human ES and iPS cells by dual inhibition of SMAD signaling. *Nat. Biotechnol.* **27**, 275–280 (2009).

162. Nallet-Staub, F. *et al.* Cell Density Sensing Alters TGF-β Signaling in a Cell-Type-Specific Manner, Independent from Hippo Pathway Activation. *Dev. Cell* **32**, 640–651 (2015).

163. Murphy, S. J. *et al.* Differential trafficking of transforming growth factor-β receptors and ligand in polarized epithelial cells. *Mol. Biol. Cell* **15**, 2853–2862 (2004).

164. Brunner, P. *et al.* AMOT130 drives BMP-SMAD signaling at the apical membrane in polarized cells. *Mol. Biol. Cell* **31**, 118–130 (2020).

165. Zaltsman, Y., Masuko, S., Bensen, J. J. & Kiessling, L. L. Angiomotin Regulates YAP Localization during Neural Differentiation of Human Pluripotent Stem Cells. *Stem Cell Reports* **12**, 869–877 (2019).

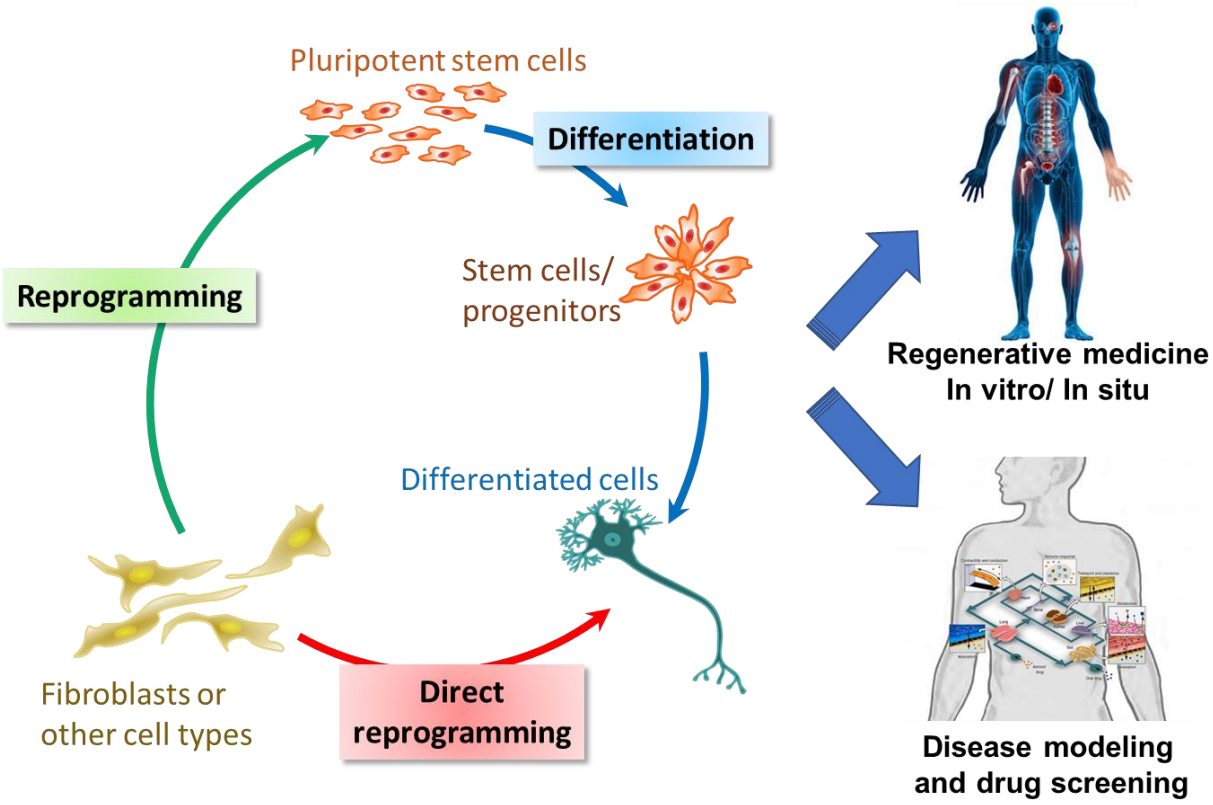

Fig. 1.1. Stem Cells and Cell Reprogramming for Biomedical Applications.

Chapter 2

Engineering Synthetic Neuromuscular Tissue to Guide Stem Cell Therapy

Abstract

Muscular denervation occurs in trauma and motor neuron disease and can cause significant morbidities, but there is currently no effective therapy. Synthetic tissue systems and organs-on-chips, which have been increasingly utilized for preclinical drug screening and disease modeling to isolate mechanisms and decrease costs, have never been applied for screening of stem cell therapies. We developed such a platform here with our synthetic neuromuscular tissue (SyNMT) using micro- and nano- topographical alignment of skeletal muscle cells together with induced pluripotent stem cell (iPSC)-derived motor neurons (MNs), whose axons form NMJs with muscle fibers. As a proof of concept, we assessed the impact of neural crest stem cell (NCSC) and bone marrow-derived mesenchymal stem cell (MSC) spheroids on SyNMT NMJ formation. NCSCs, which originate the peripheral nervous (PN) system and play key roles in early skeletal muscle formation, show enhanced secretion of pro-regenerative growth factors in spheroid form, while MSCs have a vast abundance of clinical trials for neurological and orthopedic indications. We demonstrated that only NCSC spheroids, however, improved SyNMT NMJ formation, and that benefits were contact-dependent. Results were confirmed *in vivo* by intramuscular transplantation of stem cell spheroids into a rat model of PN injury: NCSC spheroids significantly improved functional recovery via electrophysiology and gait analysis, in contrast with MSC spheroids. Interestingly, spheroids also improved long-term *in vivo* survival of NCSCs by over 15 times relative to single cell suspensions, further justifying their use. SyNMT findings were recapitulated with significant tissue improvements in NMJ innervation with NCSCs. Altogether, our work demonstrated the therapeutic potential of NCSCs for neuromuscular regeneration and the application of a synthetic tissue platform in screening cell therapies for regenerative medicine.

Introduction

Muscle denervation has broad etiologies, occurring in trauma and motor neuron diseases such as peripheral nerve injury, amyotrophic lateral sclerosis, spinal muscular atrophy, Guillain-Barre syndrome and Charcot-Marie-Tooth disease, as well as neuropathies of diabetes and alcoholism, degenerative disk disease, pernicious anemia, and Intensive Care Unit (ICU)-acquired weakness. Peripheral nerve (PN) injury alone affects over one million worldwide a year. The resultant motor impact can contribute to consequences ranging from weakness or loss of functional independence, to respiratory failure and mortality, depending on the nerve(s) involved[1–3].

Despite the prevalence and severe implications of muscle denervation, there is currently no effective therapy to overcome the critical gap of nerve injury (1 centimeter [cm] in rodents and 3 cm in humans), and much of the underlying mechanism remains unclear[1–3]. Prognosis varies widely depending on nature of injury or illness, delay before intervention, and patient characteristics[3–6]. While it is critical to accelerate axon growth for nerve regeneration, another major barrier of functional recovery is the reinnervation and the reformation of neuromuscular junctions (NMJs)[4,57]. Regeneration of NMJs is thought to be supported by growth-promoting activity and signaling by the injured nerve, Schwann cells, and target muscle[8,9]. A sustained release of growth factors (GFs) result in limited improvement[10–12], and the release kinetics remain to be optimized[13]. Stem cell transplantation has advantages over synthetic manipulation of these complex and incompletely-understood paracrine programs, as transplanted cells not only are capable of acting as environmentally responsive reservoirs of physiologic levels of paracrine signals, but also offer additional benefits such as cell communications, migration, and differentiation. In the past, cellular therapies for denervation have more often focused on the damaged nerve itself, and have not effectively addressed the unmet needs for NMJ regeneration[3,14,15]. Furthermore, appropriate types and sources of stem cells for NMJ regeneration have not been identified.

Neural crest stem cells (NCSCs) are stem cells that can be differentiated and isolated from embryonic stem cells (ESCs), embryonic neural crest, and induced pluripotent stem cells (iPSCs) and found in low abundance in adult tissues[16–18]. They have the capacity to differentiate into cell types of all three germ layers, including peripheral neurons and Schwann cells[19–21]. Transplantation of NCSCs into nerve conduits, for instance, promotes nerve regeneration and functional recovery through Schwann cell differentiation and trophic signaling[22]. In addition, NCSCs have been discovered to signal to muscle during development, playing critical roles in regulating early and sustainable myogenesis as well as regulating maintenance and differentiation of the skeletal muscle progenitor pool[23,24]. NCSCs thus represent a developmentally relevant cell type for nerve-muscle regeneration. On the other hand, mesenchymal stem cells (MSCs) isolated from bone marrow and other tissues are multipotent adult stem cells which have been widely explored for regeneration, primarily for neurological, cardiovascular, and orthopedic indications, with an abundance of clinical trials[25–29]. It remains to be determined whether NCSCs and MSCs have therapeutic effect on NMJ regeneration.

Recent development of organ-on-a-chip systems has demonstrated promising results in disease modeling and drug screening[30–32]. While various sources of neurons and myoblasts have been used to model the NMJ on unpatterned surfaces[33–38], aligned myoblasts and motor neurons in co-culture improve myodifferentiation and NMJ functional maturation[39–41]. Some of these systems were used to model disease and/or screen drugs[36,41,42]. However, it is not clear whether synthetic neuromuscular tissues and organ-on-chips in general can be used to screen cellular therapies. Here, for the first time, we provide proof of concept for this possibility by using the co-culture of NCSCs or MSCs with synthetic neuromuscular tissue, and verify the *in vitro* results *in vivo*.

Major barriers after *in vivo* transplantation exist for stem cell therapy in the form of low retention and survival rate[31,43–47]. Over 95% of cells typically migrate out of the target site within 24-48 hours, and of those remaining about 99% die by 4-6 weeks, leaving just 0.05% of the

original delivery to exert effects[45]. Besides the co-injection of biomaterials, cell spheroids can robustly enhance cell viability, including *in vivo*; additionally, spheroidal culture helps preserve phenotype and function of stem cells and increase protein synthesis[48–51]. Following this rationale, we sought to investigate whether stem cell spheroids could promote NMJ formation in both an *in vitro* synthetic neuromuscular tissue model and an *in vivo* model of denervation injury.

Results

Micro and Nano-topographical Cues Improved Cell Organization in a Synthetic Neuromuscular Tissue (SyNMT)

Our SyNMT is based on our previous approach to use micropatterned surfaces or scaffolds to induce myotube alignment[52,53]. We developed a simple and easily replicable synthetic tissue system with a geometrically-patterned scaffold and readily interchangeable components, in which muscle and neurons can align, interact, and form junctions. Stem cell therapeutics of interest may easily be added, and different aspects of stem cell function isolated and their effects on the system studied.

We first compared not only myotubes[52,53] and motor neurons alone[54,55], but also in co-culture for the formation of NMJs on microgrooves versus electrospun nanofiber scaffolds. PDMS microgrooves of physiological stiffness[56] (storage modulus of 9.14-9.87 kPa) were cast from silicon wafers as previously[52,53] (Fig. 2.1A-B). C2C12 myotubes grew and aligned (Fig. 2.1C), and subsequently formed NMJs within days of co-culture with iPSC-derived motor neurons (MNs) (Fig. 2.1D-G).

In addition, nanofiber scaffolds were electrospun[52] (Fig. 2.1H) and then aligned under stretch (Fig. 2.1I). Nanofibers enabled aligned myotube growth and NMJ formation for both C2C12s (Fig. 2.1J-N) and primary chemically induced myogenic cells (ciMCs; Fig. 2.1P-S, Suppl. Fig. 2.1). Interestingly, although both successfully aligned neuromuscular cells, the nanotopography of electrospun scaffolds was found superior in enabling development of

myotubes of more robust morphology, with a 1.5-fold increase in myotube width relative to ciMCs induced and cultured on microgrooves ($p<0.05$, Fig. 2.1O). As such, electrospun scaffolds were used for stem cell therapy screening thereafter. For increased relevance to normal physiology, we chose to use the primary ciMCs for cell screening.

Derivation and Characterization of NCSCs and Spheroids

We derived NCSCs from iPSCs following previous protocol[22] (Fig. 2.2A). All NCSCs derived from different iPSC lines were expandable. iPSC-NCSCs homogeneously expressed NCSC markers p75 neurotrophin factor (p75), HNK1/N-CAM/CD57, AP2, and nestin (Fig. 2.2B-E)[57–59]. In addition, iPSC-NCSCs were multipotent and could differentiate into cell types of ectoderm (e.g., Schwann cells, peripheral neurons) (Fig. 2.2F-I) and mesoderm (chondrocytes, adipocytes, and osteoblasts) (data not shown). Peripheral neurons were positive for neurofilament β-III tubulin (TUJ1) and peripherin (Fig. 2.2F-G). Schwann cells were positive for glial fibrillary acidic protein (GFAP) and S100β (Fig. 2.2H-I).

Spheroidal culture in other cell types helps preserve phenotype and enhanced functionality, such as differentiation capacity and protein secretion[48,49,60,61]. We wanted to evaluate the impact, if any, of spheroid formation on NCSCs. Spheroid formation with diameters from 100 to 250 μm was studied in 50 μm increments, as controlled by seeding cell suspension density (200-2,000 cells/spheroid). Live and dead staining showed that spheroids with 500 and fewer cells, a diameter approximately equal to the 150-μm diffusion limitation found in literature[62,63], had negligible cell death rate (Fig. 2.2J) and, furthermore, retained homogenous expression of p75 three days after spheroid formation (Fig. 2.2K).

PN regeneration is thought to be supported by growth-promoting activity and signaling by the injured nerve, Schwann cells, and target muscle. Among secreted signals thought to be important are ciliary neurotrophic factor (CNTF)[4,64], basic fibroblast growth factor (bFGF)[65,66], and glial cell line–derived neurotrophic factor (GDNF)[4,16,67], among many others[17,18,68]. We found that

spheroidal culture (Fig. 2.2L; bars in orange and red) improved the secretion of such important GFs in neuromuscular function when compared with single cell seeding (bars in blue) even with encapsulation, despite the higher rate of cell proliferation in 2D.

NCSCs But Not MSCs Improved NMJ Formation in SyNMT

An ongoing question in cell therapies is whether beneficial effects are a result of cell replacement or other signaling effects. Research into the mechanisms behind benefits of stem cell transplantation, for instance, point increasingly towards the importance of modulatory trophic signaling beyond direct replacement of affected cells at sites of injury[69].This distinction was thus of great interest in our study. NCSC spheroids were prepared and seeded into the SyNMT system either via co-culture or Transwell to isolate paracrine from contact-dependent effects. We evaluated NMJ formation after four days of co-culture because NMJ formation has reported to occur at this time[33].

At a gross level, NCSCs in co-culture appeared to enable improved axonal growth and extension as well as myogenic cell expansion relative to controls, in contrast to NCSC conditioned media, which appeared to improve axonal morphology to a lesser extent, with minimal differences in myotube abundance relative to controls. Magnified evaluation of NMJ formation revealed quantifiable improvements with NCSCs at the micro-level, with over 4-fold greater innervated junction formation seen with NCSC co-culture ($p<0.05$, Fig. 2.3B), but insignificant differences with NCSC spheroid conditioned media (CdM) via Transwell, relative to controls. STEM121 staining of human cytoplasm suggested tendencies of NCSCs to associate and align with axons (Suppl. Fig. 2.2), which could be a possible reason for contact-dependency being necessary for NCSC co-culture improvements.

Human bone marrow (BM)-derived MSCs have been shown to generate BM stroma (including adipocytes, local functional organization of new blood vessels) that support hematopoiesis, but are neither myogenic nor neurogenic[25–27]. Immunomodulatory roles for MSCs

also exist but are incompletely understood[26]. Given their purported utility for, it seems, almost all disease[70], we were interested in whether they might have an effect on NMJ formation. MSC spheroids were prepared and seeded in the same way as NCSCs. Although axonal morphology appeared similarly improved with MSCs, muscle morphology did not appear as robust (Fig. 2.3A). Translated into quantifiable NMJ effect, insignificant improvements were seen relative to controls even with co-culture (Fig. 2.3B). In short, the SyNMT system suggested that NCSCs had advantage over MSCs for NMJ formation and could be a candidate stem cell for NMJ regeneration.

NCSC Spheroids Drastically Improved Cell Survival In Vivo

Given the SyNMT-predicted improvements, NCSC *in vivo* results were of great interest. We first wanted to examine whether spheroidal culture could also indeed improve on the major clinical barriers of cell survival and retention relative to classical transplantation of single-cell suspensions. Luciferase-expressing NCSCs were used for noninvasive cell fate tracking. Using a rat model of sciatic nerve injury, NCSCs were transplanted intramuscularly into the gastrocnemius at the insertion of the sciatic nerve as either spheroids or single cell suspension. Although robust survival was seen in both modalities prior to transplantation (Suppl. Fig. 2.3), fate was starkly different following transplantation. Whereas NCSCs transplanted in single cell suspensions rapidly died off within three days, spheroids showed bioluminescent (Fig. 2.4A) as well as histological evidence (Fig. 2.4C) of engraftment and proliferation, with flux signal equilibrating after 2.5 weeks at approximately 31% of original levels (Fig. 2.4B). NCSCs were found to associate with various structures (Fig. 2.4C). Although our focus was on the 4-week time frame, signal remained stable throughout nine weeks (31.5±0.06% at nine weeks) before conclusion of the trial. Results definitively supported the use of NCSC spheroids moving forward.

NCSC Spheroids, but not MSCs, Enhanced Functional Recovery Following Denervation Injury

For functional evaluation, non-bioluminescent NCSCs and MSCs were formed into spheroids and again transplanted into the same injury model. Functional recovery was assessed at 4 weeks. Electrophysiology revealed a remarkable 2.40-fold recovery of NCSC-injected versus control saline-injected animals (Fig. 2.5A, $p<0.05$). Similarly, walking track analysis of gait, arguably the most functional readout of metrics, revealed significant 1.12-fold improvement in NCSC- versus saline-injected animals using the sciatic functional index[71] (SFI, Fig. 2.5B, $p<0.05$). In stark contrast with NCSC spheroids, and consistent with SyNMT predictions, all functional metrics following MSC transplantation were insignificantly different from controls ($p>0.7$, Fig. 2.5C-D).

NCSCs Promoted Microstructural Recovery.

We then examined the histological characteristics of regenerated muscle. Hematoxylin and eosin (H&E) stain of sectioned muscle showed a slight increase in muscle fiber area in NCSC-injected animals (Fig. 2.6C), in comparison to saline-injected limbs (Fig. 2.6B) ($p\approx0.25$; Fig. 2.6D). Uninjured limb muscle fibers are shown for reference (Fig. 2.6A). Muscle fibers had few centrally located nuclei, suggesting that any benefit was due not to regrowth of muscle, but maintenance of existing mass.

At the neurophysiological level, axons of pre-synaptic motor neurons were labeled with antibody for neurofilament-medium (NF-M), while post-synaptic acetylcholine receptors were stained with α-bungarotoxin (α-Btx), with overlap deemed as innervation[72]. NCSC-treated animals (Fig. 2.6G) had 2.73-times higher ratios of innervated NMJs than saline controls (Fig. 2.6F) ($p<0.05$, Fig. 2.6H). Long-term axonal reinnervation was very apparent at nine weeks (Suppl. Fig. 2.4). Staining for cell fate after four weeks revealed the vast majority of transplanted NCSCs were neither $S100\beta^+$ myelinating nor $GAP43^+$ nonmyelinating Schwann cells, nor $p75^+$ NCSCs in identity (Suppl. Fig. 2.5).

Discussion

Here, we engineer scaffolds with topographically aligned myotubes and MNs in our SyNMT platform, which enables targeted assessment of ordered NMJ formation and easily isolates different aspects of stem cell therapies potentially responsible for therapeutic effect. Furthermore, we show the feasibility and ease of utilizing a novel and highly accessible source of primary myogenic cells for such applications, in combination with a well-characterized source of iPSC-derived MNs[73]. We were able to assess the effects of two different stem cell therapies on axonal sprouting, NMJ formation, and myotube health, which would not be possible in typical 2D single-cell-type cultures. SyNMT predicted the regenerative efficacy of NCSC spheroids, which significantly improved NMJ formation and as spheroids, pose advantages in significantly improved *in vivo* survival. This was contrasted with MSCs, which SyNMT predicted to be ineffective despite their distinction of being the most abundantly studied stem cells in clinical trials[29]. Regenerative capacities were confirmed *in vivo* functionally and histologically, demonstrating this first-of-its-kind application of a synthetic tissue platform for screening stem cell therapies.

We found that the nanotopography of aligned electrospun fibers further improved on the benefits of neuromuscular alignment[39–41] over microtopography of patterned microgrooves, consistent with the role of nanotopography in directing development and function of various cell types[74–76]. A root cause, aside from native physiology of skeletal muscle, may be the increase of contact points when myoblasts are aligned, facilitating fusion. We have shown previously that nanofeatures better improve elongation of C2C12 myotubes and suppress myoblast proliferation[52], and also facilitate axonal extension[54]. ciMCs similarly displayed greater widths and striation on nanoscale rather than on microscales (Fig. 2.1), which are more similar to native nanoscale fibrous hallmarks of extracellular matrix (ECM)[31,77]. Improved skeletal muscle and axonal morphology lend themselves to enhanced NMJ formation, which is why we chose to proceed with the electrospun fibers.

Transplantation of spheroids rather than conventional single cell suspensions enabled

robust long-term survival and engraftment up to nine weeks, which otherwise would have been limited to under four days (Fig. 2.4A-B). Spheroidal culture can prevent anoikis-mediated death of single cells in suspension and enhances the survival of many cell types of varying maturity, particularly of the neural lineage[48–50,78], which may have assisted in NCSC survival.

Integration of isolated NCSC secretome results with SyNMT results highlight the value of such synthetic tissue systems. Formation of NMJs is dependent on nerve terminal-derived signals to underlying basal lamina and muscle, and is further assisted by though not dependent on muscle-secreted factors[79], so cells that could mediate this interplay would be uniquely poised to facilitate neuromuscular regeneration after PN injury. Relative to single-cell-plated conditions in flat 2D cultures, NCSC spheroids *in vitro* secreted increased pro-regenerative growth factors acting for neurogenesis or axonal health and myogenesis (IGFBP-2[66], VEGF[80]), and vascularization (IGFBP-2[66], VEGF[80], PLGF[81], PDGF-AA[66]), immunomodulation (GDF-15[82]), and maintenance of stem cell precursor proliferation (EGF[83,84]) (Fig. 2.2L). Given the enhancements in regenerative GF secretion, we could have proceeded to isolate paracrine factors, such as with encapsulation of spheroids to enable physical protection of cells while allowing for signaling, as we had developed a method for conformal spheroid encapsulation in anticipation that would have allowed for minimal GF trapping. With SyNMT, we were able to determine, however, that NCSC conditioned media alone was insufficient to recapitulate the neuromuscular benefits seen with NCSC spheroid co-culture, and thus the likely contact dependence of these pro-regenerative effects *in vivo* as well. Timelines suggested that NCSC differentiation cannot be solely responsible for the benefits, as four days is too early for differentiation to occur[22,85,86], yet benefits were already seen**.** We cannot exclude the possibility, however, of differentiation having a contribution long-term to beneficial effects *in vivo*, although NCSCs did not associate consistently with specific tissue structures (Fig. 2.4C, Suppl. Fig. 2.4).

Cellular therapies for denervation have more often focused on the damaged nerve separate from the target muscle, despite the discovery that muscle innervation by the nerve is

key for functional recovery[5,87,88], and remain limited by supply, efficacy, transplant innervation/perfusion, and/or *in vivo* cell retention, whether through migration or survival[89–93]. As both SyNMT and the biology of development predicted, NCSCs were highly migratory after transplantation, though luminescence studies indicated they remained in the general upper portion of the gastrocnemius and did not seed elsewhere in the body. Functional readouts of rat reinnervation by electrophysiology and gait confirmed predictions of SyNMT for NCSCs versus MSCs. In MSCs, we saw no overt muscle, nerve, or NMJ effects in SyNMT and *in vivo*. Bone marrow-derived MSCs support *in vivo* hematopoiesis, with possible immunomodulatory functions, and associate with blood vessel walls, but are neither myogenic nor neurogenic[25–27]. These more nonspecific secondary effects of MSCs may explain their lack of therapeutic benefit here.

In contrast, due to NCSC-transplanted animals' functional improvement, we took tissue assessment a step further and found improved NMJ innervation consistent with SyNMT. NCSCs originate Schwann cells, which dedifferentiate after PN injury to become the drivers of the remarkable regeneration of which peripheral nerves are capable[59]. NCSCs, while distinct from post-injury de-differentiated Schwann cells, may pose sufficient similarities to assist the natural regenerative processes[94]. It is possible that NCSCs lend contact-mediated support to axons as known to occur with Schwann-lineage cells and axons *in vivo*[59,95], as we witnessed the tendency for their proximity in SyNMT (Suppl. Fig. 2.1) as well as qualitative increases in axonal density and health with their co-culture (Fig. 2.3A).

NCSCs are, furthermore, critical signalers via Neuregulin1 (Nrg1) and/or NOTCH ligand Delta1 expression to muscle progenitor cells (MPCs) in early muscle formation, enabling balanced, sustainable, and progressive MPC differentiation for appropriate myogenesis[19–21,23,24]. Expression of ERBB3, which signals primarily through Nrg1, is a marker of myogenic versus skeletogenic progenitors differentiated from human PSCs[96]. NCSC sensory nerve and Schwann cell derivatives control arterial differentiation and patterning as well[97]. With these facts in mind, we can speculate that pathways that facilitate myogenesis and vascularization during

development may be recapitulated by NCSCs in maintenance or regeneration of neuromuscular function after nerve injury. At the molecular level, developmental neuregulin and Delta1 signaling may underlie contact-mediated benefits found here. Overall, the regenerative interactions of muscle and nerve after denervation are not well established, but are primed for future exploration. Whether NCSCs recapitulate developmental roles in promoting muscle progenitor expansion after adult injury, or even of Schwann cell (whether de-differentiated or not) signaling in similar ways to promote muscle progenitor expansion, is uncertain but of great future interest.

Breakthroughs in therapeutic biomedicine to make clinical impact have been on the scale of decades (e.g., gene therapy, monoclonal antibodies, and even HSCs)[47]. Given the recency of many stem cell therapeutics, including patient-derived cells for personalized medicine, it may take many years yet before their practical use in clinical medicine. Use of systems like SyNMT to bridge into *in vivo* studies may accelerate the progress of stem cell therapies towards clinically relevant regeneration.

Materials & Methods

PDMS Microgroove Fabrication

Microgrooves were fabricated as previously[52,53]. Microgrooves were cut to size for placement in 24-well dishes and then sonicated in 70% ethanol for 15 minutes for sterilization, followed by several phosphate-buffered saline (PBS) washes before air-drying. Chips were sterilely placed in 24-well dishes groove-side up with forceps. Plasma treatment was followed by overnight hESC-qualified Matrigel (Corning; #354277) coating before cell seeding.

Electrospinning Nanofibers

Nanofiber scaffolds were electrospun from a poly-l-lactide acid (PLLA) solution as before[52]. Fibers were aligned by stretching in 60^{o}C water bath. Stretched fibers were allowed to dry before cutting to size and placing into 24-well dishes. Scaffolds were sterilized by soak in 70%

ethanol for 15 minutes followed by several PBS washes before air-drying. Plasma treatment was followed by overnight Matrigel coating before cell seeding. Nerve conduits were electrospun hollow tubes composed of 2:1 Poly(lactide-co-caprolactone) [PLCL]: PLLA), 10-mm in length with a 2-mm inner diameter, as described in our previous publications[22,86].

iPSC Culture and NCSC Derivation

We used two sources of iPSCs to test different NCSC lines. The first generated an iPSC line ourselves from human skin fibroblasts (Thermo Fisher, C0135C) without the integration of reprogramming factors into the genome, as previously[22] (Fig. 2.1A). The second used human iPSCs from a collaborator (Joseph Wu, Stanford). To derive NCSCs, iPSCs were grown as embryoid body (EB)-like floating cell aggregates in suspension culture for six days in serum-free NCSC induction medium consisting of Knockout DMEM/F12 (Gibco), StemPro neural supplement (Invitrogen), 20 ng/ml basic fibroblast growth factor (bFGF; Peprotech, 100-18B) and 20 ng/ml epidermal growth factor (EGF; Peprotech, AF-100-15). EBs were then allowed to adhere to Matrigel-coated dishes, and dissociated and replated after rosette formation. NCSCs were purified by magnetic-activated cell sorting (MACS, Miltenyi Biotec) for p75 (Miltenyi Biotec, #130-097-127) positivity and SSEA-4 negativity (Miltenyi Biotec, #130-097-855), twice each. ROCK inhibitor Y27632 2HCL (Fisher, 50-863-7) was used with passaging. Differentiation assays were performed as previously[22]. For expression of luciferase, cells were transduced with EF1α-Fluc2-PGK-Puro lentiviral vector (UCLA Vector Core) in OptiMem media (Gibco; 31985062) with Protamine Sulfate (1:600) for 24 hours, followed by expansion in normal NCSC media for another two days prior to a week of puromycin selection. Cells were used or frozen thereafter.

NCSC Spheroid Characterization

Spheroid formation was scaled up via centrifugation method in microwell plates (Aggrewell™), with size control via seeding cell suspension density. Survival was assessed by

live-dead stain (Invitrogen, R37601), and the *in vitro* secretome after five days was assessed with a commercially available assay of 40 common GFs (Quantibody Assay 1, RayBiotech) on the conditioned medium. Custom-written MATLAB code was developed to analyze and interpret assay densitometry calibrated to a standard curve.

MSC Culture

Human MSCs were obtained without identifying patient information from the Texas A&M University Health Science Center College of Medicine, which follows the Tulane Center for Gene Therapy protocol for cell isolation. In short, they isolated nucleated cells from bone marrow aspirates of the iliac crest of normal, healthy adult volunteers by Ficoll/Paque density gradient, resuspended in CM (alpha-MEM, 20% FBS, P/S), and cells adherent after 24 hours were collected as "MSCs"[99] for distribution. Cells were not used beyond passage 6 for our experiments for consistent phenotype[100].

SyNMT Assembly & Culture

C2C12s or ciMCs were seeded onto Matrigel-coated microgrooves or nanofibers in expansion medium consisting of Dulbecco's Modified Eagle Medium (DMEM; Gibco, 11965), 10% fetal bovine serum (FBS; Gibco, 26140079), and 1% penicillin/streptomycin (P/S; GIBCO, 15140122), with chemicals (20 μM Forskolin, 20 μM RepSox, 50 μg/ml ascorbic acid [Sigma], and 50 ng/ml bFGF [Stemgent Inc.]) in the case of ciMCs. The media was changed once every 2-3 days. Two days after seeding, C2C12s were switched over to low-serum media (DMEM, 2% horse serum media [HSM], 1% P/S) to facilitate fusion and differentiation into myotubes. iPSC-derived GFP^+-MNs were prepared as described[73,98], with smoothened agonist (SAG, 1uM) instead of puromorphamine and maintenance media of the core MN media with 1x N2, and 10ng/ml each of BDNF, GDNF and CNTF. MNs were seeded onto myotubes after five days. If stem cells were added, the spheroids were seeded within the next day after MN adhesion either with the NM

culture, or in Matrigel-coated 0.4-μm Transwells (Falcon, #353095). Myotubes and MNs were co-cultured for a total of four days before immunohistochemical analysis.

Rat Surgery

All experimental procedures with animals were approved by the UCLA ACUC committee, and carried out according to the institutional guidelines. Adult female athymic nude rats (NIH rnu, Charles River) weighing 200-250g and aged 2 months were used. Sharp surgical scissors were used to remove 1cm of the left sciatic nerve between the sciatic notch and the trifurcation of the sciatic nerve under surgical microscope. The nerve gap was bridged with a hollow electrospun tube fabricated in-house (10mm in length, 2mm inner diameter, 2:1 Poly(lactide-co-caprolactone) [PLCL]:Poly-l-lactide acid [PLLA]) using nylon sutures on each side to anchor the tube to the connective tissue of the epineurium, as described in our previous publications.

Sampling of NCSCs for representative Live-Dead assay was used day-of surgery to assess viability. After nerve transection and bridging surgery, one million cells were resuspended prior to delivery in 50μL sterile PBS, front-loaded into a 1mL syringe, then injected into the affected gastrocnemius muscle via insertion of 19-caliber needle into the gastrocnemius muscle at the insertion point of the tibial branch of the sciatic nerve.

In Vivo Imaging

Rats were anesthetized with isoflurane in a holding chamber, injected with luciferin (150 mg/kg, IP), then moved to the optical scanner (IVIS Lumina II, Perkin Elmer) and after 7 minutes imaged dorsal-side up (10-minute exposure) under maintenance anesthesia on isoflurane. Flux analysis was conducted with Living Image software (Caliper LifeSciences).

Rat Functional Analysis

Functional recovery was assessed by gait video analysis to calculate sciatic function index (SFI), electrophysiological testing, and muscle wet weight, performed as previously[22]. SFI is defined here as $= -38.3 * \frac{EPL-NPL}{NPL} + 109.5 * \frac{ETS-NTS}{NTS} + 13.3 * \frac{EIT-NIT}{NIT} - 8.8$, where PL=print length= distance from heel to third toe, TS=toe spread= distance from first to fifth toe, ITS= intermediary TS= distance from second to fourth toe, N=normal, E=experimental[71]. Briefly, rats were videotaped in slow-motion from below, walking across a transparent glass tunnel, and the paw print video stills were analyzed for appropriate print measurements for SFI.

PolyVIWE16 data acquisition software (Astro-Med, Inc.) was used to acquire data for electrophysiology analysis. Electrical stimuli were applied to the native sciatic nerve trunk at the point 1-mm proximal to the graft suturing point, and CMAPs recorded in the gastrocnemius belly from 1V to 12V or until a supramaximal CMAP was reached. Normal CMAPs from the un-operated contralateral side of sciatic nerve were recorded for comparison. The amplitude, response latency, and conduction velocity of the action potential were used to quantify the functional recovery of the regenerated peripheral nerve, with electrophysiological recovery rate defined as the ratio of the compound muscle action potential (CMAP) between the injured and contralateral normal hindlimb. Gastrocnemius muscles were then collected and wet weight recorded before fixing, along with nerve, in 4% paraformaldehyde at 4°C for future histological analysis.

Tissue Histology & Quantification

Gastrocnemius muscle was cryosectioned for hematoxylin and eosin (H&E) staining and immunostaining. Representative slices from throughout the gastrocnemius muscle were used for quantification and analysis. Muscle fiber area was quantified using ImageJ software. Junction innervation was evaluated by identifying all *en face* junctions within these sections as stained by α-Btx that colocalized with axons as stained by NF-M (see antibodies and reagents below).

Percent innervation was calculated by dividing the number of these junctions innervated with neurofilament by the total number of whole *en face* junctions, and normalized by animal to the innervation ratio of the uninjured side, calculated the same way.

Immunofluorescent Staining and Microscopy

SyNMT samples were fixed in cold 4% paraformaldehyde (PFA; Electron Microscopy Sciences, #15710) for 15 minutes. For immunohistochemical analysis, washes were performed with 0.1% BSA in PBS (BSA; Miltenyi Biotec, #130-091-376) rather than PBS, which was used for all other non-SyNMT samples. Fixed samples were rinsed with PBS and permeabilized and blocked with 0.5% Triton X-100 (Sigma, T8787) in PBS with 5% normal donkey serum (NDS; Jackson Immunoresearch, 017000121) for 30 minutes at room temperature (RT). Primary antibodies were diluted in blocking solution and applied overnight at 4^{o}C. After three five-minute PBS washes, secondary antibodies were applied diluted in 4% NDS, together with 4',6-diamino-2-phenylindole (DAPI; Invitrogen, D3571) for one hour at RT. Secondary antibodies conjugated to Alexa Fluor® 488 or Alexa Fluor® 546 (Life Tech, Thermo Fisher) were used. Samples were epifluorescently imaged with a Zeiss Axio Observer Z1 inverted fluorescence microscope or imaged with on the Leica TCS-SP8-SMD inverted confocal microscope. Images were analyzed with ImageJ.

Primary antibodies used were: GFP (Abcam, ab13970), MF-20 (mouse, DSHB), and/or STEM121 (mouse, Takara Bio, #Y40410), nestin (Chemicon), AP2 (DSHB), p75 (Abcam; Millipore MAB5386), HNK1 (Sigma, C6680), Tuj1 (Covance), peripherin (Chemicon), glial fibrillary acid protein (GFAP; Chemicon), S100β (Abcam, ab52642), laminin (Sigma, L9393), human nuclear antigen (HNA; mouse, Millipore, MAB1281), neurofilament-medium (NF-M; ab9034, ab7794), GAP-43 (Novus, NBP1-41123SS).

Secondary antibodies used were from Life Tech (Thermo Fisher): donkey anti-mouse 488 (A21202), donkey anti-mouse 546 (A10036), donkey anti-rabbit 488 (A21206), donkey anti-rabbit

546 (A10040), donkey anti-rabbit 647 (A31573), goat anti-chicken 488 (A-11039), donkey anti-sheep 647 (A21448).

Statistics

Data were reported as mean ± standard error of the mean (S.E.M.). The sample size necessary to detect significant effect was estimated by using Power and Precision statistical software (Englewood, NJ) with the following information: minimum significant effect to be detected, data variation, power (0.8) and Type I error rate (0.05). For two-sample comparison, two-tailed Student's t-test was used. For multiple-sample comparison, analysis of variance (ANOVA) was performed to detect whether a significant difference existed between groups with different treatments, and a multiple comparison procedure Bonferonni correction used for post-analysis to identify where the differences existed. A p-value of 0.05 indicated significance, unless otherwise noted.

Acknowledgments

We would like to thank Dr. Joseph Wu (Stanford) for a line of iPSCs; Dr. Richard Wang from the UCLA DNA Microarray Core for his helpful microarray scanning assistance; Texas A&M University Health Science Center College of Medicine for deriving the MSCs and Dr. Andrea Kasko and Dr. Sam Norris from her lab for sharing them; the UCLA California Nanosystems Institute (CNSI) Advanced Light Microscopy/Spectroscopy (ALMS) Facility, particularly its staff Matt Schibler and Dr. Laurent Bentolila; Dr. April Pyle for her insightful advice, as well as Dr. Michael Hicks from her lab for generously sharing transfection reagents and muscle freezing and sectioning methods; the UCLA IMT Core/ Vector Core, particularly Janet Treger, which is supported by CURE/P30 DK041301; Dr. Dino Di Carlo's lab for kindly lending us their color camera microscope; and the CNSI Crump Preclinical Imaging Technology Center and the great help of its staff Dr. Tove Olafsen, Dishan Abeydeera, and Dr. Jason Lee.

References

1. Bongers, K. S. *et al.* Skeletal muscle denervation causes skeletal muscle atrophy through a pathway that involves both Gadd45a and HDAC4. *Am. J. Physiol. - Endocrinol. Metab.* **305**, E907–E915 (2013).
2. Tang, H. *et al.* mTORC1 Promotes Denervation-Induced Muscle Atrophy Through a Mechanism Involving the Activation of FoxO and E3 Ubiquitin Ligases. *Sci. Signal.* **7**, ra18–ra18 (2014).
3. Kress, J. P. & Hall, J. B. ICU-Acquired Weakness and Recovery from Critical Illness. *N. Engl. J. Med.* **370**, 1626–1635 (2014).
4. Ma, C. H. E. *et al.* Accelerating axonal growth promotes motor recovery after peripheral nerve injury in mice. *J. Clin. Invest.* **121**, 4332–4347 (2011).
5. Scheib, J. & Höke, A. Advances in peripheral nerve regeneration. *Nat. Rev. Neurol.* **9**, nrneurol.2013.227 (2013).
6. Herridge, M. S. *et al.* One-Year Outcomes in Survivors of the Acute Respiratory Distress Syndrome. *N. Engl. J. Med.* **348**, 683–693 (2003).
7. Fu, S. Y. & Gordon, T. Contributing factors to poor functional recovery after delayed nerve repair: prolonged axotomy. *J. Neurosci.* **15**, 3876–3885 (1995).
8. Scheib, J. & Höke, A. Advances in peripheral nerve regeneration. *Nat. Rev. Neurol.* **9**, nrneurol.2013.227 (2013).
9. Arnold, A. S. *et al.* Morphological and functional remodelling of the neuromuscular junction by skeletal muscle PGC-1Î±. *Nat. Commun.* **5**, 1–11 (2014).
10. Kang, S.-B., Olson, J. L., Atala, A. & Yoo, J. J. Functional recovery of completely denervated muscle: implications for innervation of tissue-engineered muscle. *Tissue Eng. Part A* **18**, 1912–20 (2012).
11. Heumann, R., Korsching, S., Bandtlow, C. & Thoenen, H. Changes of nerve growth factor synthesis in nonneuronal cells in response to sciatic nerve transection. *J. Cell Biol.* **104**,

1623–1631 (1987).

12. Borselli, C. *et al.* Functional muscle regeneration with combined delivery of angiogenesis and myogenesis factors. *Proc. Natl. Acad. Sci. U. S. A.* **107**, 3287–92 (2010).
13. Hoyng, S. A. *et al.* A comparative morphological, electrophysiological and functional analysis of axon regeneration through peripheral nerve autografts genetically modified to overexpress BDNF, CNTF, GDNF, NGF, NT3 or VEGF. *Exp. Neurol.* **261**, 578–593 (2014).
14. Gordon, T., Tyreman, N. & Raji, M. A. The Basis for Diminished Functional Recovery after Delayed Peripheral Nerve Repair. *J. Neurosci.* **31**, 5325–5334 (2011).
15. Schweickert, W. D. & Hall, J. ICU-Acquired Weakness. *Chest* **131**, 1541–1549 (2007).
16. Henderson, C. E. *et al.* GDNF: a potent survival factor for motoneurons present in peripheral nerve and muscle. *Science (80-.).* **266**, 1062–1064 (1994).
17. Li, R. *et al.* Single injection of a novel nerve growth factor coacervate improves structural and functional regeneration after sciatic nerve injury in adult rats. *Exp. Neurol.* **288**, 1–10 (2017).
18. Fu, S. Y. & Gordon, T. The cellular and molecular basis of peripheral nerve regeneration. *Mol. Neurobiol.* **14**, 67–116 (1997).
19. Hoppler, S. & Wheeler, G. N. DEVELOPMENTAL BIOLOGY. It's about time for neural crest. *Science* **348**, 1316–7 (2015).
20. Buitrago-Delgado, E., Nordin, K., Rao, A., Geary, L. & LaBonne, C. NEURODEVELOPMENT. Shared regulatory programs suggest retention of blastula-stage potential in neural crest cells. *Science* **348**, 1332–5 (2015).
21. Mandalos, N. P. & Remboutsika, E. Sox2: To crest or not to crest? *Semin. Cell Dev. Biol.* **63**, 43–49 (2017).
22. Huang, C.-W. *et al.* The Differentiation Stage of Transplanted Stem Cells Modulates Nerve Regeneration. *Sci. Rep.* (2017).

23. Ho, A. T. V. *et al.* Neural Crest Cell Lineage Restricts Skeletal Muscle Progenitor Cell Differentiation through Neuregulin1-ErbB3 Signaling. *Dev. Cell* **21**, 273–287 (2011).

24. Rios, A. C., Serralbo, O., Salgado, D. & Marcelle, C. Neural crest regulates myogenesis through the transient activation of NOTCH. *Nature* **473**, 532–535 (2011).

25. Sacchetti, B. *et al.* No identical 'mesenchymal stem cells' at different times and sites: Human committed progenitors of distinct origin and differentiation potential are incorporated as adventitial cells in microvessels. *Stem Cell Reports* **6**, 897–913 (2016).

26. Bianco, P. *et al.* The meaning, the sense and the significance: Translating the science of mesenchymal stem cells into medicine. *Nature Medicine* **19**, 35–42 (2013).

27. Bianco, P., Robey, P. G. & Simmons, P. J. Mesenchymal Stem Cells: Revisiting History, Concepts, and Assays. *Cell Stem Cell* **2**, 313–319 (2008).

28. Ladak, A., Olson, J., Tredget, E. E. & Gordon, T. Differentiation of mesenchymal stem cells to support peripheral nerve regeneration in a rat model. *Exp. Neurol.* **228**, 242–252 (2011).

29. Mendicino, M., Bailey, A. M., Wonnacott, K., Puri, R. K. & Bauer, S. R. MSC-based product characterization for clinical trials: An FDA perspective. *Cell Stem Cell* **14**, 141–145 (2014).

30. Park, S. E., Georgescu, A. & Huh, D. Organoids-on-a-chip. *Science* **364**, 960–965 (2019).

31. Madl, C. M., Heilshorn, S. C. & Blau, H. M. Bioengineering strategies to accelerate stem cell therapeutics. *Nature* **557**, 335–342 (2018).

32. Bhatia, S. N. & Ingber, D. E. Microfluidic organs-on-chips. *Nature Biotechnology* **32**, 760–772 (2014).

33. Umbach, J. A., Adams, K. L., Gundersen, C. B. & Novitch, B. G. Functional neuromuscular junctions formed by embryonic stem cell-derived motor neurons. *PLoS One* **7**, (2012).

34. Vilmont, V., Cadot, B., Ouanounou, G. & Gomes, E. R. A system for studying mechanisms of neuromuscular junction development and maintenance. *Dev.* **143**, 2464–2477 (2016).

35. Guo, X. *et al.* Tissue engineering the mechanosensory circuit of the stretch reflex arc with human stem cells: Sensory neuron innervation of intrafusal muscle fibers. *Biomaterials* **122**, 179–187 (2017).

36. Steinbeck, J. A. *et al.* Functional Connectivity under Optogenetic Control Allows Modeling of Human Neuromuscular Disease. *Cell Stem Cell* **18**, 134–143 (2016).

37. Santhanam, N. *et al.* Stem cell derived phenotypic human neuromuscular junction model for dose response evaluation of therapeutics. *Biomaterials* **166**, 64–78 (2018).

38. Cisterna, B. A. *et al.* Active acetylcholine receptors prevent the atrophy of skeletal muscles and favor reinnervation. *Nat. Commun.* **11**, 1–13 (2020).

39. Happe, C. L., Tenerelli, K. P., Gromova, A. K., Kolb, F. & Engler, A. J. Mechanically patterned neuromuscular junctions-in-a-dish have improved functional maturation. *Mol. Biol. Cell* **28**, 1950–1958 (2017).

40. Luo, B. *et al.* Electrospun nanofibers facilitate better alignment, differentiation, and long-term culture in an: In vitro model of the neuromuscular junction (NMJ). *Biomater. Sci.* **6**, 3262–3272 (2018).

41. Osaki, T., Uzel, S. G. M. & Kamm, R. D. Microphysiological 3D model of amyotrophic lateral sclerosis (ALS) from human iPS-derived muscle cells and optogenetic motor neurons. *Sci. Adv.* **4**, eaat5847 (2018).

42. Bakooshli, M. A. *et al.* A 3d culture model of innervated human skeletal muscle enables studies of the adult neuromuscular junction. *Elife* **8**, (2019).

43. Hill, E., Boontheekul, T. & Mooney, D. J. Regulating activation of transplanted cells controls tissue regeneration. *Proc. Natl. Acad. Sci. U. S. A.* **103**, 2494–9 (2006).

44. Ho, S. S., Murphy, K. C., Binder, B. Y. K., Vissers, C. B. & Leach, J. K. Increased

Survival and Function of Mesenchymal Stem Cell Spheroids Entrapped in Instructive Alginate Hydrogels. *Stem Cells Transl. Med.* **5**, 773–781 (2016).

45. Nguyen, P. K., Neofytou, E., Rhee, J.-W. & Wu, J. C. Potential Strategies to Address the Major Clinical Barriers Facing Stem Cell Regenerative Therapy for Cardiovascular Disease. *JAMA Cardiol.* **1**, 953 (2016).
46. Blau, H. M. & Daley, G. Q. Stem Cells in the Treatment of Disease. *N. Engl. J. Med.* **380**, 1748–1760 (2019).
47. Daley, G. Q. The promise and perils of stem cell therapeutics. *Cell Stem Cell* **10**, 740–749 (2012).
48. Korff, T. & Augustin, H. G. Integration of endothelial cells in multicellular spheroids prevents apoptosis and induces differentiation. *J. Cell Biol.* **143**, 1341–52 (1998).
49. Jiang, B. *et al.* Spheroidal formation preserves human stem cells for prolonged time under ambient conditions for facile storage and transportation. *Biomaterials* **133**, 275–286 (2017).
50. Wobma, H. M., Liu, D. & Vunjak-Novakovic, G. Paracrine Effects of Mesenchymal Stromal Cells Cultured in Three-Dimensional Settings on Tissue Repair. *ACS Biomater. Sci. Eng.* (2017). doi:10.1021/acsbiomaterials.7b00005
51. Sart, S., Tomasi, R. F.-X., Amselem, G. & Baroud, C. N. Multiscale cytometry and regulation of 3D cell cultures on a chip. *Nat. Commun.* **8**, 469 (2017).
52. Huang, N. F. *et al.* Myotube assembly on nanofibrous and micropatterned polymers. *Nano Lett.* **6**, 537–542 (2006).
53. Huang, N. F., Lee, R. J. & Li, S. Engineering of aligned skeletal muscle by micropatterning. *Am. J. Transl. Res.* **2**, 43–55 (2010).
54. Lam, H. J., Patel, S., Wang, A., Chu, J. & Li, S. In vitro regulation of neural differentiation and axon growth by growth factors and bioactive nanofibers. *Tissue Eng. - Part A* **16**, 2641–2648 (2010).

55. Wang, A. *et al.* Induced pluripotent stem cells for neural tissue engineering. *Biomaterials* **32**, 5023–5032 (2011).

56. Engler, A. J. *et al.* Myotubes differentiate optimally on substrates with tissue-like stiffness: Pathological implications for soft or stiff microenvironments. *J. Cell Biol.* **166**, 877–887 (2004).

57. Zurkirchen, L. & Sommer, L. Quo vadis: tracing the fate of neural crest cells. *Current Opinion in Neurobiology* **47**, 16–23 (2017).

58. Dupin, E., Calloni, G. W., Coelho-Aguiar, J. M. & Le Douarin, N. M. The issue of the multipotency of the neural crest cells. *Developmental Biology* **444**, S47–S59 (2018).

59. Stierli, S., Imperatore, V. & Lloyd, A. C. Schwann cell plasticity-roles in tissue homeostasis, regeneration, and disease. *Glia* **67**, 2203–2215 (2019).

60. Sart, S., Tomasi, R. F.-X., Amselem, G. & Baroud, C. N. Multiscale cytometry and regulation of 3D cell cultures on a chip. *Nat. Commun.* **8**, 469 (2017).

61. Liu, Y., Muñoz, N., Tsai, A.-C., Logan, T. M. & Ma, T. Metabolic Reconfiguration Supports Reacquisition of Primitive Phenotype in Human Mesenchymal Stem Cell Aggregates. *Stem Cells* **35**, 398–410 (2017).

62. Orive, G. *et al.* Cell encapsulation: technical and clinical advances. *Trends Pharmacol. Sci.* **36**, 537–546 (2015).

63. Lazarjani, H. A., Poncelet, D. & Faas, M. M. Polymers in cell encapsulation from an enveloped cell perspective. *Adv. Drug Deliv. Rev.* **67**–**68**, 15–34 (2014).

64. Meyer, M., Matsuoka, I., Wetmore, C., Olson, L. & Thoenen, H. Enhanced synthesis of brain-derived neurotrophic factor in the lesioned peripheral nerve: different mechanisms are responsible for the regulation of BDNF and NGF mRNA. *J. Cell Biol.* **119**, 45–54 (1992).

65. Hwang, J. H. *et al.* Combination therapy of human adipose-derived stem cells and basic fibroblast growth factor hydrogel in muscle regeneration. *Biomaterials* **34**, 6037–6045

(2013).

66. Husmann, I., Soulet, L., Gautron, J., Martelly, I. & Barritault, D. Growth factors in skeletal muscle regeneration. *Cytokine and Growth Factor Reviews* **7**, 249–258 (1996).

67. Chen, Z.-L., Yu, W.-M. & Strickland, S. Peripheral regeneration. *Annu. Rev. Neurosci.* **30**, 209–233 (2007).

68. Funakoshi, H. *et al.* Targeted expression of a multifunctional chimeric neurotrophin in the lesioned sciatic nerve accelerates regeneration of sensory and motor axons. *Proc. Natl. Acad. Sci.* **95**, 5269–5274 (1998).

69. Bollini, S., Gentili, C., Tasso, R. & Cancedda, R. The Regenerative Role of the Fetal and Adult Stem Cell Secretome. *J. Clin. Med.* **2**, 302 (2013).

70. Caplan, A. I. & Correa, D. The MSC: An injury drugstore. *Cell Stem Cell* **9**, 11–15 (2011).

71. Qian, Y. *et al.* An integrated multi-layer 3D-fabrication of PDA/RGD coated graphene loaded PCL nanoscaffold for peripheral nerve restoration. *Nat. Commun.* **9**, 323 (2018).

72. Passini, M. A. *et al.* Antisense oligonucleotides delivered to the mouse CNS ameliorate symptoms of severe spinal muscular atrophy. *Sci. Transl. Med.* **3**, 72ra18 (2011).

73. Adams, K. L., Rousso, D. L., Umbach, J. A. & Novitch, B. G. Foxp1-mediated programming of limb-innervating motor neurons from mouse and human embryonic stem cells. *Nat. Commun.* **6**, 1–16 (2015).

74. Downing, T. L. *et al.* Biophysical regulation of epigenetic state and cell reprogramming. *Nat. Mater.* **12**, 1154–1162 (2013).

75. Patel, S. *et al.* Bioactive nanofibers: Synergistic effects of nanotopography and chemical signaling on cell guidance. *Nano Lett.* **7**, 2122–2128 (2007).

76. Engler, A. J., Sen, S., Sweeney, H. L. & Discher, D. E. Matrix Elasticity Directs Stem Cell Lineage Specification. *Cell* **126**, 677–689 (2006).

77. Ku, S. H., Lee, S. H. & Park, C. B. Synergic effects of nanofiber alignment and electroactivity on myoblast differentiation. *Biomaterials* **33**, 6098–6104 (2012).

78. Chan, H. F. *et al.* Rapid formation of multicellular spheroids in double-emulsion droplets with controllable microenvironment. *Sci. Rep.* **3**, 3462 (2013).

79. Escher, P. *et al.* Neuroscience: Synapses form in skeletal muscles lacking neuregulin receptors. *Science (80-.).* **308**, 1920–1923 (2005).

80. Tateno, K. *et al.* Critical roles of muscle-secreted angiogenic factors in therapeutic neovascularization. *Circ. Res.* **98**, 1194–202 (2006).

81. Autiero, M. *et al.* Role of PlGF in the intra- and intermolecular cross talk between the VEGF receptors Flt1 and Flk1. *Nat. Med.* **9**, 936–943 (2003).

82. Kempf, T. *et al.* GDF-15 is an inhibitor of leukocyte integrin activation required for survival after myocardial infarction in mice. *Nat. Med.* **17**, 581–588 (2011).

83. Biteau, B. & Jasper, H. EGF signaling regulates the proliferation of intestinal stem cells in Drosophila. *Development* **138**, 1045–55 (2011).

84. Kojima, A. & Tator, C. H. Intrathecal Administration of Epidermal Growth Factor and Fibroblast Growth Factor 2 Promotes Ependymal Proliferation and Functional Recovery after Spinal Cord Injury in Adult Rats. *J. Neurotrauma* **19**, 223–238 (2002).

85. Lee, G. *et al.* Isolation and directed differentiation of neural crest stem cells derived from human embryonic stem cells. *Nat. Biotechnol.* **25**, 1468–1475 (2007).

86. Wang, A. *et al.* Induced pluripotent stem cells for neural tissue engineering. *Biomaterials* **32**, 5023–5032 (2011).

87. Jiang, L., Jones, S. & Jia, X. Stem Cell Transplantation for Peripheral Nerve Regeneration: Current Options and Opportunities. *Int. J. Mol. Sci.* **18**, (2017).

88. Heine, W., Conant, K., Griffin, J. W. & Höke, A. Transplanted neural stem cells promote axonal regeneration through chronically denervated peripheral nerves. *Exp. Neurol.* **189**, 231–240 (2004).

89. Guenard, V., Kleitman, N., Morrissey, T. K., Bunge, R. P. & Aebischer, P. Syngeneic Schwann cells derived from adult nerves seeded in semipermeable guidance channels

enhance peripheral nerve regeneration. *J. Neurosci.* **12**, 3310–3320 (1992).

90. Bryson, J. B. *et al.* Optical control of muscle function by transplantation of stem cell-derived motor neurons in mice. *Science* **344**, 94–7 (2014).

91. Yohn, D. C., Miles, G. B., Rafuse, V. F. & Brownstone, R. M. Transplanted mouse embryonic stem-cell-derived motoneurons form functional motor units and reduce muscle atrophy. *J. Neurosci.* **28**, 12409–18 (2008).

92. Bursac, N., Juhas, M. & Rando, T. A. Synergizing Engineering and Biology to Treat and Model Skeletal Muscle Injury and Disease. *Annu. Rev. Biomed. Eng.* **17**, 217–242 (2015).

93. Kwee, B. J. & Mooney, D. J. Biomaterials for skeletal muscle tissue engineering. *Curr. Opin. Biotechnol.* **47**, 16–22 (2017).

94. Furlan, A. & Adameyko, I. Schwann cell precursor: a neural crest cell in disguise? *Developmental Biology* **444**, S25–S35 (2018).

95. Sanes, J. R. & Lichtman, J. W. DEVELOPMENT OF THE VERTEBRATE NEUROMUSCULAR JUNCTION. *Annu. Rev. Neurosci.* **22**, 389–442 (1999).

96. Hicks, M. R. *et al.* ERBB3 and NGFR mark a distinct skeletal muscle progenitor cell in human development and hPSCs. *Nat. Cell Biol.* **20**, 46–57 (2018).

97. Mukouyama, Y. S., Shin, D., Britsch, S., Taniguchi, M. & Anderson, D. J. Sensory nerves determine the pattern of arterial differentiation and blood vessel branching in the skin. *Cell* **109**, 693–705 (2002).

98. Wichterle, H., Lieberam, I., Porter, J. A. & Jessell, T. M. Directed differentiation of embryonic stem cells into motor neurons. *Cell* **110**, 385–397 (2002).

99. Colter, D. C., Sekiya, I. & Prockop, D. J. Identification of a subpopulation of rapidly self-renewing and multipotential adult stem cells in colonies of human marrow stromal cells. *Proc. Natl. Acad. Sci. U. S. A.* **98**, 7841–7845 (2001).

100. Lee, R. H. *et al.* The CD34-like protein PODXL and ά6-integrin (CD49f) identify early progenitor MSCs with increased clonogenicity and migration to infarcted heart in mice.

Blood **113**, 816–826 (2009).

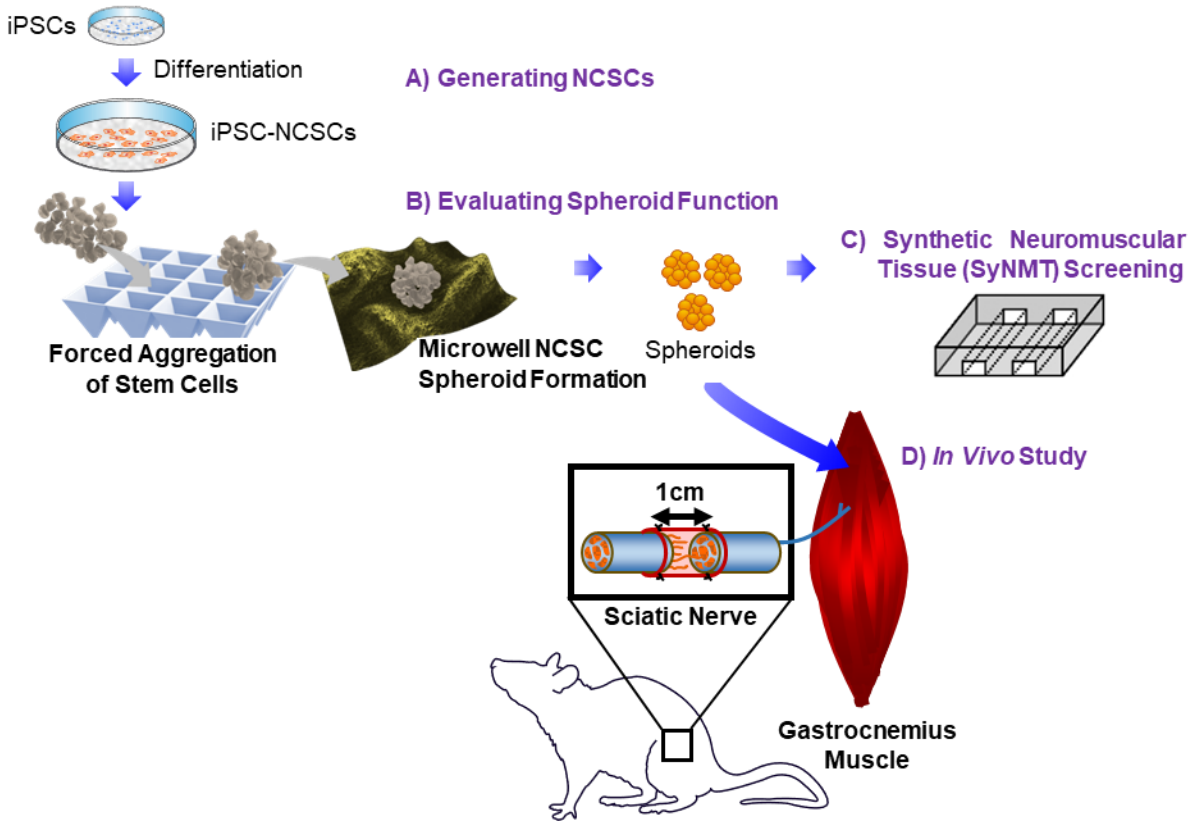

Visual Abstract.

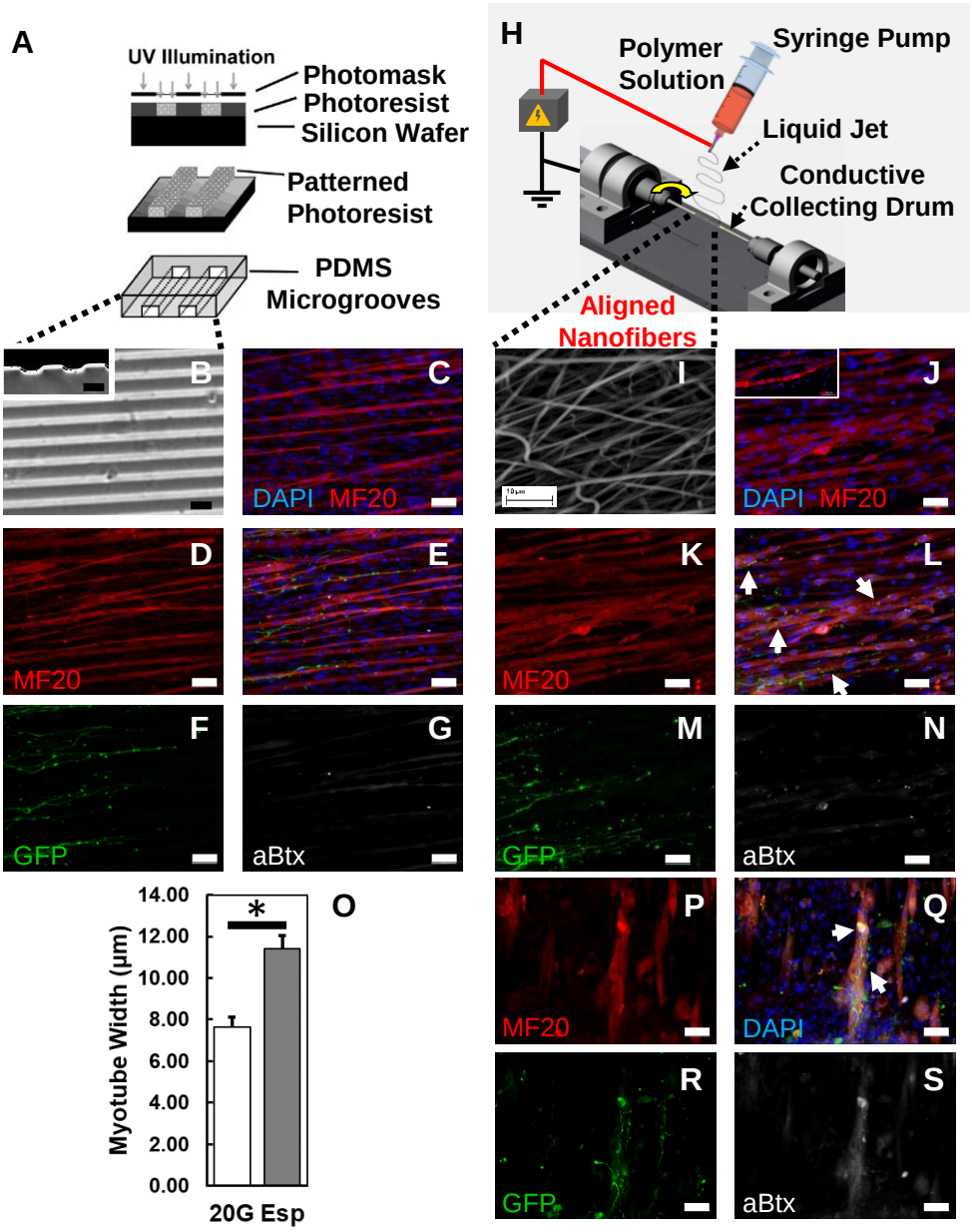

Fig. 2.1. Micro- and Nano- topographical Cues Impact Neuromuscular Cell Morphology. (A) Schematic of microgroove fabrication with soft lithography. **(B)** Fabricated microgrooves; scale bar = 20µm. **(C-G)** Immunofluorescent stains of C2C12 myotubes co-cultured with iPSC-derived MNs on the microgrooves. **(H)** Schematic of electrospinning process. **(I)** Scanning electron microscopy (SEM) of the aligned electrospun (Esp) nanofibers. **(J-N)** Stains of C2C12-MN co-culture on the Esp membranes, with an inset in **(J)** of striation formation. **(O)** Quantification of average myotube width of ciMCs cultured on the 20µm-width microgrooves (20G) versus Esp membranes *: $p<0.05$. **(P-S)** Stains of ciMCs co-cultured with iPSC-derived MNs on the Esp membrane. Arrows = innervated NMJs. Scale bars unless otherwise noted = 50µm.

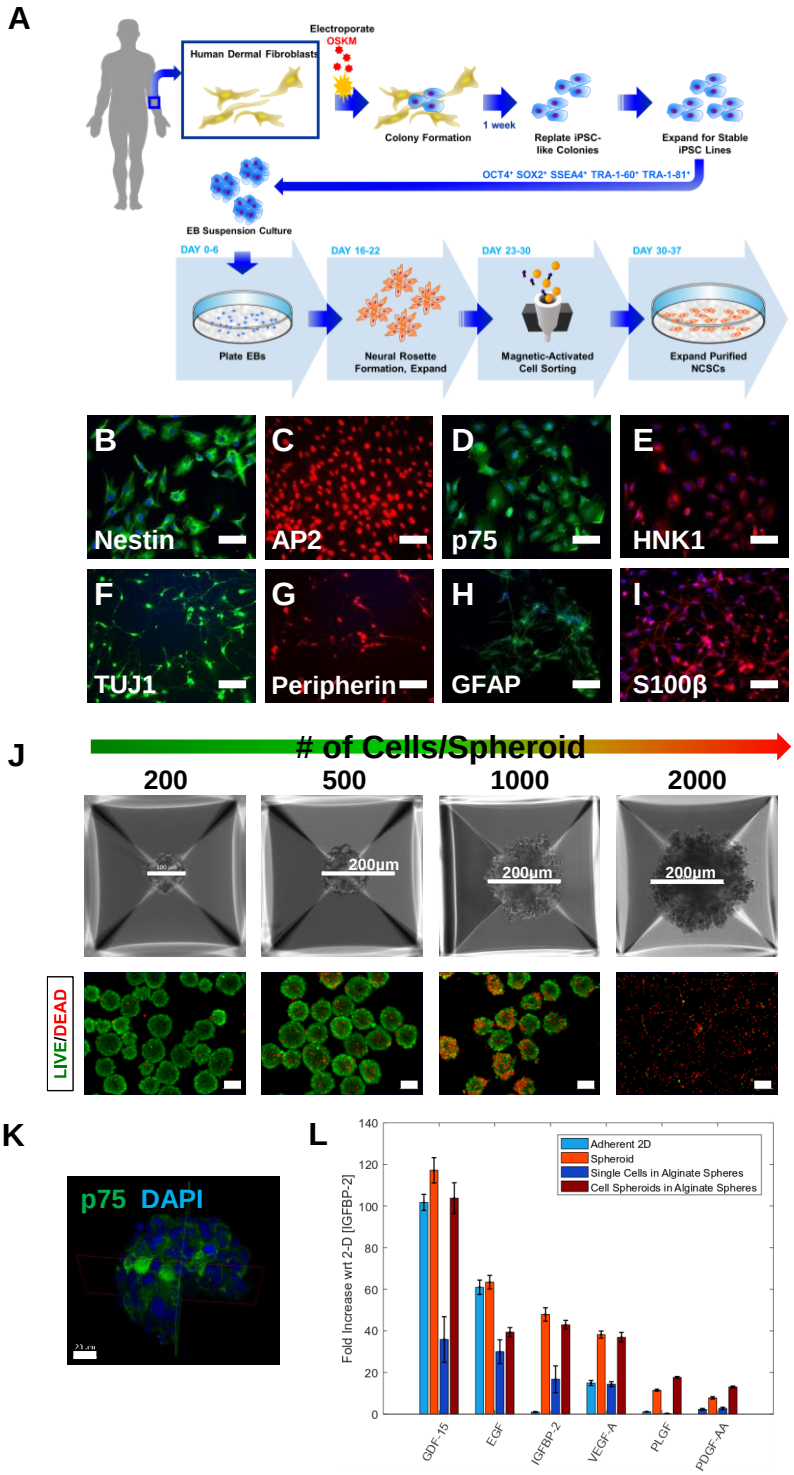

Fig. 2.2. hiPSC-derived NCSCs Have Multipotent Potential and Form Spheroids with Enhanced Regenerative Secretomes. **(A)** iPSC and NCSC derivation process. **(B-E)** NCSC expression of NCSC markers. Standard differentiation protocols were used to generate **(F-G)** peripheral neurons and **(H-I)** Schwann cells. Scale bar= 100μm. **(J)** Size-dependency of NCSC spheroid survival, Scale bar= 100μm unless otherwise specified. **(K)** 3D quarter-cutaway of NCSC stained spheroid. Scale bar= 20μm. **(L)** Regenerative secretome of NCSCs in various modalities.

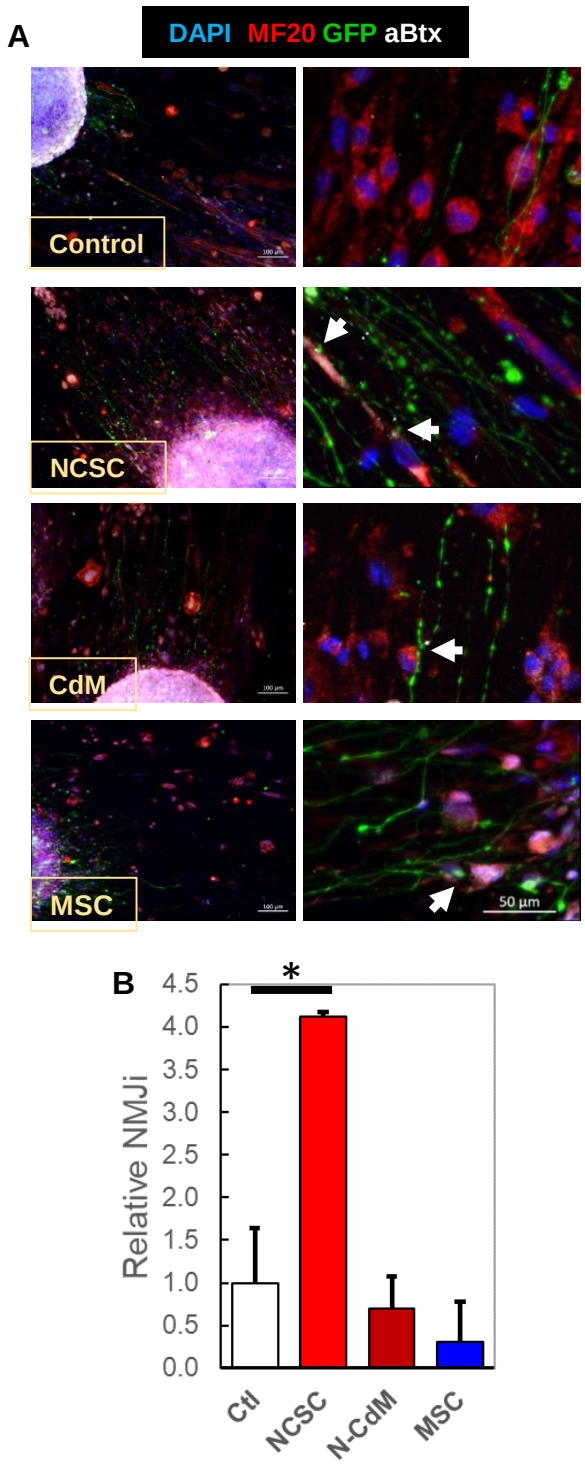

Fig. 2.3. SyNMT Screening Reveals Differences in NMJ Innervation with NCSCs versus MSCs. **(A)** Low (scale bar = 100µm) and high magnification (scale bar = 50µm) stains for NMJ formation in ciMC-MN co-culture with different stem cell conditions. NCSC and MSC denote co-culture with respective spheroids. CdM = NCSC spheroid conditioned media via Transwell. Arrows indicate NMJs. **(B)** Quantification of innervated NMJs (NMJi) relative to Control. *: $p<0.05$.

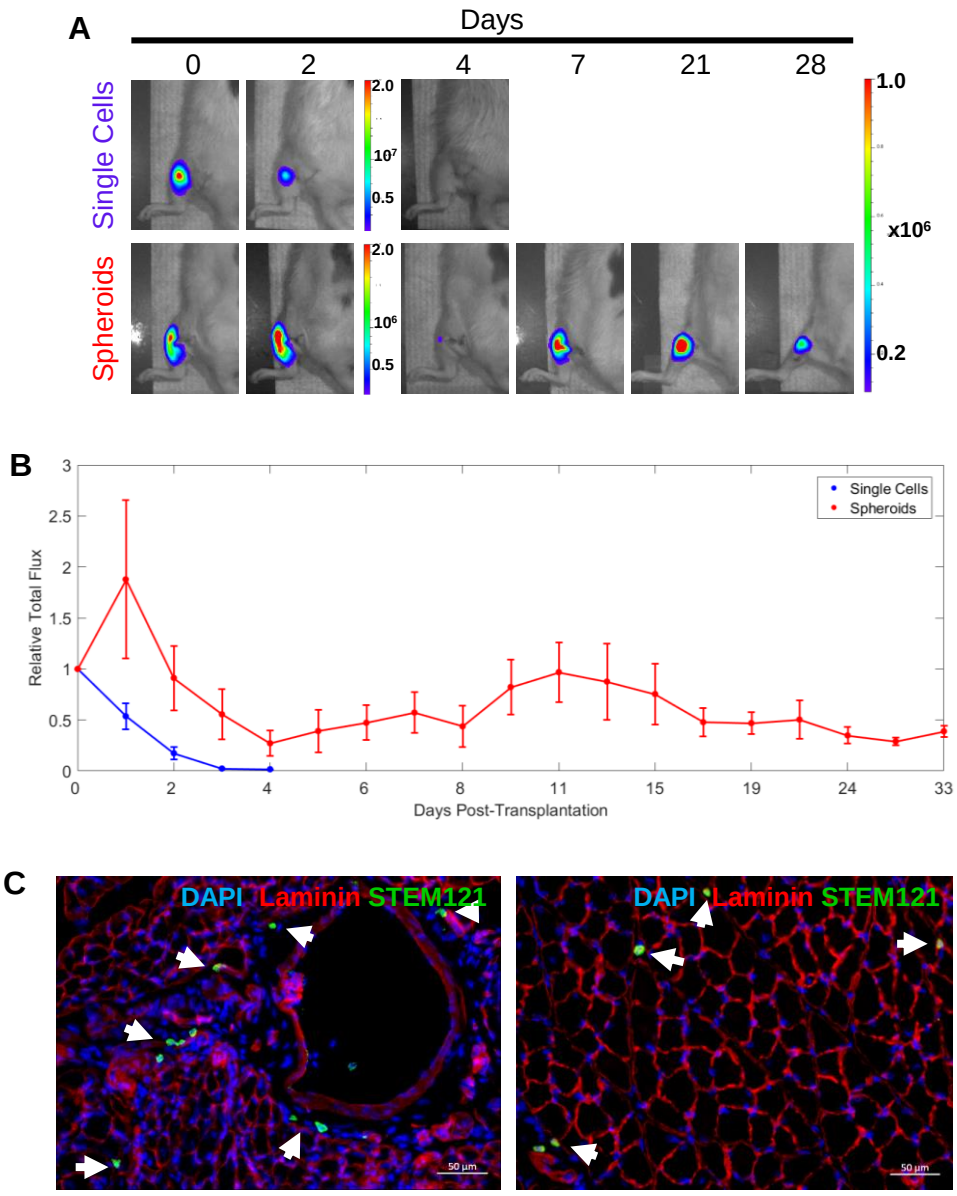

Fig. 2.4. NCSC Spheroids Improve *In Vivo* Survival Following Transplantation. **(A)** Bioluminescent noninvasive tracking of luciferase-labeled NCSC survival (total flux, in p/s) after transplantation as single-cell suspension versus spheroids, n=3 each. **(B)** Plot of total flux relative to original baseline directly following transplantation. **(C)** Distribution of NCSCs (positive for human cytoplasm STEM121 marker) in various structures as stained by laminin (red) and DAPI (blue). Scale bar = 50µm.

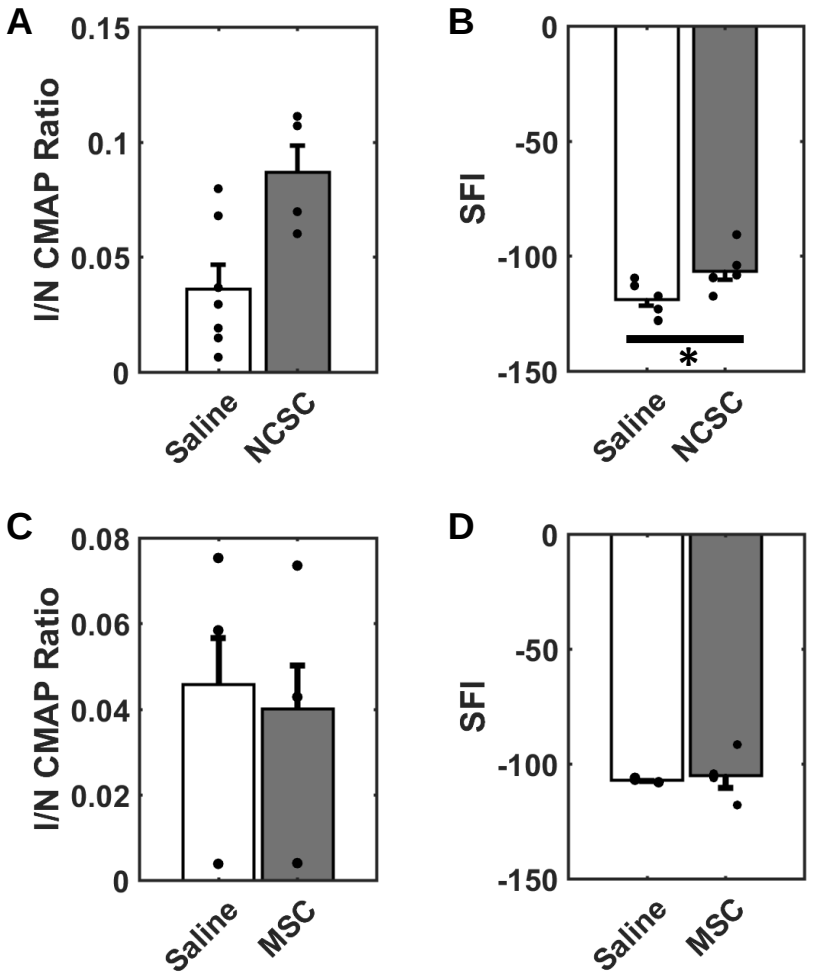

Fig. 2.5. NCSCs but Not MSCs Improve Functional Recovery 4 Weeks after Stem Cell Transplantation. **(A-B)** Functional metrics for NCSC-transplanted rats, where I/N is the ratio of the injured (I) limb to normal (N) uninjured limb for each animal, CMAP = compound muscle action potential, SFI = sciatic functional index, Controls were injected with saline rather than cells, *: $p<0.05$. **(C-D)** The same functional metrics, but for MSC-transplanted rats. Minimum n of 3.

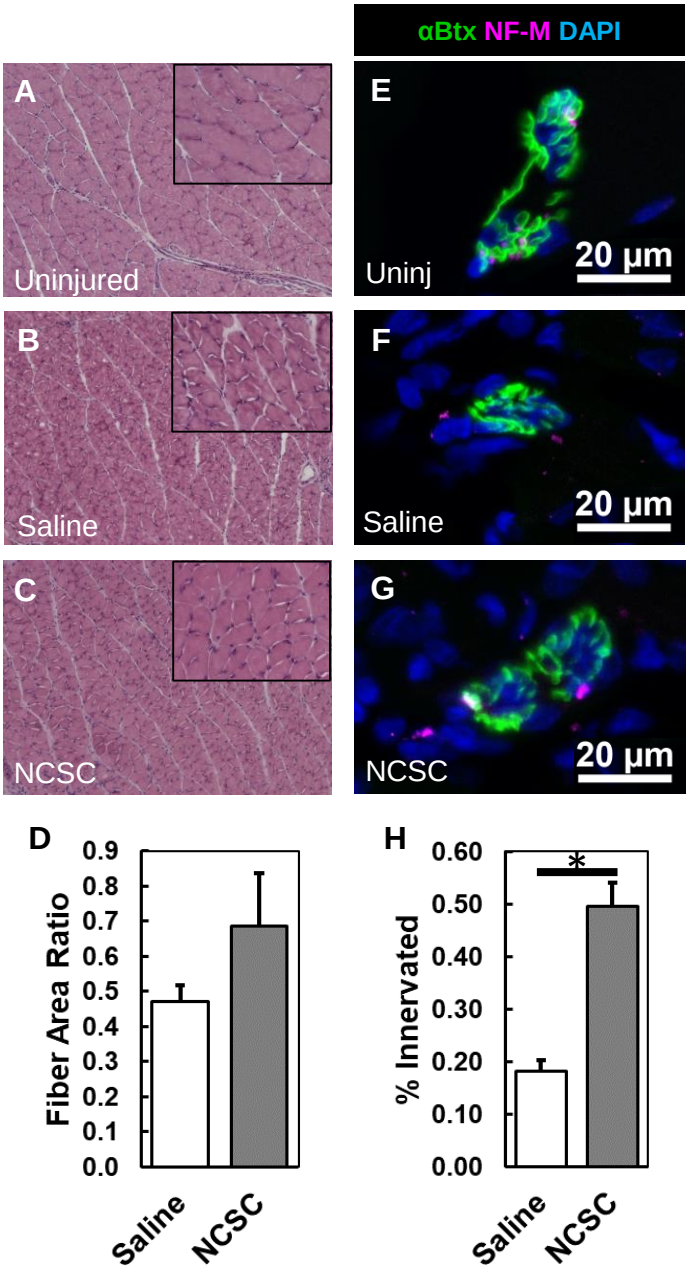

Fig. 2.6. Neuromuscular Histology is Improved 4 Weeks Following NCSC Transplantation. **(A-C)** H&E stains of sectioned gastrocnemius muscle at 4x magnification, with insets at 10x. **(D)** Quantification of average fiber area as a ratio of the injured to the uninjured side of each animal, n=4 each. **(E-G)** Representative stains of NMJs, where uninj = uninjured limb, versus saline and NCSC injected injured limbs, n=5 each. αBtx = α-Bungarotoxin, NF-M = neurofilament-medium. **(H)** Quantification of NMJs innervated with NF-M as a % of total # whole NMJs, normalized for each animal to the % innervation of its uninjured limb. *: $p<0.05$.

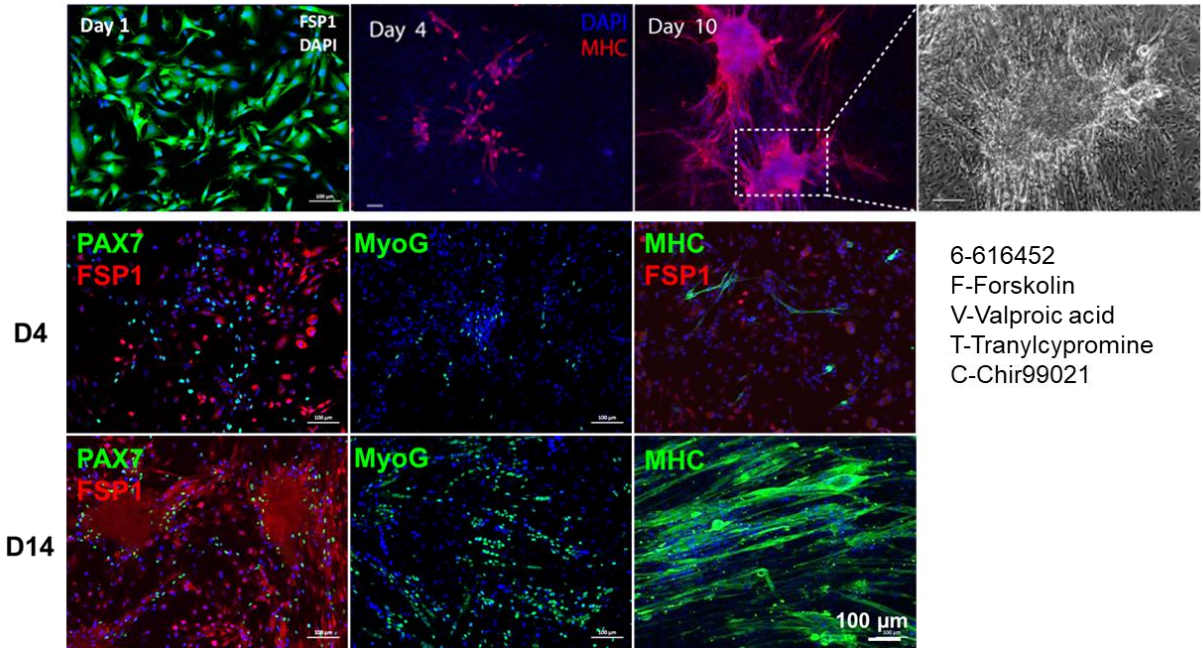

Suppl. Fig. 2.1. Chemically Induced Myogenic Cells (ciMCs). Using this chemical cocktail, ciMCs are seen at various time points, given as days (D) of chemical application. Scale bar = 100µm.

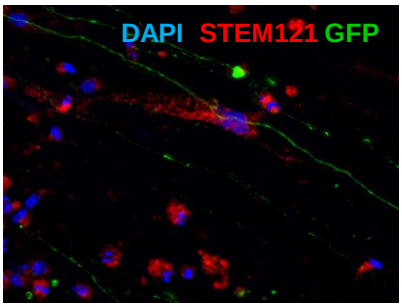

Suppl. Fig. 2.2. SyNMT NCSC Stain. ciMC-MN co-culture with NCSCs stained for STEM121 antibody to human cytoplasm to identify NCSC morphology, as well as GFP for MNs and DAPI for nuclei.

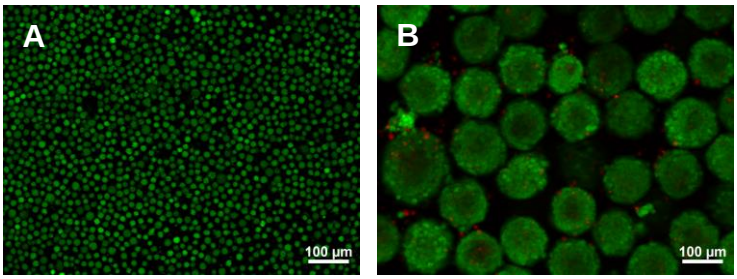

Suppl. Fig. 2.3. Survival of NCSCs Through Needle Prior to Transplantation. NCSCs were subject to live-dead stain following ejection through the needle prior to transplantation. Green = live, Red = dead. **A)** Single cell suspension, and **B)** Spheroids, are shown. Scale bar = 100µm.

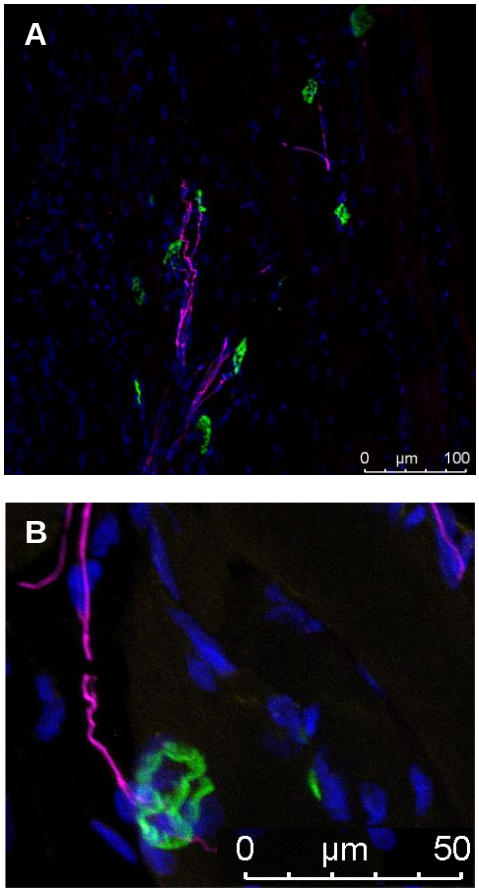

Suppl. Fig. 2.4. Long-term NMJ Reinnervation 9 Weeks After NCSC Transplantation. Axonal reinnervation via histological stain for alpha-bungarotoxin (green), neurofilament-medium (NF-M, purple), and DAPI (blue) of longitudinal gastrocnemius section at nine weeks. **(A)** low-magnification view, **(B)** high-magnification view.

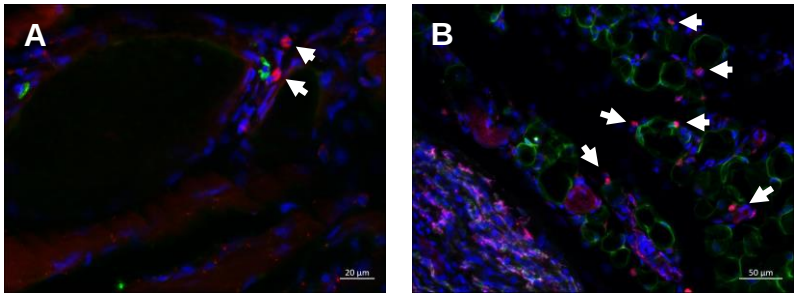

Suppl. Fig. 2.5. Staining for Schwann and Neural Crest Identity of NCSCs 4 Weeks Following Transplantation. **(A)** Stains for human nuclear antigen HNA (red), Schwann cells of myelinating S100β (green) and nonmyelinating GAP43 (violet) subtypes, together with DAPI (blue). Scale bar = 20µm. **(B)** Stains for human nuclear antigen HNA (red) and neural crest marker p75 (green) together with DAPI (blue). Scale bar = 50µm. Arrows = transplanted human cells (HNA^+).

Chapter 3

Spatial Promotion of Neuronal Reprogramming in Three-Dimensional Spheroids

Abstract

Direct reprogramming of adult human somatic cells into neuronal fate, known as “induced neurons” (iNs), has tremendous potential for disease modeling and therapeutic regeneration, but is still hindered by low and variable conversion efficiencies. Biophysical cues play profound roles in development and shaping multi-cellular behavior, but their involvement in direct reprogramming is still not well understood. Here we show that three-dimensional (3D) multicellular spheroids enhance iN conversion efficiency by over 67-fold relative to conventional 2D culture. Moreover, reprogramming displayed characteristic spatial patterns of peripheral neural enrichment of spheroids. Cell-contact-dependent NOTCH signaling, spheroid surface-area-to-volume ratios, proliferation, pH manipulation, global histone acetylation, and absolute mechanical tension had no effect on these patterns, but the disruption of spheroid surface adhesive polarity eliminated peripheral reprogramming promotion. Conversely, chemical inhibition of both the TGF-β and BMP pathways disinhibited reprogramming within the spheroid to further improve conversion. In summary, we unraveled a mechanism of enhanced iN conversion in spheroids that enabled us to develop a novel approach to significantly improve reprogramming efficiency. This strategy will greatly facilitate the translation of iN technology for drug screening, disease modeling, and tissue regeneration.

Introduction

The discovery that differentiated cells can be reprogrammed into pluripotent cells and other cell types spurred the development of new technologies for engineering cell identity for biomedical applications. Understanding how to traverse this new landscape of cell fate would

have tremendous implications not only for basic science, but also for improving accessibility to cells for disease modeling and therapeutic testing, functionalizing knowledge for engineering improved replacement cells and tissues, and *in situ* regeneration and healing without the cancer risks of pluripotent cell products[1–3]. Direct reprogramming or transdifferentiation of adult somatic cells into neuronal fate, "induced neurons" (iNs), has been extensively investigated as a model of reprogramming into non-pluripotency[1]. The conversion of human fibroblasts to neurons is realized by the forced expression of neural lineage transcription factors (TFs; here, *Ascl1, Brn2, Myt1l*, and *NeuroD1*, together known as BAMN), and additional TFs can be included to further specify the subtypes of neurons[4–6].

Despite this wealth of knowledge and potential, low and variable efficiencies in generating iNs and incomplete comprehension of underlying mechanisms of this conversion are significant roadblocks to their application[2,6,7]. The majority of the field has focused on understanding direct reprogramming through the lens of transcription factors and biochemical signaling for gene regulation, and indeed, in multicellular systems, gradients of morphogens contribute to development of cellular identity and morphology[8]. Cell reprogramming occurs in a complex environment, however. Such signaling does not exclude the involvement of biophysical regulation, nor the possibility of mechano-chemical coupling, which have both been important shapers of reprogramming and differentiation in other cell types[9–12]. Morphogen concentration and reaction-diffusion theory, for instance, cannot exclusively account for the patterning observed in multicellular tissues, and parsimonious integration of cytoskeletal properties and mechanotransduction into existing models have provided more accurate and comprehensive representations of reality[13–15]. Attempts to improve on iN conversion from fibroblasts thus far, however, have focused primarily on using small molecules to disrupt or promote certain gene networks[3,16–18]. Yet in its nascency for identifying roles in general reprogramming, the utility of biophysical cues for direct reprogramming is not well understood.

Three-dimensional (3D) multicellular aggregates, termed “spheroids” (though not necessarily spherical in shape), were first applied for promoting germline differentiation in embryonic cells[19–21], and were found thereafter in pluripotent stem cells (PSCs), termed “embryoid bodies” (EBs), to facilitate differentiation into almost any cell type, including the neural lineage[22,23]. Indeed, neural cells seem to particularly favor the spheroidal form; in the nervous system, spheroids, termed “neurospheres”[24], arise naturally when isolating neural cells from nervous tissue, and culture in this form enhances physiological responses and survival of neurons *in vitro*[25,26] as well as *in vivo* after grafting back into the brain[27]. More recently, discoveries that multi-cellular clustering via prolonged pile-up aggregation and compression may facilitate lineage switching[28] and de-differentiation[28,29] in the absence of other factors have opened up intriguing questions on application of spheroids for direct reprogramming. It is not clear, however, whether and how 3D spheroid culture affects direct neuronal reprogramming.

Remarkable progress has been made in engineering organoids and model systems of increasing complexity and capability, but fundamental mechanisms shaping identity and patterning of multicellular structures require further study for understanding. Simplified multicellular systems such as spheroids enable better isolation of variables, and once their influence is grasped, will illuminate the determinism behind as yet stochastically-understood direct reprogramming processes[32]. As such, we examined the impact of spheroidal culture on iN direct reprogramming of human neonatal dermal fibroblasts (hNDFs) with the BAMN factors.

Results

Spheroid Culture Enhances Direct Reprogramming of Fibroblasts into Neurons

Direct reprogramming involves both disruption of the existing regulatory network (generally early on) and establishment of another. The initial nonspecific disruption is often mechanistically associated with cell cycle regulation, cell senescence, chromatin inactivation, and genome stability[1]. To assess the impact of mechanobiological changes associated with spheroid

culture[28] on direct reprogramming, primary human neonatal dermal fibroblasts (hNDFs) were transduced with doxycycline (dox)-inducible lentiviral vectors for the BAMN factors[5]. After dox induction in monolayer to ensure unbiased activation of the transgenes, hNDFs were either plated onto Matrigel-coated cover slips as 2D controls or centrifuged in microwells to form 3D aggregates, or "spheroids" (Fig. 3.1A). The expression of neuron-specific β-tubulin III (Tuj1) was used as a marker of neuronal fate, as is convention[4,5]. Tuj1 expression began earlier in spheroids than in 2D culture, appearing as early as day two (two days after dox induction and one day after spheroid formation) (Fig. 3.1B-C).

To evaluate relative reprogramming efficiency, spheroids were replated after three days onto Matrigel-coated cover slips. We did not use enzymatic disaggregation because we found that neurons had disproportionate difficulty in recovering from and re-adhering after spheroid dissociation, perhaps due to the increased sensitivity of interconnected extended processes in spheroids to mechanical trituration. This was in agreement with previously published findings on dissociating neural precursor spheroids, which suffered from sluggish growth attributed to possible removal of vital receptors by enzyme-mediated dissociation, and even in the absence of enzyme dissociators, over 50% cell death after spheroid dissociation[33]. At two weeks post-dox induction, monolayer iNs still displayed very few $Tuj1^+$ cells (0.06%; Fig. 3.1E). Spheroid iNs, in contrast, had dramatically improved neural conversion (4.06%, Fig. 3.1D), by over 67-fold ($p<0.05$, Fig. 3.1F).

Spheroid Reprogramming Progresses in a Spatial Pattern

In order to assess the dynamic direct reprogramming process, we tracked the expression of Tuj1 over time. We knew that onset would be more rapid (Fig. 3.1B) and ultimately greater than in 2D (Fig. 3.1D-F), but what was unexpected was to see a consistent and distinct spatial pattern of Tuj1 expression. Rather than a gradual and spatially homogenous increase, expression began on the periphery of the spheroid (Fig. 3.2A-C), moving somewhat inward over time but remaining

concentrated on the exterior (Fig. 3.2D-I). N-cadherin was also preferentially expressed at the spheroid surface at day 3, indicating early spatial differences in adhesion within the spheroid as well (Fig. 3.2J-L).

The cell surface receptor Notch mediates cell-cell contact-dependent signaling, and has key roles throughout development[34]. It has been shown that NOTCH signaling regulates neuronal development and morphogenesis[35], and that indirect NOTCH inhibition with N-[N-(3,5-difluorophenacetyl)-L-alanyl]- S-phenylglycine t-butyl ester (DAPT), a γ-secretase inhibitor, promotes direct neural reprogramming of human astrocytes[36]. In our hands, however, DAPT had no effect on spatial patterns ofTuj1 expression (Fig. 3.3A-D), suggesting cell-contact dependent NOTCH signaling was not responsible.

Surface Area-to-Volume Ratios & Proliferation in Reprogramming Spheroids

Decreased surface area-to-volume ratios (SA:V) improve neural reprogramming of hPSC-derived cerebral organoids, although this had to be balanced with the propensity to fail to develop into organoids and to generate fewer neuroepithelial buds if EBs were too small[37]. We sought to investigate whether spheroid reprogramming was similarly sensitive to changing SA:V, and whether decreased SA:V could reprogram the spheroid core. We compared spheroids of 500 cells, around 90μm in diameter (Fig. 3.3E-G), versus 2,000 cells, around 170μm in diameter (Fig. 3.3H-J). Although both formed spheroids, showing they remained within size allowances, we found that Tuj peripheral expression patterns invariably remained.

Faster cell cycles and thus increased proliferation are associated with increased reprogramming efficiency in some cell types[38,39]. Proliferation ($Ki67^+$) was also assessed in these spheroids after synchronizing cell cycles (Fig. 3.3F, I). The distribution of $Ki67^+$ cells did not closely correlate with the spatial pattern of Tuj^+ reprogramming, however, suggesting proliferation was not the key driver of reprogramming patterns in our system (Fig. 3.3G, J).

Interestingly, reducing spheroid size did not improve iN conversion efficiency as drastically as our original size either (Fig. 3.3K-L). Ratios are, of course, open to future optimization.

Effects of Metabolic Gradients and Epigenetic Regulation on the Spatial Pattern of Reprogramming

Core acidity and metabolic differences in 3D spheroids can result in chemical gradients and impact cell function and reprogramming[40]. To assess metabolic effects, we varied the pH of surrounding media at levels of 6.5, 7.2, 8.5, and 9. Spatial reprogramming patterns were not disrupted, suggesting that metabolic gradients were not responsible (Fig. 3.4A-B).

The manipulation of metabolism is linked with epigenetic modification. Histone acetylation, for instance, is strongly regulated by intracellular pH (pH_i), with acidic conditions promoting global histone deacetylase (HDAC) activity in a fashion self-limited by coupled proton export from the cell[41], and decreases in histone acetylation via diminished aerobic glycolysis and acetyl-CoA product[40]. Although varying pH, which is associated with HDAC activity, did not alter reprogramming patterns, given the reported role of the global HDAC inhibitor valproate in promoting neural fate in multipotent neural progenitor cells[42] and human fibroblasts[17], as well as in reprogramming mouse fibroblasts to pluripotency[43], we examined the effect of valproate on iNs. Multicellular aggregation by lateral confinement triggers an increase in nuclear plasticity along with the reorganization of epigenetic and chromosome packing within the nucleus to prime the nucleus for reprogramming[28], so we thought it feasible that this could also occur in our spheroids. However, although reprogramming appeared intensified, spatial patterns were unaffected (Fig. 3.4C), suggesting that broad epigenetic trends of acetylation are not responsible for the spatial pattern of reprogramming.

The Role of Mechanical Tension in the Spatial Pattern of Reprogramming

In spheroids formed by centrifugation-driven aggregation, the few cell layers on the periphery display a distinct circumferential contractile tension on the order of 10s of Pascals. This peripheral contraction drives profiles of significantly-larger (kilopascals) compressive stress within the bulk in the radial and circumferential directions which peak just inside the peripheral region[44]. Staining of actin filaments with phalloidin confirmed that our spheroids displayed cytoskeletal tension patterns that varied with relative radial location, appearing to align more on the periphery (Fig. 3.5A), unlike cells in 2D which had no consistent patterns (Fig. 3.5B). Cortical tension is primarily created by actomyosin contractility[45]. To query whether the mechanical tension in the spheroid peripheral region was responsible for the spatial pattern of neuronal reprogramming, we treated spheroids with blebbistatin, a specific inhibitor of non-muscle myosin II[46]. Disruption of actin-myosin contraction did not eliminate the peripheral preference of neuronal reprogramming (Fig. 3.5C), suggesting either that higher mechanical tension at the spheroid periphery does not account for the spatial reprogramming pattern, or that it is the differential tension rather than the net contractile force that is responsible[45,47]. Staining of F-actin at two weeks post-dox treatment showed the more contractile phenotype characteristic of fibroblasts and other mesenchymal cells with their prominent stress fibers, in contrast to converted neurons (Fig. 3.5D).

Adhesive Encapsulation Disrupts the Spatial Pattern

Cells on the surface of spheroids have apical polarity in the absence of cell-matrix adhesion. To determine whether this cell adhesion polarity affected neuronal reprogramming, we encapsulated spheroids in hyaluronic acid (HA) hydrogels conjugated with the tri-amino acid adhesive peptide arginine-glycine-aspartate (RGD), the primary integrin-binding domain found in many extracellular matrix (ECM) proteins[48], to enable adhesion of the cells on the surface of spheroids. Spheroid cells attached readily in these gels, beginning to migrate within days (Fig. 3.6A). In this setting of disrupted polarity, Tuj1 expression was drastically lowered on the spheroid

surface, and the peripheral advantage of spheroids was lost (Fig. 3.6B-C). F-actin was more prominent in migratory cells pushing out of the spheroid into the surrounding hydrogel (Fig. 3.6D). Ki67$^+$ cells were also found on the periphery of spheroids in HA-RGD, but was not correlated with iN conversion, lending further credence to the idea that cell division was not responsible for the spatial patterns (Fig. 3.6E).

Rescuing Core Reprogramming with Combined Pathway Inhibition.

Mesenchymal cells are more prone to spheroid formation and compaction[49], and cells of higher contractile power like fibroblasts and other mesenchymal cells are thought to assemble in the core of spheroids preferentially over less contractile cells[50]. The bone morphogenetic protein (BMP) and transforming growth factor β (TGF-β)-Activin-Nodal signaling pathways have key roles in mesenchymal differentiation[10,51]. In addition, although single pathway inhibition is insufficient, dual pathway inhibition efficiently induces neural conversion from PSCs[52], hPS-derived spheroids modeling the forebrain[53], and fibroblast reprogramming with small-molecules[18]. We therefore investigated whether dual pathway inhibition might affect spatial expression patterns in spheroids. Inhibition of the TGF-β/Activin/Nodal pathway with the TGF-β type I receptor ALK4/5/7 inhibitor, A83-01[55,56] (A) (Fig. 3.7C), or the BMP pathway with BMP7 type I receptor kinase ALK2 inhibitor, K02288[57–59] (K) (Fig. 3.7D), alone did not much affect spatial Tuj1$^+$ reprogramming patterns relative to no-treatment controls (Fig. 3.7A). Application of both chemicals for dual pathway inhibition, however, enhanced Tuj1 expression on the spheroid interior without eliminating peripheral expression (Fig. 3.7B). These results suggest that the mesenchymal identity in the core of spheroids may be the barrier to neuronal reprogramming.

Discussion

Biophysical cues are acknowledged to play profound roles in development and multi-cellular assembly, but their role in cell reprogramming is not well understood. Here we discovered

that 3D spheroids can enhance iN direct reprogramming efficiency by over 67-fold relative to conventional 2D methods and provide a rational basis for a robust approach to generate iNs. In addition, the inhibition of TGF-β/Activin and BMP pathways can remove the spatial heterogeneity of reprogramming, and further boost the reprogramming efficiency. This combination of 3D spheroid culture and chemical inhibitors in iN generation will be a powerful technology to enable the translation of iN conversion into applications such as disease modeling, drug screening, and tissue regeneration.

Enhancement of reprogramming in our spheroids was not homogenous, but displayed a characteristic spatial distribution of a peripheral layer enriched with neurons surrounding an unreprogrammed core (Fig. 3.2A-I). Mesenchymal cells, including fibroblasts, display enhanced sphere-forming ability, and there is evidence that 3D spheroid formation may conversely simulate certain mesenchymal processes and perhaps even promote mesenchymal phenotype[50,60,61]. Additionally, cells of higher contractile power like fibroblasts and other mesenchymal cells tend to favor the core of spheroids[51]. Spheroid surface cells, in contrast, are distinct from interior cells due to lack of cell-cell adhesion on their apical surface. Cadherin staining in our spheroids confirmed surface-core adhesion protein differences (Fig. 3.2J-L). This difference in adhesion is a component of the acknowledged surface boundary differences of multicellular aggregates like spheroids, under the umbrella term “mechanical polarization”[62–64]. Enhanced mesenchymal phenotype in the interior of spheroids may underlie the low reprogramming efficiency there.

Mesenchymal modulation was highlighted as a crux of spheroid reprogramming by our subsequent finding that dual inhibition of the TGF-β/Activin and BMP pathways, which also suppresses mesenchymal phenotype, enabled iN conversion in the core of spheroids. Both pathways play key roles in reprogramming as well as neurogenesis of hPSCs and iNs[10,18,52–54]. Activin and its associated TGF-β pathway promote the mesodermal lineage, and TGF-β is a cytokine commonly used to induce and maintain the mesenchymal state. Their inhibition destabilizes networks to facilitate differentiation as well as mesenchymal-to-epithelial transition

(MET)[18,53]. BMP promotes the endodermal lineage, and naturally occurring BMP inhibitory factors like noggin, chordin, and follistatin are key inducers of neural fate[53]. It has been shown that the inhibition of the TGF-β/Activin/Lefty pathway via inhibition of the ALK4/5/7 receptors enhances neural induction[53], and PSC neural conversion requires the synergy of combined TGF-β/BMP pathway inhibition rather than either alone[53], similar to our findings in iN spheroids here. That pathway inhibitors suppressing mesenchymal identity would promote spheroid interior reprogramming, rather than merely and exclusively heightening existing patterns of surface reprogramming, was revealing: these results suggested that mesenchymal identity was more a barrier to iN conversion in the core of spheroids than on the surface, and inhibition of mesenchymal fate was the critical roadblock to whole-spheroid reprogramming.

Moreover, our results illuminated the importance of identifying biophysical cues undergirding iN spheroid conversion patterns. By manipulating a variety of factors, biophysical and otherwise, we ultimately identified that only introduction of cell-ECM adhesion in a 3D hydrogel eliminated the peripheral enhancement of reprogramming in spheroids (Fig. 3.6), demonstrating the key role specifically of adhesive polarity in dictating the reprogramming patterns in our system. Cell-ECM adhesion on the spheroid surface would disrupt adhesion and thus cell polarity[65,66] in addition to decreasing the effective intercellular adhesion[48,67]. It is possible that such encapsulation may also promote preservation or promotion of the fibroblast mesenchymal phenotype that inhibits iN conversion, creating an environment more similar to the core of unencapsulated spheroids[60].

Together with adhesion, biological properties, transport, and mechanics are all important, often interdependent, influencers of spheroid formation and behavior[11,65]. Just as important as what did impact spatial patterning was what did not. Biologically, indirect inhibition of the essential surface receptor in contact-dependent signaling between cells, Notch, did not affect our system (Fig. 3.3A-D), likely because one of our iN TFs, *Myt1*, in fact silences NOTCH to promote the neural program[36]. Proliferation or active cell cycles, which has been associated with privileged

improvement in direct reprogramming to pluripotency[39,40], was neither sufficient nor necessary for iN reprogramming in this system (Fig. 3.3F-G, I-J), corroborating previous findings in chemically reprogrammed iNs[16,17]. Similarly, decreasing SA:V had no impact on iNs (Fig. 3.3E, H, K-L) despite its improvement of PSC-derived cerebral organoid neurogenesis[38], possibly due to differences between PSC differentiation and iN reprogramming. Transport gradients and accumulated acidity from metabolic byproducts were further ruled out by manipulating pH of surrounding media (Fig. 3.4A-B), likely because we were well within size limitations of nutrient diffusion, commonly estimated as radii around 200μm[68]. Epigenetic manipulation with the global HDAC inhibitor VPA (Fig. 3.4C) suggested that broad epigenetic spatial trends were not responsible either – also not unreasonable given the varying role of epigenetic marks at different developmental stages and for different lineages[41], although interrogation of epigenetic activation of more specific markers could be of potential future interest. With regards to mechanics, surface cortical tension is a key driver of spheroid force profiles[45] and has been closely correlated with stemness[69], but absolute cytoskeletal contractility and cortical tension were not directly responsible for the spatial pattern of reprogramming here (Fig. 3.5C). This does not rule out, however, the importance of relative force profiles or mechanical gradients, whose investigation has been greatly enabled by the recent development of dispersible force sensor technologies[45,70–72]. Profiling the spatial transcriptional profile at single cell resolution could be of great future interest as well[73,74].

In conclusion, here we examined the impact of the most fundamental multicellular building block, spheroids, on direct reprogramming. Our results complement recent findings of de-differentiation and enhanced reprogramming of self-assembled multicellular clusters of various human cell types after compression[30], lateral confinement[29], or growth on low attachment surfaces[75]. We presented a strategy to significantly enhance iN direct reprogramming efficiency which may illuminate more fundamental roles for tissue polarity in reprogramming cell fate. Although forced expression of TFs and application of exogenous chemicals play important roles

in direct reprogramming, biophysical factors, which arise naturally in development, pathology, and healing, are also of great physiological importance, and can be engineered *in vitro* and *in vivo* to significantly boost reprogramming efficiency[12,14,76,77]. Understanding the processes underlying spheroid reprogramming will enable not only isolating and optimizing aspects to improve conversion efficiencies, but also, in turn, modular scaling up of organoid assembly for tissue engineering and regenerative medicine.

Materials and Methods

Lentivirus Preparation

Doxycycline-inducible lentiviral constructs of Tet-O-FUW-Ascl1, Tet-O-FUW-Brn2, Tet-O-FUW-Myt1l and Tet-O-FUW-NeuroD1 were used to produce the lentivirus for the transduction of fibroblasts. Lentivirus was prepared using calcium phosphate transduction and concentrated using Lenti-X Concentrator (Clontech, #631232) according to the manufacturer's protocol. Once the virus was collected it was stored at -80°C until further use.

Cell Culture

Primary human neonatal fibroblasts (HDFa, Life Technologies) were cultured in complete medium (CM) containing Dulbecco's Modified Eagle Medium (DMEM; Gibco, 11965), 10% fetal bovine serum (FBS; Gibco, 26140079), and 1% penicillin/streptomycin (Pen/Strep; GIBCO, 15140122). Passaging used 0.25% trypsin. Cells were grown to confluency before infection with dox-inducible lentiviruses. For cell cycle-synchronized studies, FBS content of media was lowered to 1% when cells reached 80% confluency and maintained for 24 hours prior to viral application. Plated hNDFs were incubated with lentivirus for BAMN together with polybrene (8 µg/mL, Sigma, #H9268) and fresh CM overnight for up to 24 hours before being replaced with fresh CM containing doxycycline (Dox; 2 ug/ml, Sigma) for transgene activation.

In the cases of chemical inhibition, chemicals were added into CM with dox and applied at the same time as transgene activation. Chemicals included: 5uM DAPT[37], 1mM Valproic acid (VPA; Cayman Chemical, Cat # 13033), 0.5μM TGF-β type I receptor ALK4/5/7 inhibitor, A83-01[55,56] (Sigma, Cat # 616454), and/or 0.5μM BMP receptor kinase ALK2 inhibitor, K02288[57,58] (Tocris Bioscience, Cat # 4986).

Spheroid Formation

Spheroids were formed 12-24 hours after dox induction. Quick aggregation has been shown to greatly enhance mESC neurogenesis over slow aggregation in petri dishes[78]. As such, we utilized a rapid centrifugation method of spheroid formation in microwells (Aggrewell). For pH studies, starting with the time of spheroid formation and onward, basal media used was HEPES-buffered DMEM buffer base (Gibco, 12430047) adjusted to pH 6.5, 7.2, 8.5, and 9 via NaOH and HCl (Sigma) titration with a benchtop digital pH meter, with the same antibiotic and FBS components. For long-term culture (beyond three days), CM was changed to N2-B27 medium: DMEM/F12 (Gibco, 11320033), N-2 supplement (Gibco, 17502048), B-27 supplement (Gibco, 17504044), 1% penicillin/streptomycin, and doxycycline (2ng/ml). Half-media changes were performed every 2-3 days.

Efficiency Calculation

Spheroids were collected from Aggrewells after three days and replated on Matrigel-coated 18-mm coverslips. Efficiency of neuronal induction was calculated as originally published[5]. Neurons were defined as Tuj1-positive cells (upon immunostaining) with a round cell body and cell process three times the length of the cell body. This number was divided by the total number of cells plated (minimum 2,000 cells). All cells on the coverslip were assessed in this way. Minimum n of 3.

Encapsulation of Spheroids in ECM

Thiolated hyaluronic acid (Lifecore, 5mg/mL at 700kDa) was mixed with 4-armed thiol terminated PEG (Laysan Bio, 2mg/ml at 20kDa) and 8-armed norbornene terminated PEG, (Jenkem, 4 mg/mL at 20 kDa). RGD peptide (Genscript, GCGYGRGDSPG) or L-Cysteine (Sigma) was added at a final concentration of 250 uM, and LAP (Sigma) at 0.025%. Crosslinking was initiated by exposure with UV light (Analytik Jena, 365 nm) for 15 seconds. Storage modulus as interrogated by rheology was around 100 Pa.

Immunofluorescent Staining and Microscopy

Cells were fixed with cold 4% paraformaldehyde (PFA; Electron Microscopy Sciences, #15710) in PBS before rinse with PBS for storage or stain. Monolayers were fixed at room temperature for 10 minutes. Spheroids were fixed at room temperature for 30 minutes to one hour, depending on size. Encapsulated spheroids were fixed at 4^{o}C overnight. Spheroids intended for cryosectioning were sequentially dehydrated thereafter, using ascending concentrations of EtOH for free spheroids (overnight), or of sucrose in OCT for encapsulated spheroids (3 days).

For staining, fixed samples or slides were rinsed three times with PBS, then permeabilized with 0.5% Triton X-100 (Sigma, T8787) in PBS for 5 minutes at room temperature (RT) for monolayers or sections, or one hour for spheroids. Samples were blocked for one hour at RT with 5% normal donkey serum (NDS; Jackson Immunoresearch, 017000121) (monolayer, sections) or 5% NDS with 0.3% Triton-X-100. Primary antibodies were diluted in blocking solution and applied overnight at 4^{o}C. Antibodies included: Tuj1 (mouse and rabbit, Biolegend #801202, 802001, respectively), N-cadherin (rabbit, Abcam, ab12221), and Ki-67 (rabbit, Abcam, ab16667). When phalloidin was applied, samples were incubated with Phalloidin Texas-Red-X (Molecular Probes, T-7471) for one hour at RT following primary antibody incubation where applicable and preceding secondary antibody. Following three PBS washes, samples were incubated with secondary antibodies diluted in 4% NDS, together with 4',6-diamino-2-phenylindole (DAPI;

Invitrogen, D3571) for one hour at RT. Secondary antibodies conjugated to Alexa Fluor® 488 or Alexa Fluor® 546 (Life Tech, Thermo Fisher) were used: donkey anti-mouse 488 (A21202), donkey anti-mouse 546 (A10036), donkey anti-rabbit 488 (A21206), donkey anti-rabbit 546 (A10040). Monolayers and sections were epifluorescently imaged with a Zeiss Axio Observer Z1 inverted fluorescence microscope and whole-spheroid images (and their corresponding monolayer controls, as applicable) were taken with a confocal inverted Leica TCS-SP8-SMD confocal microscope. 3D renderings and manipulations were performed using the Leica software.

Statistics

For two-sample comparison, two-tailed, unpaired Student's t-test was used. For multiple-sample comparison, analysis of variance (ANOVA) was performed to detect whether a significant difference existed between groups with different treatments, and a multiple-comparison Bonferonni correction applied. A p-value less than 0.05 indicated significance.

Acknowledgements

Many thanks to Dr. Marius Wernig from Stanford University for providing the BAMN constructs for iN reprogramming, and to Dr. Siavash Kurdistani from UCLA for insightful discussion of pH-related epigenetics. We would also like to thank the UCLA California Nanosystems Institute (CNSI) Advanced Light Microscopy/Spectroscopy (ALMS) Facility, particularly its staff Matt Schibler and Dr. Laurent Bentolila.

References

1. Aydin, B. & Mazzoni, E. O. Cell Reprogramming: The Many Roads to Success. *Annu. Rev. Cell Dev. Biol.* **35**, 433–452 (2019).
2. Amamoto, R. & Arlotta, P. Development-inspired reprogramming of the mammalian central nervous system. *Science* **343**, (2014).
3. Brumbaugh, J., Stefano, B. Di & Hochedlinger, K. Reprogramming: Identifying the mechanisms that safeguard cell identity. *Development (Cambridge)* **146**, (2019).
4. Vierbuchen, T. *et al.* Direct conversion of fibroblasts to functional neurons by defined factors. *Nature* **463**, 1035–1041 (2010).
5. Pang, Z. P. *et al.* Induction of human neuronal cells by defined transcription factors. *Nature* **476**, 220–223 (2011).
6. Vignoles, R., Lentini, C., d'Orange, M. & Heinrich, C. Direct Lineage Reprogramming for Brain Repair: Breakthroughs and Challenges. *Trends in Molecular Medicine* **25**, 897–914 (2019).
7. Herdy, J. *et al.* Chemical modulation of transcriptionally enriched signaling pathways to optimize the conversion of fibroblasts into neurons. *Elife* **8**, (2019).
8. Cederquist, G. Y. *et al.* Specification of positional identity in forebrain organoids. *Nature Biotechnology* **37**, 436–444 (2019).
9. Downing, T. L. *et al.* Biophysical regulation of epigenetic state and cell reprogramming. *Nat. Mater.* **12**, 1154–1162 (2013).
10. Warmflash, A., Sorre, B., Etoc, F., Siggia, E. D. & Brivanlou, A. H. A method to recapitulate early embryonic spatial patterning in human embryonic stem cells. *Nat. Methods* **11**, 847–854 (2014).
11. Kinney, M. A., Hookway, T. A., Wang, Y. & McDevitt, T. C. Engineering three-dimensional stem cell morphogenesis for the development of tissue models and scalable regenerative therapeutics. in *Annals of Biomedical Engineering* **42**, 352–367 (Kluwer Academic

Publishers, 2014).

12. Song, Y., Soto, J., Chen, B., Yang, L. & Li, S. Cell engineering: Biophysical regulation of the nucleus. *Biomaterials* **234**, 119743 (2020).
13. Recho, P., Hallou, A. & Hannezo, E. Theory of mechanochemical patterning in biphasic biological tissues. *Proc. Natl. Acad. Sci. U. S. A.* **116**, 5344–5349 (2019).
14. Howard, J., Grill, S. W. & Bois, J. S. Turing's next steps: The mechanochemical basis of morphogenesis. *Nature Reviews Molecular Cell Biology* **12**, 400–406 (2011).
15. Xue, X. *et al.* Mechanics-guided embryonic patterning of neuroectoderm tissue from human pluripotent stem cells. *Nat. Mater.* **17**, 633–641 (2018).
16. Li, X. *et al.* Small-Molecule-Driven Direct Reprogramming of Mouse Fibroblasts into Functional Neurons. *Cell Stem Cell* **17**, 195–203 (2015).
17. Hu, W. *et al.* Direct Conversion of Normal and Alzheimer's Disease Human Fibroblasts into Neuronal Cells by Small Molecules. *Cell Stem Cell* **17**, 204–212 (2015).
18. Ladewig, J. *et al.* Small molecules enable highly efficient neuronal conversion of human fibroblasts. *Nat. Methods* **9**, 575–578 (2012).
19. Holtfreter, J. A study of the mechanics of gastrulation. *J. Exp. Zool.* **95**, 171–212 (1944).
20. Moscona, A. Cell suspensions from organ rudiments of chick embryos. *Exp. Cell Res.* **3**, 535–539 (1952).
21. Pierce, G. B., Dixon, F. J. & Verney, E. Testicular teratomas. I. Demonstration of teratogenesis by metamorphosis of multipotential Cells. *Cancer* **12**, 573–583 (1959).
22. Steinberg, M. S. Mechanism of tissue reconstruction by dissociated cells, II: Time-course of events. *Science (80-.).* **137**, 762–763 (1962).
23. Pas, S. P. The rise of three-dimensional human brain cultures. *Nature* **553**, 437–445 (2018).
24. Seeds, N. W. Biochemical differentiation in reaggregating brain cell culture. *Proc. Natl. Acad. Sci. U. S. A.* **68**, 1858–1861 (1971).

25. Honegger, P. & Richelson, E. Biochemical differentiation of aggregating cell cultures of different fetal rat brain regions. *Brain Res.* **133**, 329–339 (1977).

26. Strecker, R. E., Miao, R. & Loring, J. F. *Survival and function of aggregate cultures of rat fetal dopamine neurons grafted in a rat model of Parkinson's disease*. *Exp Brain Res* **76**, (1989).

27. Keller, G. Embryonic stem cell differentiation: Emergence of a new era in biology and medicine. *Genes and Development* **19**, 1129–1155 (2005).

28. Watanabe, K. *et al.* Directed differentiation of telencephalic precursors from embryonic stem cells. *Nat. Neurosci.* **8**, 288–296 (2005).

29. Roy, B. *et al.* Laterally confined growth of cells induces nuclear reprogramming in the absence of exogenous biochemical factors. *Proc. Natl. Acad. Sci. U. S. A.* **115**, E4741–E4750 (2018).

30. Li, Y. *et al.* Compression-induced dedifferentiation of adipocytes promotes tumor progression. *Sci. Adv.* **6**, eaax5611 (2020).

31. Abbott, A. Biology's new dimension. *Nature* **424**, 870–872 (2003).

32. Mueller-Klieser, W. Three-dimensional cell cultures: from molecular mechanisms to clinical applications. *Am. J. Physiol. Physiol.* **273**, C1109–C1123 (1997).

33. Brassard, J. A. & Lutolf, M. P. Engineering Stem Cell Self-organization to Build Better Organoids. *Cell Stem Cell* **24**, 860–876 (2019).

34. Svendsen, C. N., Caldwell, M. A. & Ostenfeld, T. Human Neural Stem Cells: Isolation, Expansion and Transplantation. *Brain Pathol.* **9**, 499–513 (1999).

35. Henrique, D. & Schweisguth, F. Mechanisms of notch signaling: A simple logic deployed in time and space. *Development (Cambridge)* **146**, (2019).

36. Mall, M. *et al.* Myt1l safeguards neuronal identity by actively repressing many non-neuronal fates. *Nature* **544**, 245–249 (2017).

37. Zhang, L. *et al.* Small Molecules Efficiently Reprogram Human Astroglial Cells into

Functional Neurons. *Cell Stem Cell* **17**, 735–747 (2015).

38. Lancaster, M. A. *et al.* Guided self-organization and cortical plate formation in human brain organoids. *Nat. Biotechnol.* **35**, 659–666 (2017).
39. Guo, S. *et al.* Nonstochastic reprogramming from a privileged somatic cell state. *Cell* **156**, 649–662 (2014).
40. Smith, Z. D., Nachman, I., Regev, A. & Meissner, A. Dynamic single-cell imaging of direct reprogramming reveals an early specifying event. *Nat. Biotechnol.* **28**, 521–526 (2010).
41. Intlekofer, A. M. & Finley, L. W. S. Metabolic signatures of cancer cells and stem cells. *Nature Metabolism* **1**, 177–188 (2019).
42. McBrian, M. A. *et al.* Histone Acetylation Regulates Intracellular pH. *Mol. Cell* **49**, 310–321 (2013).
43. Hsieh, J., Nakashima, K., Kuwabara, T., Mejia, E. & Gage, F. H. Histone deacetylase inhibition-mediated neuronal differentiation of multipotent adult neural progenitor cells. *Proc. Natl. Acad. Sci. U. S. A.* **101**, 16659–16664 (2004).
44. Huangfu, D. *et al.* Induction of pluripotent stem cells by defined factors is greatly improved by small-molecule compounds. *Nat. Biotechnol.* **26**, 795–797 (2008).
45. Lee, W. *et al.* Dispersible hydrogel force sensors reveal patterns of solid mechanical stress in multicellular spheroid cultures. *Nat. Commun.* **10**, 1–14 (2019).
46. Miroshnikova, Y. A. *et al.* Adhesion forces and cortical tension couple cell proliferation and differentiation to drive epidermal stratification. *Nat. Cell Biol.* **20**, 69–80 (2018).
47. Brunet, T. *et al.* Evolutionary conservation of early mesoderm specification by mechanotransduction in Bilateria. *Nat. Commun.* **4**, 1–15 (2013).
48. Amack, J. D. & Manning, M. L. Knowing the boundaries: Extending the differential adhesion hypothesis in embryonic cell sorting. *Science* **338**, 212–215 (2012).
49. Bellis, S. L. Advantages of RGD peptides for directing cell association with biomaterials. *Biomaterials* **32**, 4205–4210 (2011).

50. Mani, S. A. *et al.* The Epithelial-Mesenchymal Transition Generates Cells with Properties of Stem Cells. *Cell* **133**, 704–715 (2008).

51. Youssef, J., Nurse, A. K., Freund, L. B. & Morgan, J. R. Quantification of the forces driving self-assembly of three-dimensional microtissues. *Proc. Natl. Acad. Sci. U. S. A.* **108**, 6993–6998 (2011).

52. Etoc, F. *et al.* A Balance between Secreted Inhibitors and Edge Sensing Controls Gastruloid Self-Organization. *Dev. Cell* **39**, 302–315 (2016).

53. Chambers, S. M. *et al.* Highly efficient neural conversion of human ES and iPS cells by dual inhibition of SMAD signaling. *Nat. Biotechnol.* **27**, 275–280 (2009).

54. Birey, F. *et al.* Assembly of functionally integrated human forebrain spheroids. *Nature* **545**, 54–59 (2017).

55. Zhang, M. *et al.* Pharmacological reprogramming of fibroblasts into neural stem cells by signaling-directed transcriptional activation. *Cell Stem Cell* **18**, 653–667 (2016).

56. Miura, S. & Suzuki, A. Generation of Mouse and Human Organoid-Forming Intestinal Progenitor Cells by Direct Lineage Reprogramming. *Cell Stem Cell* **21**, 456-471.e5 (2017).

57. Sanvitale, C. E. *et al.* A New Class of Small Molecule Inhibitor of BMP Signaling. *PLoS One* **8**, e62721 (2013).

58. Przanowski, P. *et al.* Pharmacological reactivation of inactive X-linked Mecp2 in cerebral cortical neurons of living mice. *Proc. Natl. Acad. Sci. U. S. A.* **115**, 7991–7996 (2018).

59. Macías-Silva, M., Hoodless, P. A., Tang, S. J., Buchwald, M. & Wrana, J. L. Specific activation of Smad1 signaling pathways by the BMP7 type I receptor, ALK2. *J. Biol. Chem.* **273**, 25628–25636 (1998).

60. Sart, S. *et al.* Mapping the structure and biological functions within mesenchymal bodies using microfluidics. *Sci. Adv.* **6**, eaaw7853 (2020).

61. Jeon, S. *et al.* Shift of EMT gradient in 3D spheroid MSCs for activation of mesenchymal

niche function. *Sci. Rep.* **7**, 1–13 (2017).

62. Maruthamuthu, V., Sabass, B., Schwarz, U. S. & Gardel, M. L. Cell-ECM traction force modulates endogenous tension at cell-cell contacts. *Proc. Natl. Acad. Sci. U. S. A.* **108**, 4708–4713 (2011).

63. Mertz, A. F. *et al.* Scaling of traction forces with the size of cohesive cell colonies. *Phys. Rev. Lett.* **108**, (2012).

64. Krens, S. F. G., Möllmert, S. & Heisenberg, C. P. Enveloping cell-layer differentiation at the surface of zebrafish germ-layer tissue explants. *Proceedings of the National Academy of Sciences of the United States of America* **108**, E9–E10 (2011).

65. Laurent, J. *et al.* Convergence of microengineering and cellular self-organization towards functional tissue manufacturing. *Nature Biomedical Engineering* **1**, 939–956 (2017).

66. Luxenburg, C. *et al.* Wdr1-mediated cell shape dynamics and cortical tension are essential for epidermal planar cell polarity. *Nat. Cell Biol.* **17**, 592–604 (2015).

67. Manning, M. L., Foty, R. A., Steinberg, M. S. & Schoetz, E. M. Coaction of intercellular adhesion and cortical tension specifies tissue surface tension. *Proc. Natl. Acad. Sci. U. S. A.* **107**, 12517–12522 (2010).

68. Alessandri, K. *et al.* Cellular capsules as a tool for multicellular spheroid production and for investigating the mechanics of tumor progression in vitro. *Proc. Natl. Acad. Sci. U. S. A.* **110**, 14843–8 (2013).

69. Guo, J., Wang, Y., Sachs, F. & Meng, F. Actin stress in cell reprogramming. *Proc. Natl. Acad. Sci. U. S. A.* **111**, E5252–E5261 (2014).

70. Campàs, O. *et al.* Quantifying cell-generated mechanical forces within living embryonic tissues. *Nat. Methods* **11**, 183–189 (2014).

71. Dolega, M. E. *et al.* Cell-like pressure sensors reveal increase of mechanical stress towards the core of multicellular spheroids under compression. *Nat. Commun.* **8**, 1–9 (2017).

72. Mohagheghian, E. *et al.* Quantifying compressive forces between living cell layers and within tissues using elastic round microgels. *Nat. Commun.* **9**, 1–14 (2018).

73. Wang, X. *et al.* Three-dimensional intact-tissue sequencing of single-cell transcriptional states. *Science (80-.).* **361**, (2018).

74. Eng, C. H. L. *et al.* Transcriptome-scale super-resolved imaging in tissues by RNA seqFISH+. *Nature* **568**, 235–239 (2019).

75. Su, G. *et al.* The effect of forced growth of cells into 3D spheres using low attachment surfaces on the acquisition of stemness properties. *Biomaterials* **34**, 3215–3222 (2013).

76. Madl, C. M., Heilshorn, S. C. & Blau, H. M. Bioengineering strategies to accelerate stem cell therapeutics. *Nature* **557**, 335–342 (2018).

77. Ingber, D. E. Mechanical control of tissue growth: Function follows form. *Proceedings of the National Academy of Sciences of the United States of America* **102**, 11571–11572 (2005).

78. Eiraku, M. *et al.* Self-Organized Formation of Polarized Cortical Tissues from ESCs and Its Active Manipulation by Extrinsic Signals. *Cell Stem Cell* **3**, 519–532 (2008).

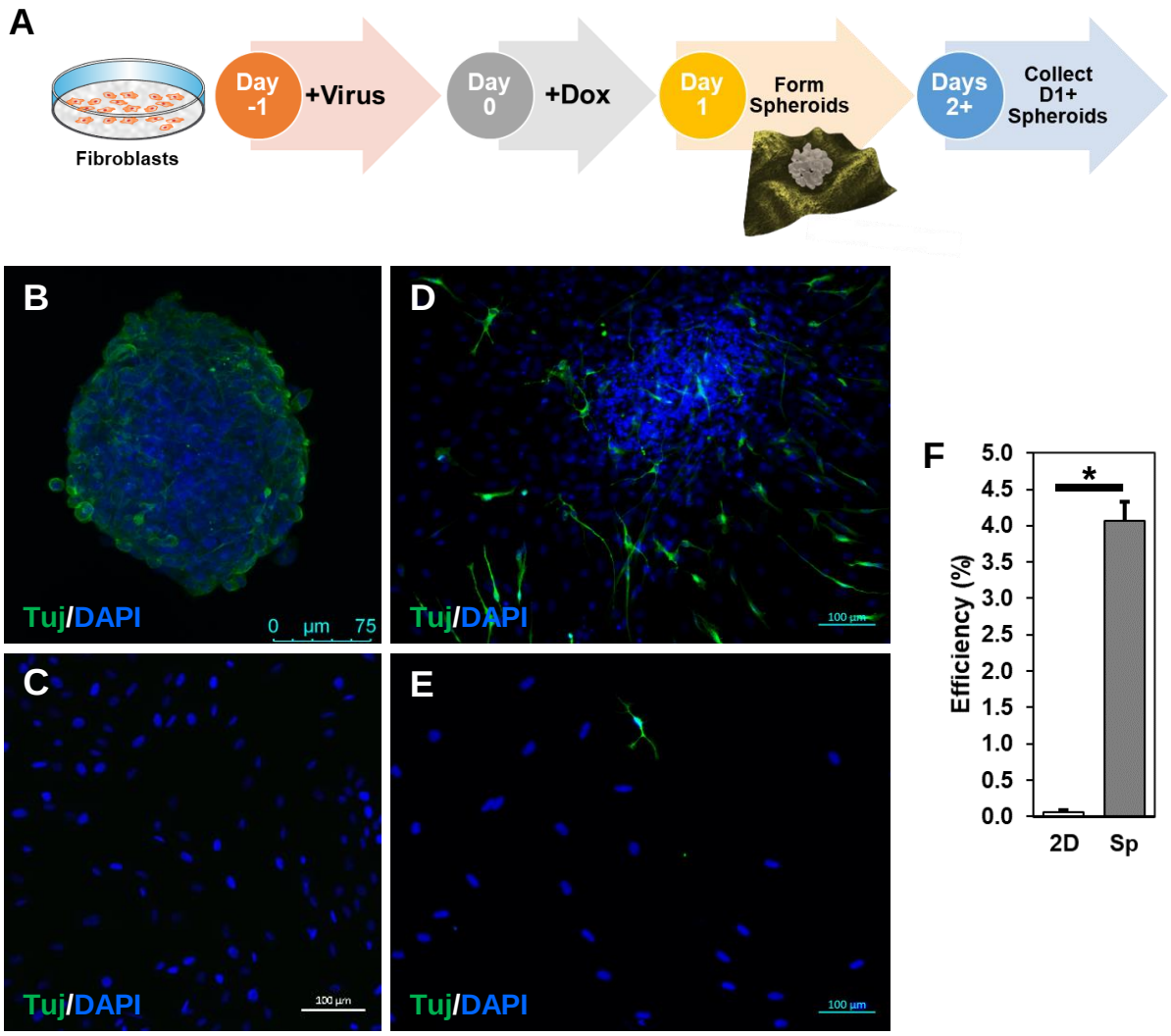

Fig. 3.1. 3D Spheroids Reprogram Earlier and More Efficiently Than 2D culture. **(A)** Schematic of reprogramming timeline. **(B-C)** Staining of β-tubulin III (Tuj1) and nuclei (DAPI) in **(B)** iN spheroids (scale bar = 75µm) and **(C)** 2D culture (scale bar = 100µm) at 2 days after Dox activation (1 day after spheroid formation). **(D-E)** Tuj1 staining of **(D)** replated spheroids and **(E)** replated single cells at 2 weeks after reprogramming induction, scale bar = 100µm. **(F)** Quantification of conversion efficiency after two weeks of reprogramming. *$p < 0.05$ (n=3).

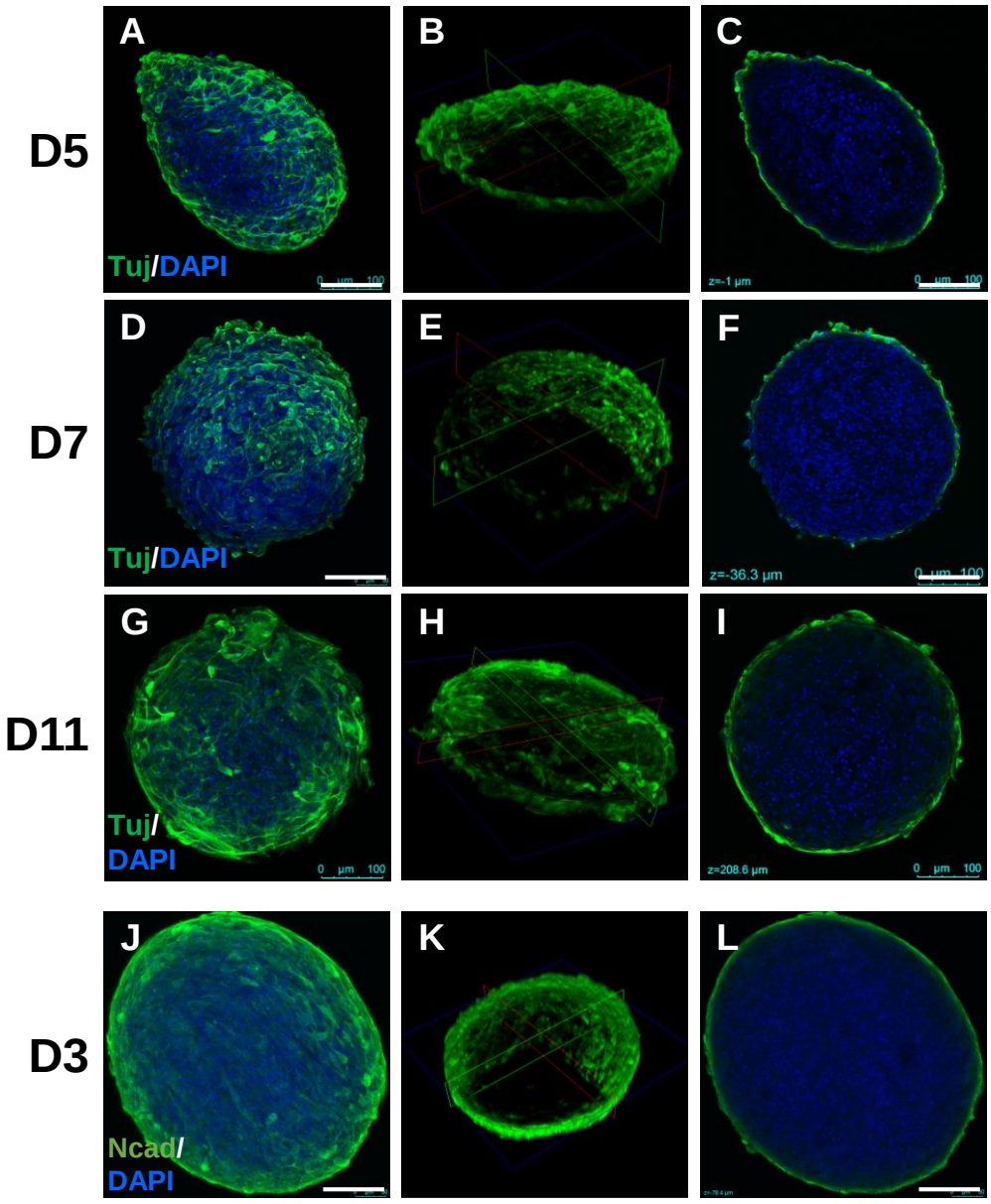

Fig. 3.2. iN Spheroid Reprogramming Displays Spatiotemporal Patterns. Confocal imaging of spheroids stained for Tuj1 (green) and DAPI (blue) at Day 5 with **(A**) maximum intensity projections of z-stacks, **(B**) 3D reconstruction of spheroid images with a quarter quadrant removed, and **(C**) an optical section through the middle of the spheroid. The same for Day 7 **(D-F)**, and Day 11 **(G-I)** are also shown. **(J-L)** N-cadherin (Ncad) and DAPI stains of spheroids at Day 3, given maximum intensity projections and quarter-sphere cutaways of 3D renderings. Scale bar = 100µm.

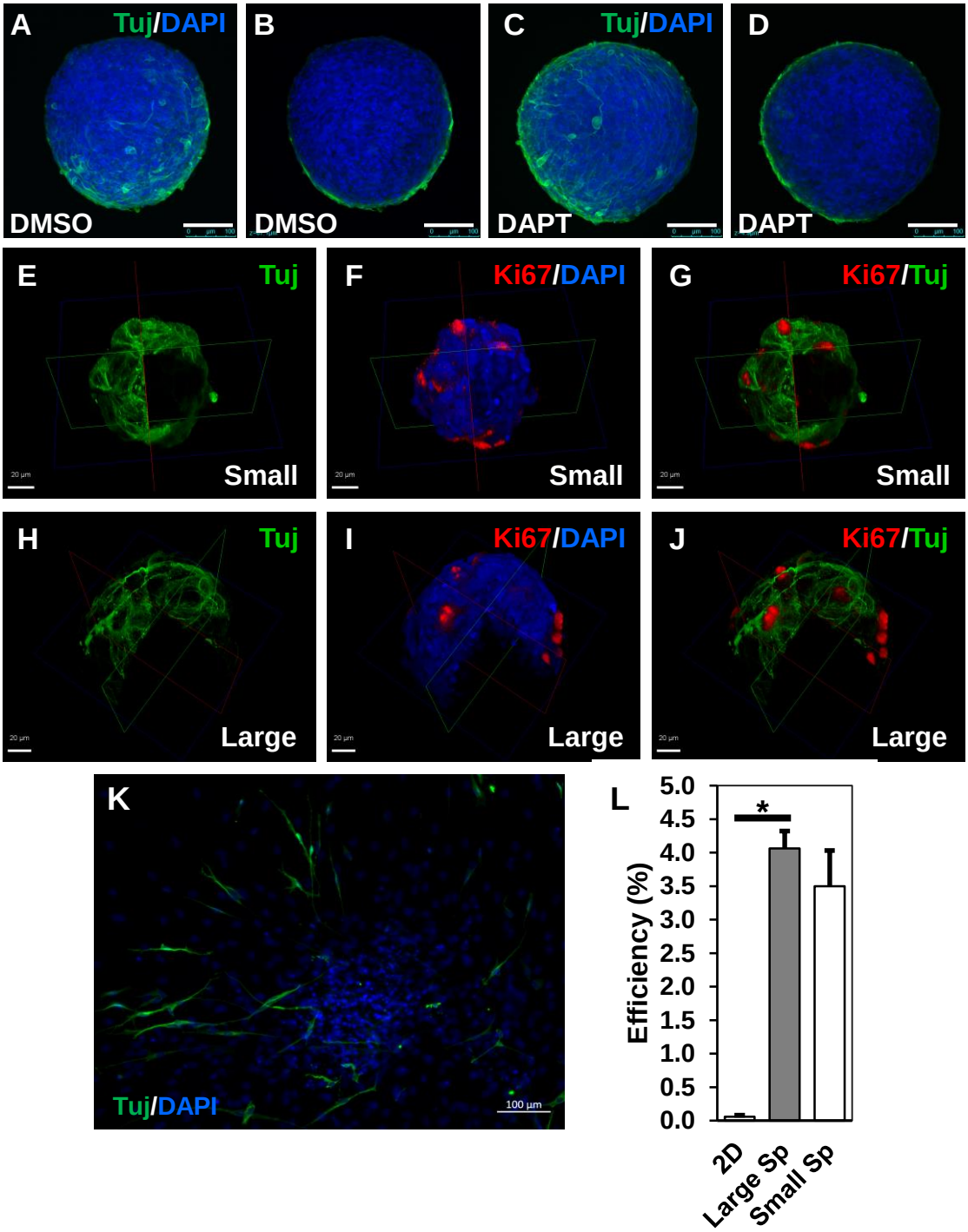

Fig. 3.3. Indirect NOTCH Inhibition and Surface Area-to-Volume Ratios Do Not Impact Spatial Patterns. Spheroids were stained for Tuj1 with DAPI in the presence of DMSO **(A-B)** or indirect NOTCH inhibitor DAPT **(C-D)** after 4 days of reprogramming. Maximum intensity projections and optical sections of the middle of spheroids are shown (scale bar = 100µm). Three days after dox induction, 3D renderings with quadrant cut-away of smaller spheroids, stained for **(E)** Tuj1, **(F)** Ki67 proliferative marker overlaid with DAPI, and **(G)** Tuj1 overlaid with Ki67 (scale bar = 20µm). **(H-J)** Depict the same for larger spheroids (scale bar = 20µm). **(K)** Spheroids were plated after 3 days and reprogrammed for a total of 2 weeks before fixation and staining for Tuj1 and DAPI nuclei, scale bar = 100µm). **(L)** Quantification of conversion efficiency after two weeks of reprogramming. Sp = spheroid. *$p < 0.05$, n=3.

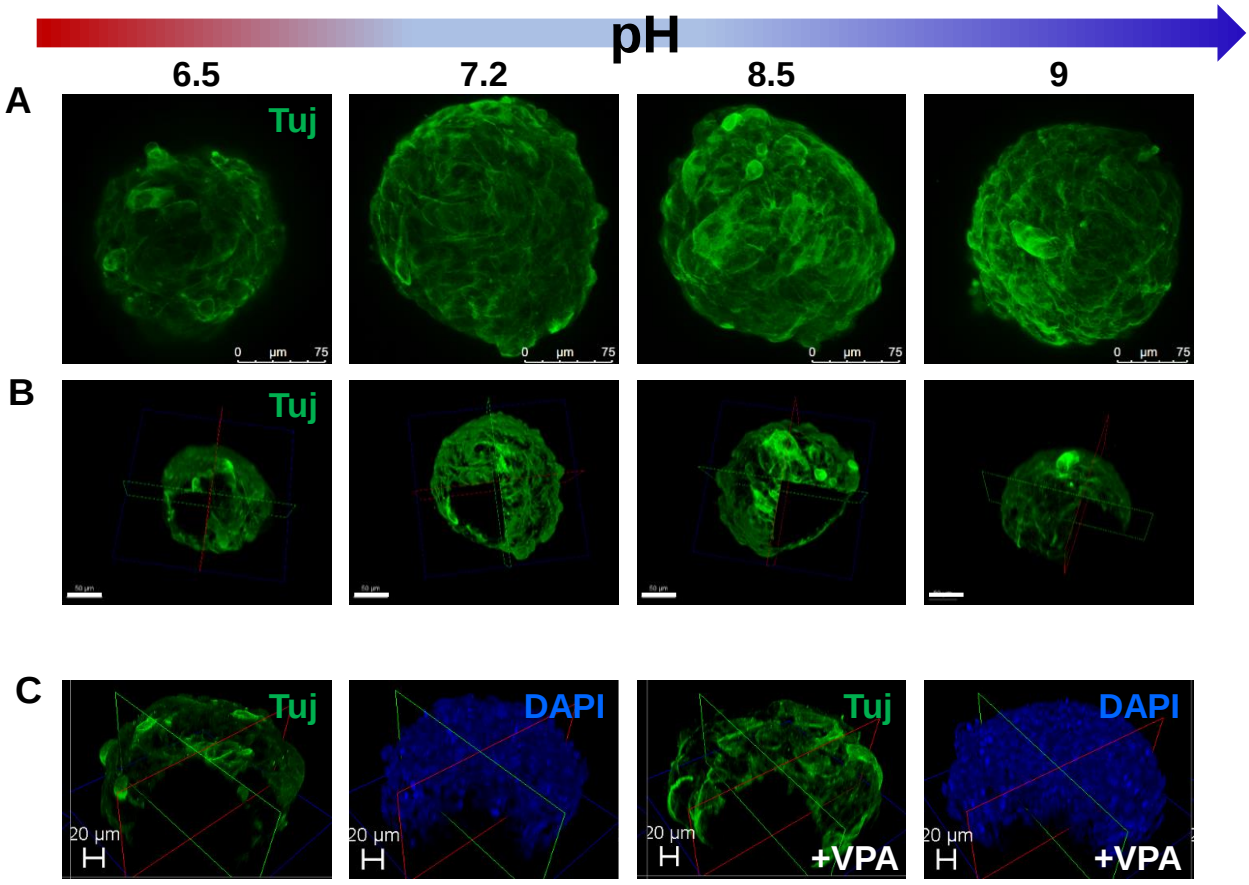

Fig. 3.4. pH Variation and HDAC Inhibition Do Not Change Reprogramming Patterns. (A-B) Tuj1 stains portrayed at pH 6.5, 7.2, 8.5, and 9 via (**A**) maximum intensity projections(scale bar = 75µm) and (**B**) 3D rendering of spheroid hemispheres with quadrant cut-aways (scale bar = 50µm). **(B)** With and without the addition of valproate (VPA), 3D renderings with a quarter cutaways of spheroids with stained for Tuj1 and DAPI (scale bar = 20µm). Same exposure conditions were used within each experiment.

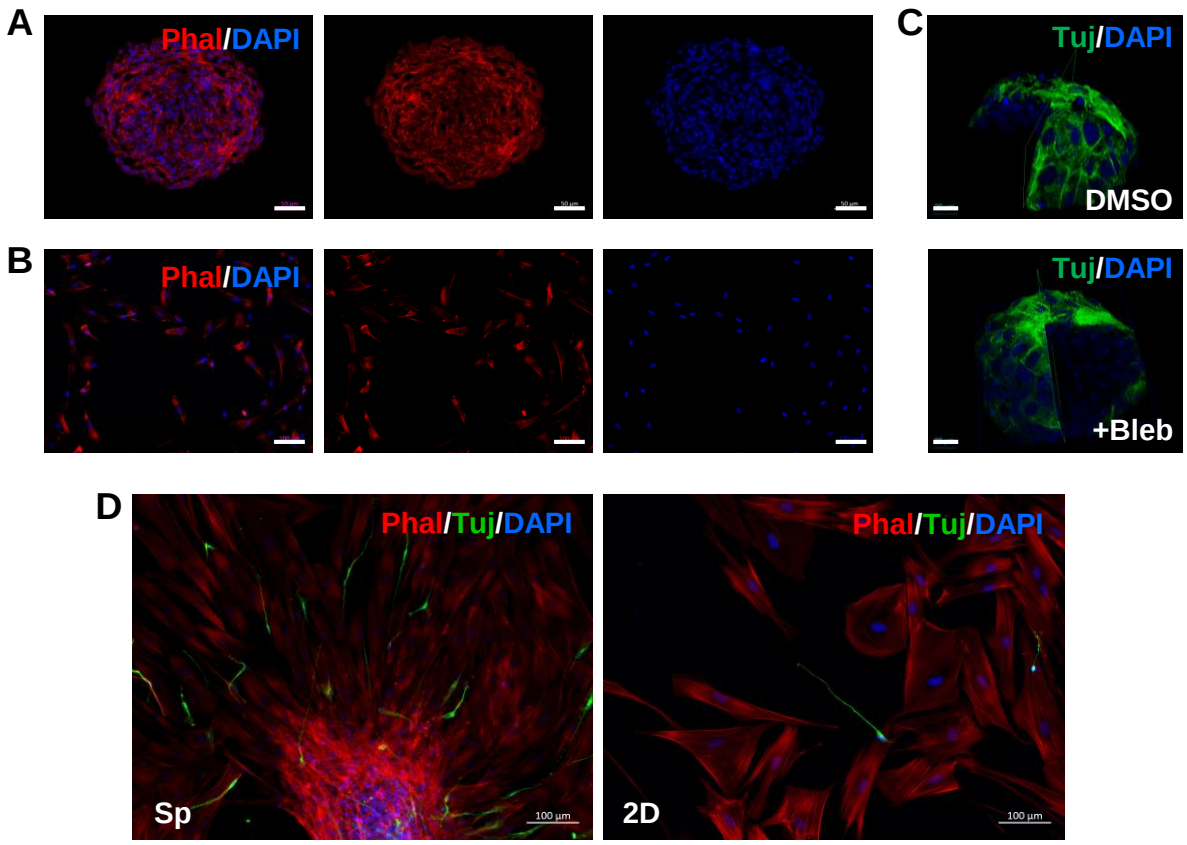

Fig. 3.5. Absolute Mechanical Tension Does Not Dictate Spatial Patterns. Phalloidin (red) and DAPI (blue) stains of **(A)** spheroid cryosections (scale bar = 50µm) and **(B)** 2D monolayers (scale bar = 100µm), 3 days after dox induction. **(C)** At the same time point, 3D renderings of Tuj1 stains with and without the addition of blebbistatin (Bleb) (scale bar = 20µm). **(D)** iN cells were replated 3 days after dox induction. Stains for phalloidin, Tuj1, and DAPI after 2 weeks of reprogramming were imaged for spheroids (Sp) and 2D culture (scale bar = 100µm).

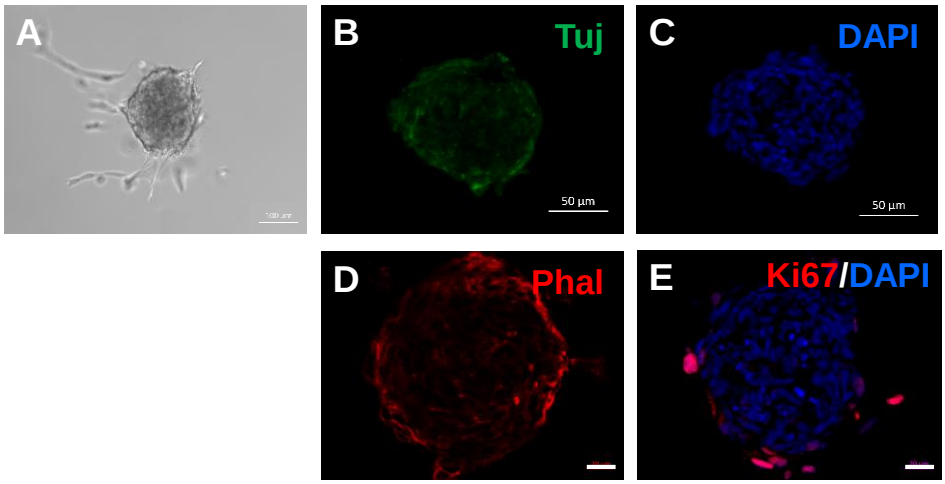

Fig. 3.6. Disruption of Adhesive Polarity Eliminates Peripheral Reprogramming. (A) Brightfield image of a spheroid embedded in HA-RGD for one day (scale bar = 100µm). **(B-E)** Spheroids encapsulated in HA-RGD for two days were stained for **(B)** Tuj1, green and **(C)** DAPI, blue (scale bar = 50µm), and **(D)** phalloidin, red, and **(E)** Ki67, red, and DAPI, blue (scale bar = 20µm).

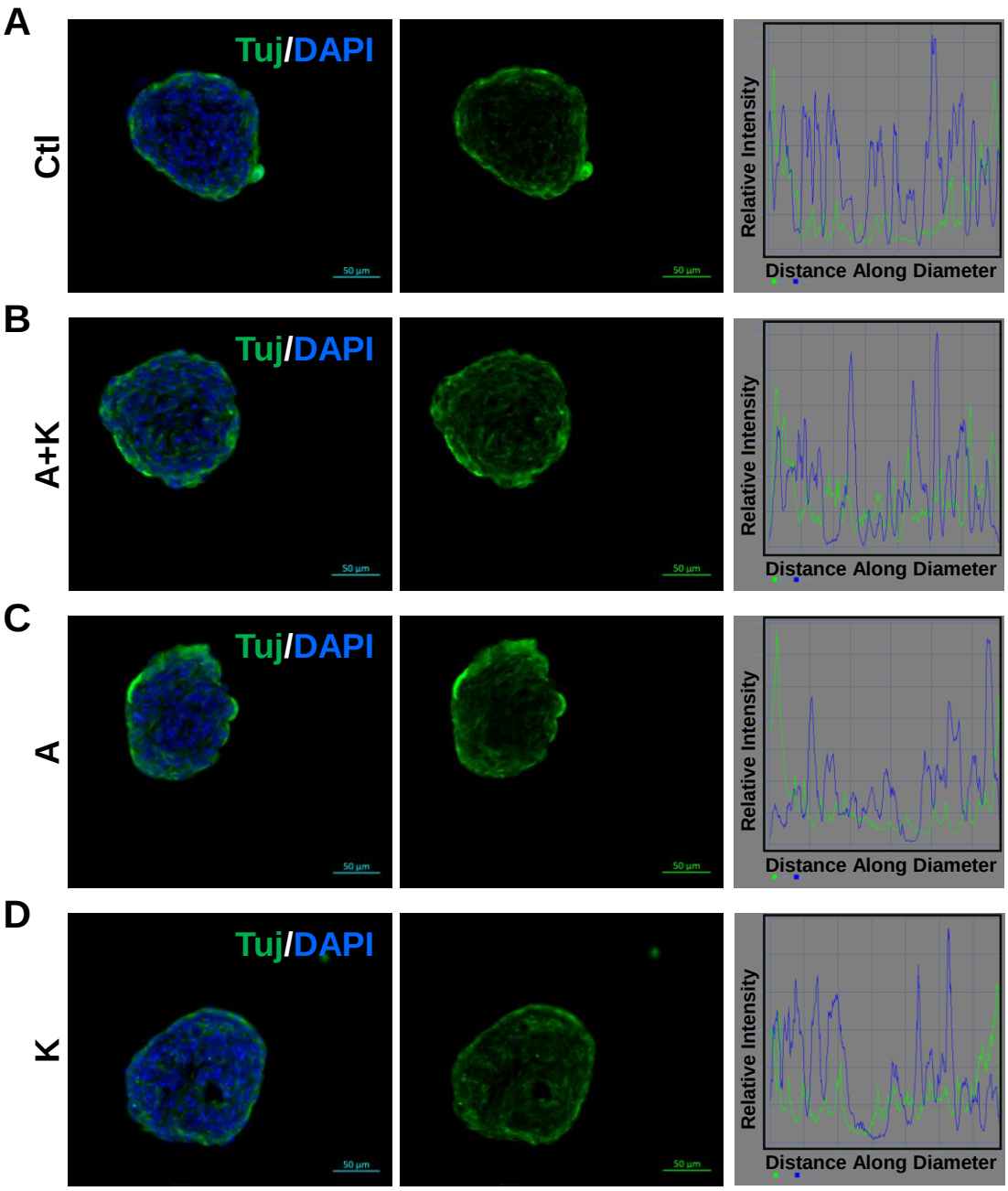

Fig. 3.7. TGF-β and BMP Pathway Inhibition Rescue Spheroid Core Reprogramming. After 3 days of reprogramming, staining of spheroids for Tuj1 (green) and DAPI (blue), including graphical depictions of their relative intensity over the diameter of the spheroid, for **(A)** controls, **(B)** application of both TGF-β type I receptor ALK4/5/7 inhibitor, A83-01 (A), and BMP receptor kinase ALK2 inhibitor, K02288 (K), **(C)** A alone, and **(D)** K alone. Scale bar = 50µm.

Chapter 4

Conclusions and Future Directions

My thesis addressed questions at the interface of cell engineering, neuroengineering, and regenerative medicine. We showed an unprecedented proof-of-concept that engineered synthetic neuromuscular tissue (SyNMT) can guide stem cell therapy to treat denervation injuries, thus developing a new stem cell therapeutic for peripheral nerve injury (PNI), and that three-dimensional (3D) spheroids can be harnessed to dramatically improve direct reprogramming into neurons.

SyNMT screening corroborated *in vivo* results in showing that neural crest stem cells (NCSCs) pose greater and more direct advantages in promoting functional neuromuscular regeneration after intramuscular transplantation for PNI, in contrast with the more nonspecific secondary effects of mesenchymal stem cells (MSCs). Our SyNMT distilled the environmental and physiological cues most relevant to our inquiry, building off our previous work in myotube alignment[1,2], into a simple and easily replicable synthetic tissue system with a geometrically-tuned, mechanically-patterned scaffold and readily interchangeable components, in which muscle and neurons could align, interact, and form junctions. Stem cell therapeutics of interest were easily added, and different aspects of stem cell function isolated and their effects on the system studied. This system as well as our mode of spheroid formation using microwells, which enables production of hundreds of spheroids from a single well, is easily scalable for higher-throughput screening.

From this initial proof of concept, there is rich potential for optimization and further development by us and others. Many and varied organ-on-a-chip systems of increasing physiological relevance are being rapidly innovated by the talented scientific community, and we hope to see them soon applied to assist in spurring on stem/cell therapy translation towards their

full potential. An intuitive future adaptation of our SyNMT system would be the placement of muscle and motor neurons (MNs) on separate electrospun membranes in two chambers of a microfluidic chip (e.g., polydimethylsiloxane [PDMS]-fabricated, similar to our microgrooves) to enable physical separation and perfusion/shear flow, perhaps with the presence of microvasculature cells as well. Other possible variations include 3D alignment and bundle formation such as with encapsulating hydrogel, electrical stimulation[3] for neuromuscular junction (NMJ) maturation[4], addition of inflammatory cytokines to simulate an inflammatory environment, matching MN and muscle position *hox* genes[5], incorporating optogenetic systems to more easily study functional connectivity[6], use of human cells, and tuning of components to improve further on myotube formation and neuromuscular (NM) assembly. Nanoscale patterning was found to be so advantageous in our system, and alternative methods of integrating these cues with these variations, such as with tuning of hydrogel ECM composition, are also possible. Sourcing MNs and/or skeletal muscle from patient tissue, or for induced pluripotent stem cell (iPSC)- or chemically induced myogenic cells (ciMC)-derivation of these cell types, would additionally provide a more personalized model of disease and therapeutic response.

The mechanistic basis for the therapeutic effect of NCSC spheroids is also of great future interest. As discussed more in Chapter 2, it is possible that NCSCs act by posing sufficient similarities to post-injury de-differentiated Schwann cells to facilitate regenerative processes, or recapitulate myogenesis and vasculogenesis enhancing processes from development in the adult. The basis of contact-dependency of regenerative benefits similarly can be postulated as involving such mechanisms, such as neuregulin and Delta1 signaling at the molecular level, but cell study at greater resolution is necessary for conclusivity. Although post-denervation interactions of nerve and muscle are not well understood, they are of great importance. Single-cell tracking and fate analysis of NCSCs could pose a unique window into these processes. Mechanistic understanding would better enable optimization of desired therapeutic outcomes.

Furthermore, we used athymic nude rats here to isolate assessment of cell benefit from any potential immunoinflammatory background that could result from xenogeneic human cell injection, but optimizing regenerative effects *in vivo* with immunocompetent animals would be a natural succession. The possibility of cell therapies immunologically compatible for functional survival within all patients is currently being explored in the field, and allele-specific knockout of the "self" immune marker human leukocyte antigen (HLA) in NCSCs or in the iPSC cell source of NCSCs could be an alternative route to explore[7,8]. If NCSC spheroids work effectively in an immunocompetent small animal model, follow-up studies in large-animal models may lead to translation into clinical applications.

On the induced neuron (iN) side, we have found that the biophysical environment of 3D spheroids can impact and drastically promote neural reprogramming, improving conversion efficiency by over 67 times. Although these improvements displayed characteristic spatial patterns localized to spheroid surfaces, we were able to rescue spheroid core reprogramming to levels on par with the spheroid periphery with the application of dual transforming growth factor- β (TGF-β)/Activin and bone morphogenic protein (BMP) pathway inhibition, which inhibits core mesenchymal phenotype for enhanced conversion to a neural one. It will be of great interest in the future to examine whether the 3D niche of spheroids can synergize with biochemical and TF inhibition as well as other methods of reprogramming promotion[9,10] to enhance conversion efficiency even further. Others, for instance, have also found that applying *in vivo* geometric boundary conditions to *in vitro* culture can promote stem cell self-organization, such as with microfabricated crypt and villi structures that directed intestinal stem cell organization into small intestinal epithelium[11], or hydrogel topographical cues for tissue formation[12–14]. At the tissue level, incorporating physiological mechanical factors improves tissue size, complexity, and tone over conventional reliance exclusively on biological cues[15]. Better understanding of mechanisms of differentiation and reprogramming may even be applied to treat cancers, a strategy termed

"differentiation therapy"[16]. Fleshing out the nuances of mechanism will enable design of tunable niches that harness mechanical and microenvironmental cues to improve cell reprogramming.

Details of mechanism may be further explored in a number of ways. Assessment of polarity from a biological marker standpoint can be performed by examining apicobasal polarity with other markers such as Par3 and E-cadherin[17], as well as closer assessment of nucleus-centrosome orientations[18]. Interactions can also be examined at single cell resolution, both mechanically and biologically: recent dispersible force sensor technology can be harnessed to quantify cell-cell as well as regional mechanical dynamics of spheroid reprogramming[19–22], and advancements in *in situ* sequencing technologies that preserve spatial information as well[23,24]. Such data would enable tighter relation of biophysical inputs to biological outputs, and vice versa. For spheroidal consistency, further studies could also be performed to determine whether different methods of spheroid formation result in different mechanobiological and reprogramming outputs. Of interest, too, would be examining whether spheroid-derived iNs had a higher tendency towards subtypes for which apicobasal polarity was more significant, such as cortical neurons[25].

Despite the advantages of successful and efficient iN reprogramming, much of this is still unrealized potential which needs to be fleshed out before clinical use. Gene and protein expression of iNs relative to primary neurons are similar but distinct, with some differences quite large[26,27]. Characterizing as well as minimizing differences at the gene, chromatin, protein, epigenetic, and functional levels are necessary if these cells are to be translated into the clinical realm. The results of transdifferentiation from cells found in proximity to the native brain open up the possibility in the more distant future of *in vivo* transdifferentiation for CNS healing[28]. Long-term stability of conversion after *in vivo* conversion or transplantation will also need to be ensured, though, as the environmental cues acknowledged to have such great impact on reprogramming similarly need to be considered for establishing longevity.

"Organoid" is the general term for multicellular structures derived from PSCs or adult organs which possess some tissue-level function[29]. Spheroids have the advantage of

reproducibility and high-throughput production, over more complex organoids[30], and in fact may aid in building complexity. Tissues formed by assemblies of spheroids compact in a more structurally stable manner with improved macro-shape relative to bioprinting single cells directly in patterns, whose contraction eliminates tissue shape[31]. As illustrated above, mechanical form and force is not just a byproduct of but also an important driver of morphogenesis and biological signaling[32,33]. Understanding of the impact of mechanical cues is thus not only valuable from a fundamental science standpoint, but also from a therapeutic one.

Barriers to central nervous system and peripheral nervous disease treatment are indubitably multifactorial, including not just scientific, but also regulatory, clinical, economic (e.g., accessible costs), and ethical components[34]. Efficacy and implementation are major barriers to current interventions for neurological disorders, and any improvement will rely jointly on innovation of treatment or prevention strategies, as well as access to and enactment of strategies of already-proven efficacy[35]. Even for conditions for which fatality is currently inevitable, rendering some patients more willing to take on risks, ethical medical practice necessitates not just safety of a therapy as a minimum standard, but also understanding of efficacy[34].

The ability to reprogram cells and stem cells lay the foundation for a new branch of regenerative medicine predicated on reconnoitering these paths and directing navigation to generate cells and tissues for regenerative replacement, disease modeling, and therapeutic testing[36–38]. Synthetic multi-tissue systems incorporating biophysical cues like ours have great potential in facilitating optimization of stem cell therapy regenerative effects, teasing out likely mechanisms of improvement in finer detail, and also moving beyond purifying and characterizing stem cells in isolation to improved evaluation of stem cells for translation to reduce the risk of complications. Significant hurdles to clinical translation remain in managing the intricacy of cell-tissue function and organized tissue assembly[29]. Engineering approaches may assist, such as with the development of self-organizing cell collectives using synthetic and biological environmental modulation of spatially designed cell building blocks. Understanding the

fundamental biological and biophysical bases of spheroid reprogramming will enable not only isolating and optimizing aspects to improve reprogramming, but also, in turn, modular scaling up of organoid assembly[30,39–41]. Altogether, integration of these considerations may assist in mutually informing and maximizing the synergy between cell and tissue engineering and regenerative medicine.

References

1. Huang, N. F. *et al.* Myotube assembly on nanofibrous and micropatterned polymers. *Nano Lett.* **6**, 537–542 (2006).
2. Huang, N. F., Lee, R. J. & Li, S. Engineering of aligned skeletal muscle by micropatterning. *Am. J. Transl. Res.* **2**, 43–55 (2010).
3. Pitsalidis, C. *et al.* Transistor in a tube: A route to three-dimensional bioelectronics. *Sci. Adv.* **4**, eaat4253 (2018).
4. Sanes, J. R. & Lichtman, J. W. DEVELOPMENT OF THE VERTEBRATE NEUROMUSCULAR JUNCTION. *Annu. Rev. Neurosci.* **22**, 389–442 (1999).
5. Lippmann, E. S. *et al.* Deterministic HOX patterning in human pluripotent stem cell-derived neuroectoderm. *Stem Cell Reports* **4**, 632–644 (2015).
6. Steinbeck, J. A. *et al.* Functional Connectivity under Optogenetic Control Allows Modeling of Human Neuromuscular Disease. *Cell Stem Cell* **18**, 134–143 (2016).
7. Gornalusse, G. G. *et al.* HLA-E-expressing pluripotent stem cells escape allogeneic responses and lysis by NK cells. *Nat. Biotechnol.* **35**, 765–772 (2017).
8. Xu, H. *et al.* Targeted Disruption of HLA Genes via CRISPR-Cas9 Generates iPSCs with Enhanced Immune Compatibility. *Cell Stem Cell* **24**, 566-578.e7 (2019).
9. Hu, W. *et al.* Direct Conversion of Normal and Alzheimer's Disease Human Fibroblasts into Neuronal Cells by Small Molecules. *Cell Stem Cell* **17**, 204–212 (2015).
10. Ladewig, J. *et al.* Small molecules enable highly efficient neuronal conversion of human fibroblasts. *Nat. Methods* **9**, 575–578 (2012).
11. Wang, Y. *et al.* A microengineered collagen scaffold for generating a polarized crypt-villus architecture of human small intestinal epithelium. *Biomaterials* **128**, 44–55 (2017).
12. Stevens, K. R. *et al.* InVERT molding for scalable control of tissue microarchitecture. *Nat. Commun.* **4**, 1–11 (2013).
13. Brandenberg, N. & Lutolf, M. P. In Situ Patterning of Microfluidic Networks in 3D Cell-Laden

Hydrogels. *Adv. Mater.* **28**, 7450–7456 (2016).

14. Xiao, W. *et al.* Brain-mimetic 3D culture platforms allow investigation of cooperative effects of extracellular matrix features on therapeutic resistance in glioblastoma. *Cancer Res.* **78**, 1358–1370 (2018).
15. Poling, H. M. *et al.* Mechanically induced development and maturation of human intestinal organoids in vivo /692/4020/2741/520/1584. *Nat. Biomed. Eng.* **2**, 429–442 (2018).
16. De Thé, H. Differentiation therapy revisited. *Nature Reviews Cancer* **18**, 117–127 (2018).
17. Luxenburg, C. *et al.* Wdr1-mediated cell shape dynamics and cortical tension are essential for epidermal planar cell polarity. *Nat. Cell Biol.* **17**, 592–604 (2015).
18. Thé, M. *et al.* Anisotropy of cell adhesive microenvironment governs cell internal organization and orientation of polarity. *Proc. Natl. Acad. Sci. U. S. A.* **103**, 19771–19776 (2006).
19. Lee, W. *et al.* Dispersible hydrogel force sensors reveal patterns of solid mechanical stress in multicellular spheroid cultures. *Nat. Commun.* **10**, 1–14 (2019).
20. Campàs, O. *et al.* Quantifying cell-generated mechanical forces within living embryonic tissues. *Nat. Methods* **11**, 183–189 (2014).
21. Dolega, M. E. *et al.* Cell-like pressure sensors reveal increase of mechanical stress towards the core of multicellular spheroids under compression. *Nat. Commun.* **8**, 1–9 (2017).
22. Mohagheghian, E. *et al.* Quantifying compressive forces between living cell layers and within tissues using elastic round microgels. *Nat. Commun.* **9**, 1–14 (2018).
23. Wang, X. *et al.* Three-dimensional intact-tissue sequencing of single-cell transcriptional states. *Science (80-.).* **361**, (2018).
24. Eng, C. H. L. *et al.* Transcriptome-scale super-resolved imaging in tissues by RNA seqFISH+. *Nature* **568**, 235–239 (2019).
25. Hakanen, J., Ruiz-Reig, N. & Tissir, F. Linking cell polarity to cortical development and malformations. *Frontiers in Cellular Neuroscience* **13**, 244 (2019).

26. Caiazzo, M. *et al.* Direct generation of functional dopaminergic neurons from mouse and human fibroblasts. *Nature* **476**, 224–227 (2011).

27. Yoo, A. S. *et al.* MicroRNA-mediated conversion of human fibroblasts to neurons. *Nature* **476**, 228–231 (2011).

28. Srivastava, D. & DeWitt, N. In Vivo Cellular Reprogramming: The Next Generation. *Cell* **166**, 1386–1396 (2016).

29. Takebe, T. & Wells, J. M. Organoids by design. *Science* **364**, 956–959 (2019).

30. Brassard, J. A. & Lutolf, M. P. Engineering Stem Cell Self-organization to Build Better Organoids. *Cell Stem Cell* **24**, 860–876 (2019).

31. Vrij, E. *et al.* Directed Assembly and Development of Material-Free Tissues with Complex Architectures. *Adv. Mater.* **28**, 4032–4039 (2016).

32. Rivron, N. C. *et al.* Tissue deformation spatially modulates VEGF signaling and angiogenesis. *Proc. Natl. Acad. Sci. U. S. A.* **109**, 6886–6891 (2012).

33. Nelson, C. M. *et al.* Emergent patterns of growth controlled by multicellular form and mechanics. *Proc. Natl. Acad. Sci. U. S. A.* **102**, 11594–11599 (2005).

34. Lindvall, O. Why is it taking so long to develop clinically competitive stem cell therapies for CNS disorders? *Cell Stem Cell* **10**, 660–662 (2012).

35. Feigin, V. L. *et al.* Global, regional, and national burden of neurological disorders, 1990–2016: a systematic analysis for the Global Burden of Disease Study 2016. *Lancet Neurol.* **18**, 459–480 (2019).

36. Aydin, B. & Mazzoni, E. O. Cell Reprogramming: The Many Roads to Success. *Annu. Rev. Cell Dev. Biol.* **35**, 433–452 (2019).

37. Amamoto, R. & Arlotta, P. Development-inspired reprogramming of the mammalian central nervous system. *Science* **343**, (2014).

38. Brumbaugh, J., Stefano, B. Di & Hochedlinger, K. Reprogramming: Identifying the mechanisms that safeguard cell identity. *Development (Cambridge)* **146**, (2019).

39. Guven, S. *et al.* Multiscale assembly for tissue engineering and regenerative medicine. *Trends in Biotechnology* **33**, 269–279 (2015).

40. Birey, F. *et al.* Assembly of functionally integrated human forebrain spheroids. *Nature* **545**, 54–59 (2017).

41. Xiang, Y. *et al.* hESC-Derived Thalamic Organoids Form Reciprocal Projections When Fused with Cortical Organoids. *Cell Stem Cell* **24**, 487-497.e7 (2019).

Chapter 5

Appendix A: Two-Phase Flow & Droplet Modeling for Therapeutic Encapsulation

Introduction

Microfluidic devices are used to manipulate volumes in “micro”-small amounts, and have acquired popularity in part due to the advantages they pose in reducing reagent usage and thus cost[1]. Tissue engineering has emerged in recent years as a way of harnessing and learning from the body’s structures and processes to treat disease, but therapy retention and longevity within the body remain the major clinical barriers to fulfilling their significant regenerative potential[2–4]. Therapeutics below the scale of whole organs span everything from cell therapies to organoids, nanoparticles to scaffolds, and are many and variable in size. Use of microfluidics could help enable various aspects of tissue engineering, including therapeutic formation, bioreactions, encapsulation, and therapeutic manipulation and isolation. Larger tissue engineering applications, however, require larger sizes than produced by conventional soft lithography (SL) [1].

The same small volumes that pose advantages for reagents have also made achieving the synthesis rates necessary for commercialization and large-scale production difficult, a difficulty exacerbated by the manufacturing variation and multi-step assembly seen with conventional SL techniques[3]. Conventional channel-based systems can be grouped into hydrodynamically-driven methods (the classic flow focusing, co-axial, and T-junction geometries) and external force-driven methods (e.g., electromagnetic fields, pneumatic micropumps)[1]. In recent years, new methods to increase throughput such as gradient confinement and parallelization of conventional structures (e.g., vertical stacking, increasing number of microfluidic units within each device, parallelized channels for simultaneous flow) have been used. A major issue accompanying parallelization, however, is that of polydispersity due to channel geometry variation and impacted fluid stream[1,5].

Riche, et al. combined parallelization and principals from gradient confinement to create a parallelizable 3D generator that also addressed the issue of flow variance. Here, the disperse phase increasingly occludes the outlet until upstream continuous phase pressure is released via shearing of the droplets at the vertical bend in the channel geometry[6]. This mechanism of droplet formation makes droplet size dependent on outlet tubing inner diameter rather than flow rates and ratios[5,7]. Furthermore, 3D printing enables greater manufacturing standardization and assembly-free use, which is advantageous over conventional soft lithography[5], as well as ability to accommodate larger dimensions that may be desired in constructs such as for tissue engineering applications described above[1].

The problem here was to handle larger therapeutics on the scale of hundreds of microns at small volumes using a scalable device. I examined two-phase flow in a 3D-printed device developed by a collaborator[6]. Specifically, I wanted to investigate how two-phase fluid flows through such a device, as well as what kind of stresses a therapeutic might experience within it.

In addition to the reasons for using this specific device as detailed above, developing a model in COMSOL Multiphysics to address these questions has several motivations. First, if a quantitatively predictive model could be developed for this device, it could be adapted in theory for other similar devices. Computer models reduce the many confounding variations (e.g., tubing clogs, material differences, premature gelation) found between real-world trials which should be identical in theory, to enable isolated examination of cause-effect and also quantification of phenomena.

Second, the many parameters that affect droplet formation not only enable minute tuning, but also necessitate empirical trial-and-error for each new combination of geometry and material in order to maintain droplet size, formation rate, and other chip demands. If a model were created, theoretical starting points for each new scenario could be calculated first to decrease usage of reagents and wet lab time[8].

Third is the biological rationale. Examining whether cells or cell constructs survive or remain intact upon device transit is a low bar. Beyond mere survival, it is becoming increasingly recognized that the stresses and forces that a cell experiences can profoundly shape its behavior, function, and phenotype. Fluid shear stress, for instance, has been found to promote cancer cell motility[9] and shape stem cell differentiation and organogenesis[10], while solid stress can activate fibroblasts to promote pancreatic cancer cell migration[11]. Biophysical cues are also now known to play a critical role in regulating epigenetic state and cell reprogramming[12,13]. As such, quantification of the forces within such a device are critical for therapeutic safety.

Methods

The ultimate goal here was to examine two-phase flow in this device. A number of assumptions were taken. 1) Empirically discovered flow ratios would hold up in the model, although I did vary these numbers to experiment with their effects as well. 2) For non-Newtonian fluid (ungelled alginate hydrogel), physical properties could be estimated to be Newtonian with constant (average) values when run at low velocity (thus low shear and stress), with the curves over a small interval appearing almost linear. 3) Flow followed the Stokes regime, as inertial effects could be neglected (capillary number calculations found later). And 4) Fully developed flow emerged from each inlet.

An analogous 2D geometry (Fig. A.1), whose computation times enabled more nimble parameter evaluation, was first used to establish droplet formation capacity for the model. To confirm the first assumption and determine whether empirically determined numbers would indeed be reasonable to use for computational modeling of the device, flow rates were tuned for droplet formation, from starting values I had previously empirically determined given these materials to form appropriate droplets in the lab. The effect of outlet tubing cut-outs in the geometry on the flow patterns and droplet formation process was next explored. The impact of fluid-wall interactions was thereafter evaluated by adding in a contact angle for the three phases, calculated with the equation: $\cos\theta_{wo} = \frac{\gamma_o \cos\theta_o - \gamma_w \cos\theta_w}{\gamma_{wo}}$, where θ_{wo}= the contact angle between water (representing aqueous gel phase) and Novec 7500 oil, γ_o= surface tension of the oil wrt (with respect to) air, θ_o= contact angle of the oil on the solid, γ_w= surface tension of water, θ_w= contact angle of water on the solid, and γ_{wo} = the interfacial tension between water and Novec. Values were found from literature and plugged in to give a final contact angle of around 99° wrt

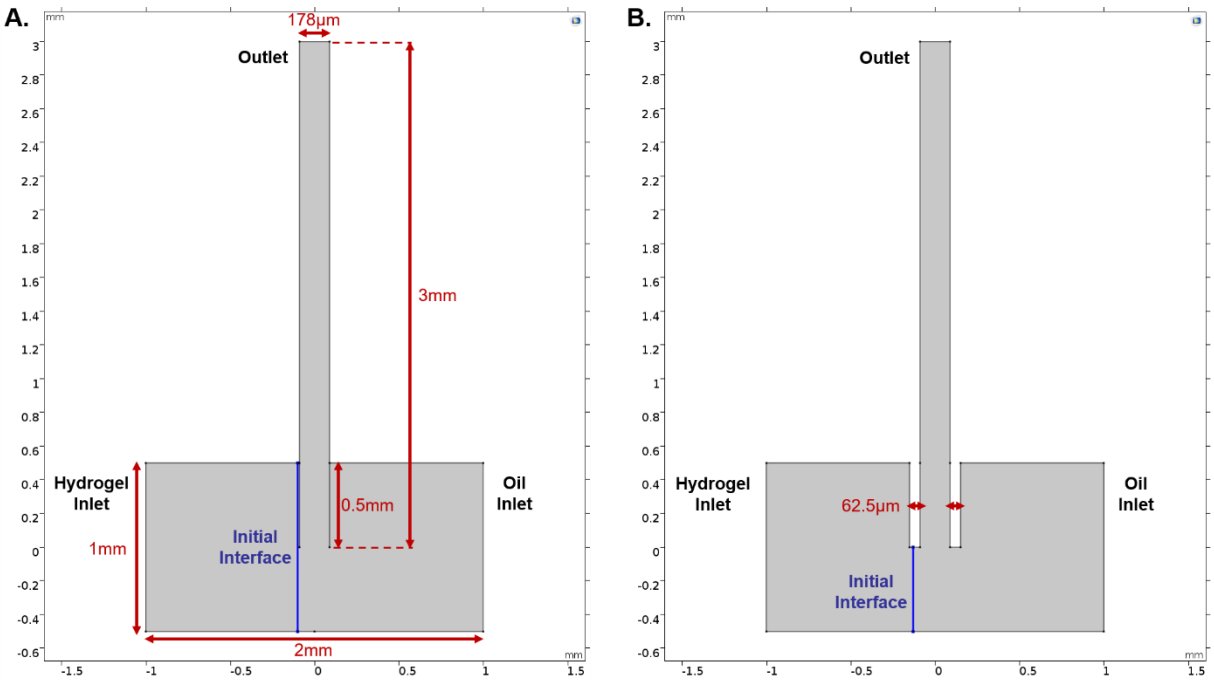

Fig. A.1. Device 2D Geometries. Two geometries were tested, the only difference between the two being the definition of interior walls without removal **(A)**, vs. the presence of the gaps around the outlet **(B)** to signify the tubing thickness and presence within the channel.

the aqueous phase, which made sense given the hydrophobic nature of the PEEK (polyether ether ketone) outlet tubing used. Volume fraction, pressure gradient, velocity magnitude and streamlines, and their timelines were studied for laminar versus Stokes flow, to assess the impact of inertial effects and the validity of the third assumption. The effect of interfacial tension on the droplet formation process was also examined. Shear stress was calculated using the equation $\tau_w = \dot{\gamma}_x \mu$, where τ_w= wall shear stress, $\dot{\gamma}_x$= shear rate, and μ = dynamic (absolute) viscosity of the phase in question (here, the gel phase is what would carry any biologics, so $\mu = \mu_{alginate}$ = 0.035 Pa*s, as defined in material properties). Maxima were calculated by taking the domain maximum of these, and relevant total stress values were calculated by taking the Total Stress in the y-direction (COMSOL's spf.T_stressy).

In 3D, I used the level set model of two-phase flow because of its ability to better visualize the interface between the fluids, which was important to me for droplet formation[13–15]. From the CAD (.stl) file of the device obtained from the Di Carlo lab, I distilled the design to the geometry where fluid interactions were most critical. Thereafter I varied a number of parameters and investigated their effect on results: 1) Inlet channel length, to examine the impact of geometry and the ability to simplify geometries (Fig. A.2); 2) Meshing, to examine the impact on visualization; 3) Inlet velocity; 4) Outlet diameter; 5) Time steps and range; 6) Location of the initial interface; and 7) Interfacial tension. Results were distilled into the figures below, and compared to 2D results

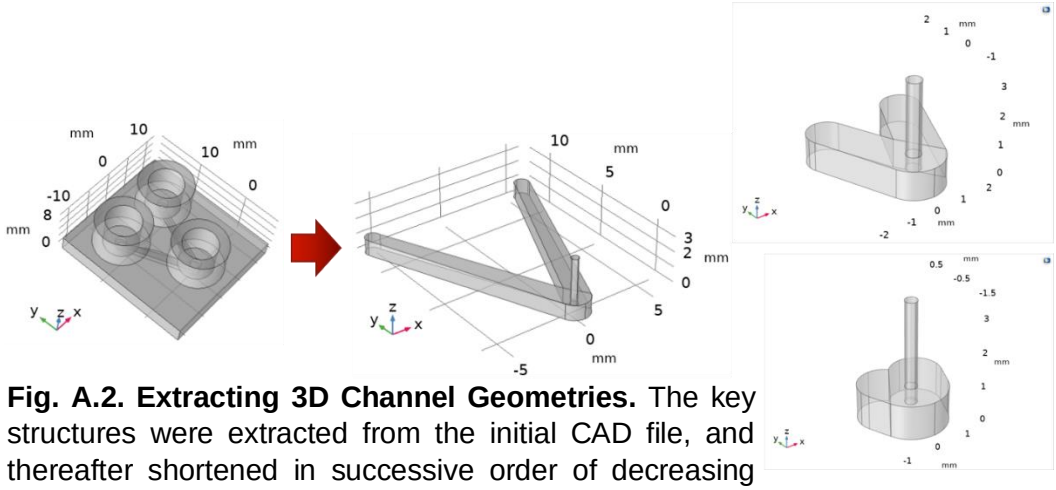

Fig. A.2. Extracting 3D Channel Geometries. The key structures were extracted from the initial CAD file, and thereafter shortened in successive order of decreasing length for 3 cases of models.

to deduce 3D flow patterns.

Results.

Running the 2D model with the inlet flow rates (Q_{in}) previously found suitable in the lab proved to be too slow to achieve reasonable times in which flows could stabilize for computed visualization. That is, fluid moved too slowly towards the outlet given computation speed. Cranking up the flow rates too high, by a few orders of magnitude, however, resulted in jetting. Q_{in} were tuned until values of $1*10^{-9}$ and $5*10^{-9}$ m^3/s for hydrogel ($Q_{in,H}$) and oil ($Q_{in,O}$), respectively, proved successful within somewhat more reasonable computation times (Fig 3). In both geometries, with and without outlet tubing cut-outs, the flow patterns and droplet formation process were not significantly different and stabilized to the same result (Fig. A.3A-D), so for simplicity the interior walls were not removed for simulations thereafter in 2D and 3D. Droplet

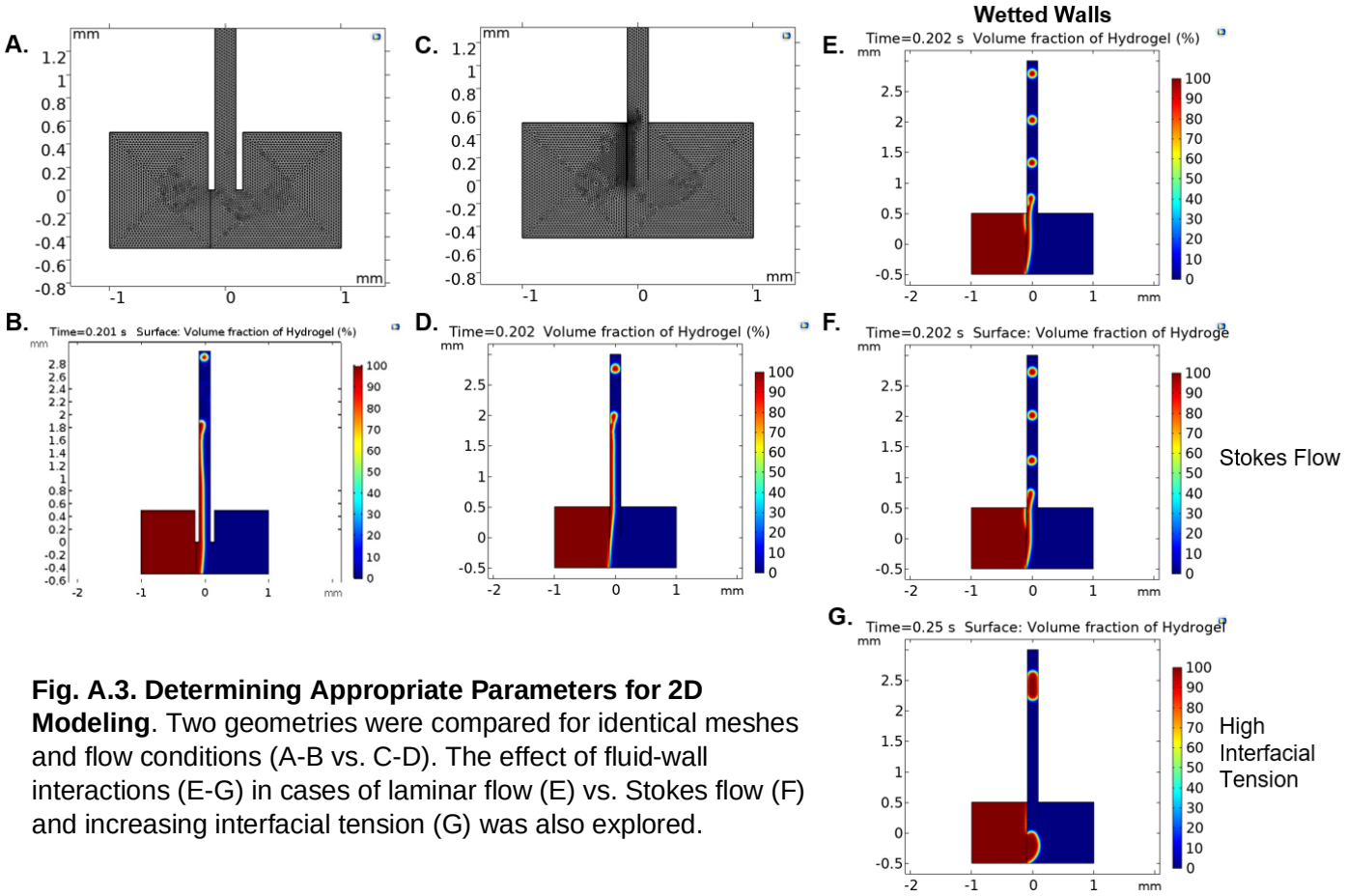

Fig. A.3. Determining Appropriate Parameters for 2D Modeling. Two geometries were compared for identical meshes and flow conditions (A-B vs. C-D). The effect of fluid-wall interactions (E-G) in cases of laminar flow (E) vs. Stokes flow (F) and increasing interfacial tension (G) was also explored.

formation was almost identical for laminar vs. Stokes flow (Fig. A.3E, F), which confirmed Assumption #3 (see “Methods”). Including consideration of wall wetting (Fig. A.3E-G) facilitated droplet formation, as it became energetically favorable to minimize contact surface area (i.e., to form droplets).

Of interest is the evolution of the pressure gradients over the course of droplet formation (Fig. A.4). In the initial stationary condition, pressure builds up at the corner of the initial interface, peaking in front of the vertical outlet (~204.83 Pascals, or Pa). Pressure builds on the hydrogel side, as the more viscous gel pushes against the lower-viscosity but faster-flowing oil ($Q_{in,O}$ is five-fold higher). The entire interface develops a slightly parabolic curve, in keeping with the flow profile, as the edge of the initial interface closest to the outlet opening where pressure is greatest, pushes the hydrogel out and into the outlet. As hydrogel increasingly stretches into the outlet, pressure first builds on the side of the hydrogel inlet, then propagates higher up the outlet tubing,

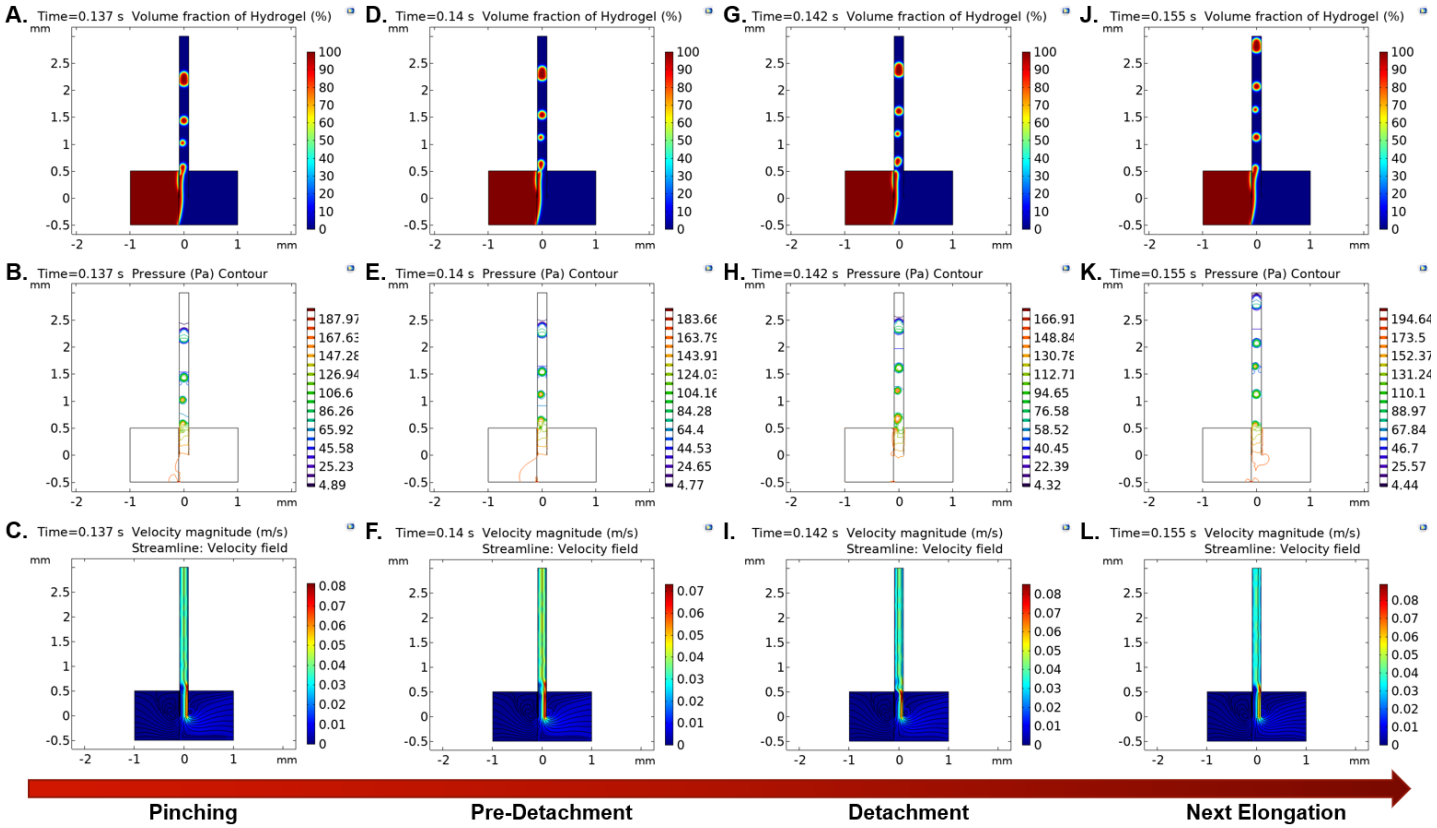

Fig. A.4. 2D Gel-in-Oil Droplet Generation: Hydrogel Fractional Volume, Pressure, and Velocity Profiles.

preferentially increased on the side of the outlet tubing closest to the hydrogel inlet. Droplet formation begins around 0.09 seconds (sec), and reaches droplet equilibrium size at around 0.14 sec. A gel droplet emerges from the homogenously outstretched gel when the increase of pressure on the gel side and balance of interfacial energies favors pinching off of the droplet, as seen in the pressure drop around the pinch (Fig. A.4A-C). An area of low pressure encircles the droplet of higher-pressure hydrogel. Pressure builds on either side of the pinching gel just prior to detachment due to the back-up of oil behind the gel drop partially occluding the outlet, with resultant eddies of low pressure surrounding each side of the partial occlusion and a simultaneous velocity increase of the adjacent oil phase (Fig. A.4D-F). Upon detachment (Fig. A.4G-I), velocity magnitude increases as pressure is released. The gel itself always flows at slower velocity than the oil. Pressure build up again on the oil side leads to the next droplet stretching out, an increase of pressure on the inlet side, followed by the next detachment (Fig. A.4J-L). Overall, plot results revealed that the area of greatest pressure was at the beginning of the outlet tubing, as could be expected, while velocity was high there as well but achieved greatest magnitude further downstream, with the speed of oil directly after droplet formation with pressure release. Velocity slowed wherever hydrogel (including hydrogel droplets) was found, and was greatest close to the outlet midline. Pressure and velocities decreased as droplets flowed further downstream.

Single phase flow follows the Stokes profile, with highest velocity in the middle of the channel (Fig. A.5B-C), but transition to two-phase flow compresses the velocity surface to one side of the outlet. This phenomenon seen in 2D (Fig. A.5A) would be expected to be replicated in the 3D channel. Similarly, the velocity field streamlines (black) demonstrate how the 2D patterns of entering the outlet tubing from either side (Fig. A.5D) occurs in 3D: namely, fluid flow does not

only enter the outlet via the side proximal to the inlet, but also wraps around the tube to enter the outlet tubing from all directions, though still preferentially on the half near the material's inlet.

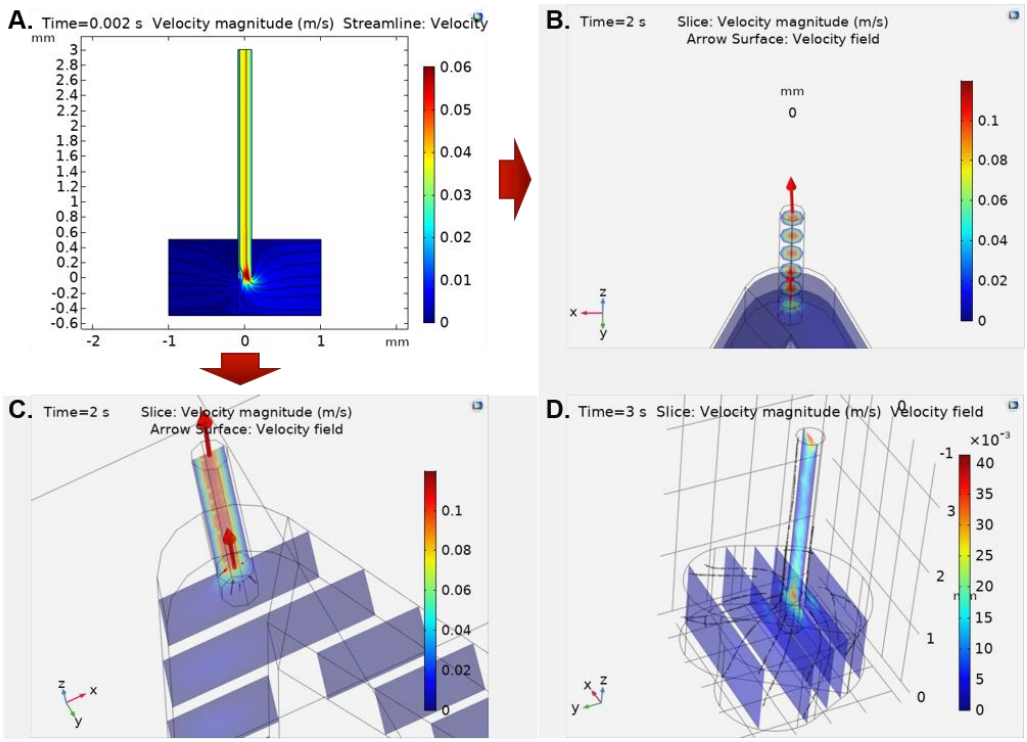

Fig. A.5. Comparison of 2D vs. 3D Velocity Magnitudes and Streamlines.

Similarly, 2D model comparison to 3D results can shed light on likely pressure and gel fractional volume patterns. In 2D, the pressure magnitudes in the outlet tubing decrease as one moves further downstream. This was already seen in the pressure contours of 3D models prior to droplet formation (Fig. A.6A) regardless of degree of channel truncation, and could be inferred to continue being the case with the pressure disturbances seen around droplet formation. For gel fractional volume, computation was too slow to see the gradual emergence of larger proportions of hydrogel (closer to red) into the channel, but the flow of the lower fractional volumes (green, Fig 6B) likely heralded the continued flow pattern of hugging the side closest to the outlet tubing by larger fractions of gel in the 3D channel as well, as seen in 2D.

As described above, shear stress and total stress have profound influences on cells' behavior, function, and phenotype, and are a critical concern in the use of microfluidics for cellular therapies as well as other biologics. Plots were generated in order to quantify these forces at work on the particle. The maximum forces that therapeutics like spheroids would have to withstand was of greatest concern. First the maximum shear stress in the device including all boundaries except the oil inlet was calculated for each time point (Fig. A.7A). Cross-examination of the peak of ~280 Pa at ~0.066 sec in Fig. A.7A with Fig. A.7B shows that the high total stress values are found at the bottom of the oil inlet and initial interface, suggesting that they result from the flow of oil rather than gel and that initial spikes in oil flow resulted in higher shear stress and total stress values that a therapeutic would not be exposed to. In all graphs, values became regularly oscillatory after steady-state droplet production was achieved at around 0.09 seconds. This reflected the modality of droplet formation via gel occlusion of the continuous oil phase. Max shear stress thereafter seemed to stay less than around 220 Pa, decreasing further perhaps with increased steadiness of flow.

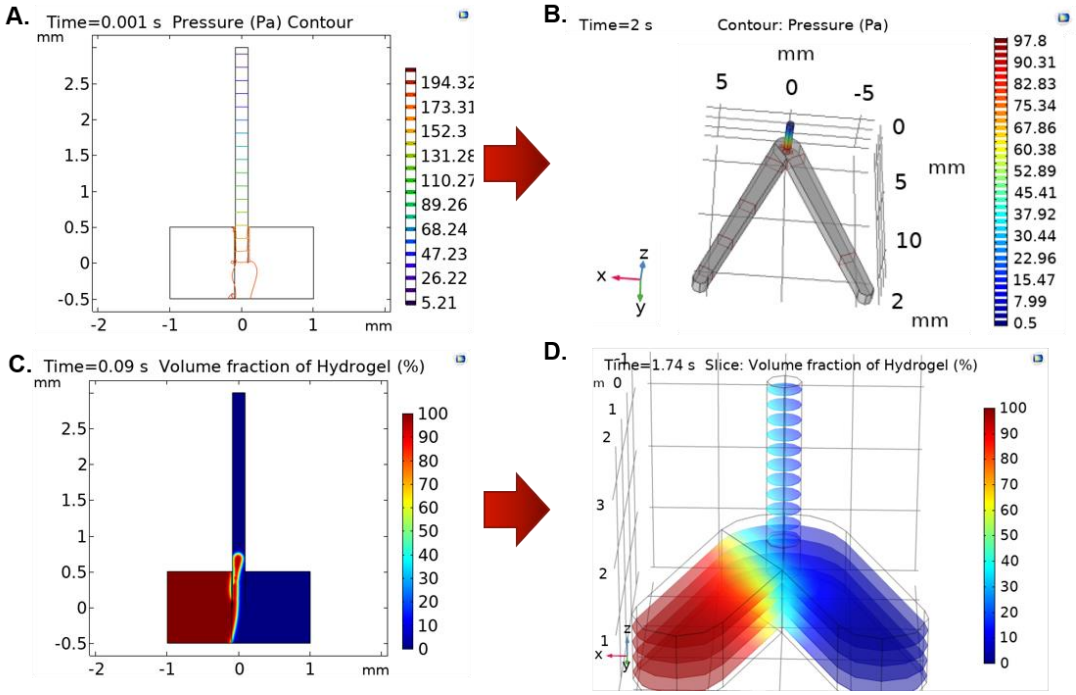

Fig. A.6. Comparison of 2D vs. 3D Pressure and Gel Fractional Volume

Examination of shear stress along the length of the outlet as well as in outlet cross-sections was further enlightening. From Fig. A.7D it is apparent that the high shear values reside on the side of the outlet tubing closest to the oil inlet, i.e., from the faster flow of fluorinated oil. The gel phase itself, which Fig. A.4 and now Fig. A.7E shows was primarily found on the side of the gel inlet at the channel opening where shear stresses are greatest, appears to reach a peak of around 38.25 Pa at the inlet opening, which when cross-referenced with the Outlet Opening boundary (cyan) of Fig. A.7B, appears at ~0.065 seconds, when droplet sizes of either extreme appear, and stabilizes after droplet formation equilibrium to levels no more than 12.75 Pa.

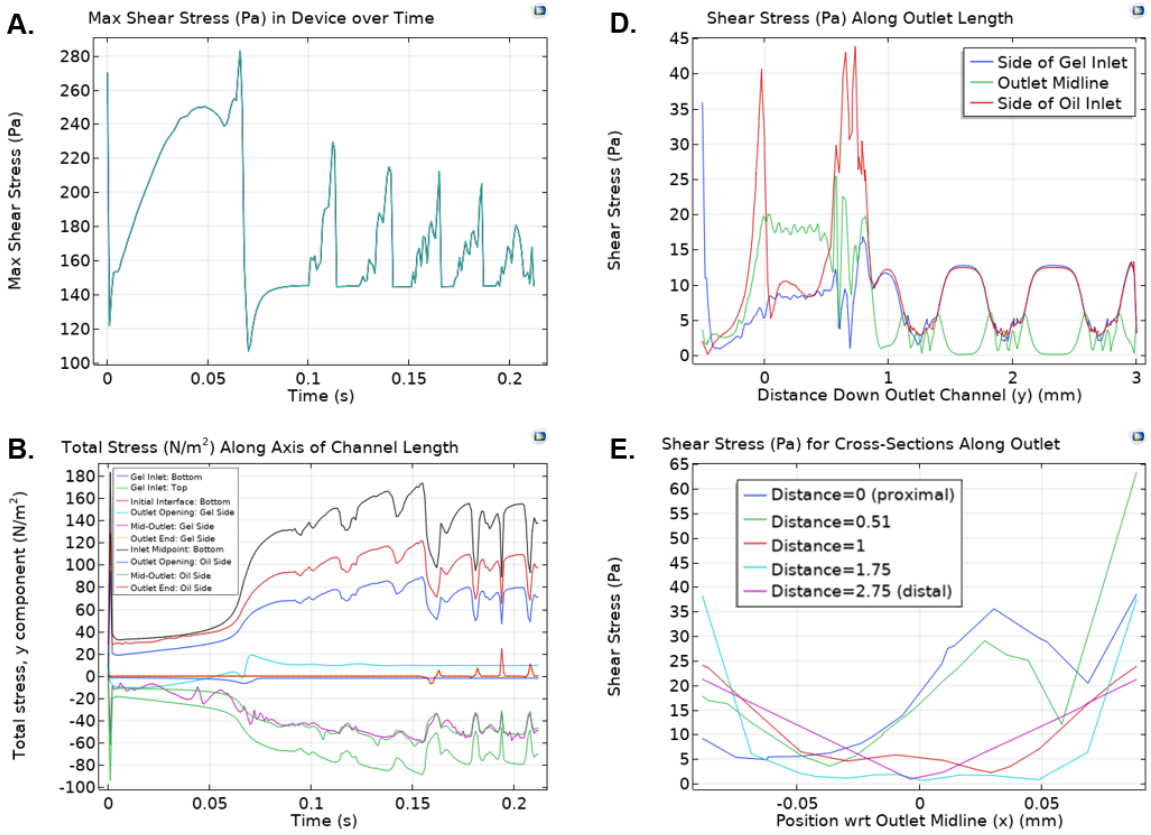

Fig. A.7. Forces Produced in 2D Two-Phase

Discussion.

Here I characterized physical phenomena of biological relevance arising from two-phase flow of alginate and fluorinated oil in a 3D-printed device. Transitioning the model into 3D required significantly longer computation times. As such, it was found that the most practical examination of 3D flows given computational constraints would focus on the differences in flow prior to droplet formation, itself also a period of importance, exploring this preceding interval in greater detail, and directed comparison with 2D. At these scales, liquids behave in a regime described by Reynolds number (Re), which is the ratio of inertial to viscous forces, and generally in microfluidics accepted ≤1, i.e., viscous forces more important, unless the device is specifically designed to harness inertia[1]. Indeed, Re is around 0.001. Microfluidic droplet formation is determined by the physics of confinement as well as the relation between viscous forces and surface tension. Other numbers, capillary number (η_d=0.035 Pa*s for alginate, $U_{d,mc}$=0.001m/s, γ_{eq}= 0.005 N/m[16]) of 0.007 (<1) and We number of <<1 (fluid inertial force $2.4015*10^{-7}$ N/m), indicates interfacial and surface tension forces govern generation and stabilization of droplets here and inertia is insignificant. The marked impact on model droplets of including fluid-wall interactions and changing interfacial tensions show too how models can aid surfactant and material design decisions.

Study of device flow patterns develop intuition of how different geometries impact flow, and aid understanding of how to harness different aspects of a device to study specific questions[17,18]. For instance, shear stress may be more significant for shaping cell behavior than simply shear rate[10]. Force quantification revealed our site of greatest concern for therapeutic shear stress was the area of sudden cross-sectional transition (outlet tube), and at its walls. Due to high wetting of walls with Novec, it is perhaps not unreasonable to consider that a sheath of oil could carry gel particles, protecting aqueous phase contents from direct shearing contact. If so, the shear stresses just inside outlet wall boundaries after equilibrium is reached are of more relevant concern. Shear rates >5000 s^{-1} are considered pathologic[17]. Values here peaked at 8000

s^{-1}, equilibrating to <6000 s^{-1}. However, we recall that flow rates were increased by a little more than an order of magnitude from lab-used values, so actual forces adjust to be well within safe range. Overall, results illustrate the utility of quantitative models, and biological safety via decreased shear transit of larger 3D-printed devices.

References.

1. Mashaghi, S., Abbaspourrad, A., Weitz, D. A. & van Oijen, A. M. Droplet microfluidics: A tool for biology, chemistry and nanotechnology. *TrAC - Trends in Analytical Chemistry* **82**, 118–125 (2016).
2. Hill, E., Boontheekul, T. & Mooney, D. J. Regulating activation of transplanted cells controls tissue regeneration. *Proc. Natl. Acad. Sci. U. S. A.* **103**, 2494–9 (2006).
3. Ho, S. S., Murphy, K. C., Binder, B. Y. K., Vissers, C. B. & Leach, J. K. Increased Survival and Function of Mesenchymal Stem Cell Spheroids Entrapped in Instructive Alginate Hydrogels. *Stem Cells Transl. Med.* **5**, 773–781 (2016).
4. Nguyen, P. K., Neofytou, E., Rhee, J.-W. & Wu, J. C. Potential Strategies to Address the Major Clinical Barriers Facing Stem Cell Regenerative Therapy for Cardiovascular Disease. *JAMA Cardiol.* **1**, 953 (2016).
5. Choi, A., Seo, K. D., Kim, D. W., Kim, B. C. & Kim, D. S. Recent advances in engineering microparticles and their nascent utilization in biomedical delivery and diagnostic applications. *Lab Chip* **17**, 591–613 (2017).
6. Riche, C. T., Roberts, E. J., Gupta, M., Brutchey, R. L. & Malmstadt, N. Flow invariant droplet formation for stable parallel microreactors. *Nat. Commun.* **7**, 10780 (2016).
7. Gu, H., Duits, M. H. G. & Mugele, F. Droplets formation and merging in two-phase flow microfluidics. *International journal of molecular sciences* **12**, 2572–2597 (2011).
8. Bhattacharjee, N., Urrios, A., Kang, S. & Folch, A. The upcoming 3D-printing revolution in microfluidics. *Lab on a Chip* **16**, 1720–1742 (2016).
9. Lee, H. J. *et al.* Fluid shear stress activates YAP1 to promote cancer cell motility. *Nat. Commun.* **8**, 1–14 (2017).
10. Yamamoto, K. *et al.* Fluid shear stress induces differentiation of Flk-1-positive embryonic stem cells into vascular endothelial cells in vitro. *Am. J. Physiol. - Hear. Circ. Physiol.* **288**, (2005).

11. Kalli, M., Papageorgis, P., Gkretsi, V. & Stylianopoulos, T. Solid Stress Facilitates Fibroblasts Activation to Promote Pancreatic Cancer Cell Migration. *Ann. Biomed. Eng.* **46**, 657–669 (2018).
12. Downing, T. L. *et al.* Biophysical regulation of epigenetic state and cell reprogramming. *Nat. Mater.* **12**, 1154–1162 (2013).
13. Huebsch, N. *et al.* Harnessing traction-mediated manipulation of the cell/matrix interface to control stem-cell fate. *Nat. Mater.* **9**, 518–526 (2010).
14. Modeling and Simulation of Multiphase Flow in COMSOL®: Part 1 | COMSOL Blog. Available at: https://www.comsol.com/blogs/modeling-and-simulation-of-multiphase-flow-in-comsol-part-1/. (Accessed: 23rd March 2019)
15. CFD Software for Simulating Fluid Flow Applications. Available at: https://www.comsol.com/cfd-module. (Accessed: 23rd March 2019)
16. Lucio, A. A. *et al.* Spatiotemporal variation of endogenous cell-generated stresses within 3D multicellular spheroids. *Sci. Rep.* **7**, 12022 (2017).
17. Costa, P. F. *et al.* Mimicking arterial thrombosis in a 3D-printed microfluidic: In vitro vascular model based on computed tomography angiography data. *Lab Chip* **17**, 2785–2792 (2017).
18. Choi, N. W. *et al.* Microfluidic scaffolds for tissue engineering. *Nat. Mater.* **6**, 908–915 (2007).

Chapter 6

Appendix B: Adult Stem Cells in Vascular Remodeling

IVYSPRING INTERNATIONAL PUBLISHER

Theranostics

2018; 8(3): 815-829. doi: 10.7150/thno.19577

Review

Adult Stem Cells in Vascular Remodeling

Dong Wang[1*], LeeAnn K. Li[1, 2*], Tiffany Dai[3], Aijun Wang[4], Song Li[1, 5]✉

1. Department of Bioengineering, University of California, Los Angeles, CA 90095, USA;
2. David Geffen School of Medicine, University of California, Los Angeles, CA 90024, USA;
3. Department of Bioengineering, University of California, Berkeley, CA 94720, USA;
4. Surgical Bioengineering Laboratory, Department of Surgery, School of Medicine, University of California, Davis, Sacramento, CA 95817, USA;
5. Department of Medicine, University of California, Los Angeles, CA 90095, USA.

* Equal contribution

✉ Corresponding author: Song Li, Ph.D., phone: +1 310-2065819, email: songli@ucla.edu

Received: 2017.02.08; Accepted: 2017.10.01; Published: 2018.01.01

Abstract

Understanding the contribution of vascular cells to blood vessel remodeling is critical for the development of new therapeutic approaches to cure cardiovascular diseases (CVDs) and regenerate blood vessels. Recent findings suggest that neointimal formation and atherosclerotic lesions involve not only inflammatory cells, endothelial cells, and smooth muscle cells, but also several types of stem cells or progenitors in arterial walls and the circulation. Some of these stem cells also participate in the remodeling of vascular grafts, microvessel regeneration, and formation of fibrotic tissue around biomaterial implants. Here we review the recent findings on how adult stem cells participate in CVD development and regeneration as well as the current state of clinical trials in the field, which may lead to new approaches for cardiovascular therapies and tissue engineering.

Key words: Cardiovascular disease; Stem cell; atherosclerosis; vascular grafts; vascular smooth muscle cell.

Introduction

Cardiovascular diseases (CVDs) such as ischemic heart disease, stroke, and peripheral artery disease are the leading cause of mortality and morbidity around the world: about 30% of global deaths and 10% of global disease burden a year are due to CVDs [1, 2]. In the past three decades, these diseases have been increasing in underdeveloped and developing countries. Although deaths from CVDs have declined in some developed countries with better healthcare interventions and systems and primary prevention, population growth and aging will drive up global CVDs in coming decades [1, 2].

Atherosclerosis is a chronic inflammatory disease resulting in clogged arteries or unstable plaque rupture [3, 4]. Currently, treatment of atherosclerosis includes reducing risk factors such as treatment of hypercholesterolemia and hypertension [1, 2] and, for advanced disease, surgery such as stent implantation and bypass surgery using autologous vessels or tissue-engineered vascular grafts [5]. However, thrombosis and secondary atherosclerosis are common complications following stent and graft implantation, particularly in small-diameter arteries and grafts [6]. New therapies are thus urgently needed for better prevention and treatment of atherosclerosis.

It is widely accepted that endothelial cell (EC) dysfunction, inflammatory cell recruitment, and vascular smooth muscle cell (SMC) de-differentiation contribute to atherogenesis [3, 4, 7]. In the past two decades, several types of vascular stem cells (VSCs), in addition to circulating progenitors, have been identified and characterized, with evidence that they are not only involved, but also play pivotal roles in blood vessel remodeling and disease development. VSCs or similar stem cells in mesenchymal tissues, for instance, also participate in the regeneration of blood vessels following the implantation of vascular grafts.

Elucidating the regulatory mechanisms of these VSCs is fundamental to understanding vascular remodeling and may pave the way to developing novel, successful therapies for atherosclerosis. In this review, we analyze vascular remodeling through the lens of stem cells, and discuss the challenges we face in developing improved therapies for vascular diseases and regeneration.

Overview of atherosclerotic vascular remodeling

Large and medium size blood vessels have three distinct layers: 1) the tunica intima, an inner lining of ECs, which may contain a small number of endothelial progenitor cells (EPCs) [8, 9]; 2) the tunica media, a thick middle layer composed of smooth muscle cells (SMCs) and a small number of stem cells; and 3) the tunica adventitia, an outer layer of connective tissue containing a heterogeneous population of cells, including fibroblasts, resident inflammatory cells (including macrophages, dendritic cells, T cells and B cells), microvascular (vasa vasorum) ECs around which pericytes reside, adrenergic nerves, and also stem cells (including multipotent mesenchymal stem cells, or MSCs) and progenitor cells (including those with macrophage, endothelial, smooth muscle, and hematopoietic potential) [10-18]. All these cells contribute, to varying extents, to the pathogenesis of atherosclerosis and vascular remodeling.

Atherosclerosis is thought to be initiated by dysfunctional or activated ECs [3, 7]. Various risk factors include genetic defects and environmental risks, behaviors like cigarette smoking and harmful use of alcohol, as well as disturbed blood flow, hypertension, hypercholesterolemia, infections, and other chronic conditions such as diabetes, obesity, autoimmune diseases, and aging [1, 2]. The injured endothelial area may be repaired by adjacent EC proliferation or EPCs from bone marrow or resident endothelium [19]. Disease begins when such endothelial repair does not occur properly.

Malfunctioning ECs secrete cytokines and upregulate expression of surface adhesive molecules to recruit circulating platelets, monocytes, T cells, neutrophils, dendritic cells, and mast cells to adhere to the site of endothelial injury and infiltrate into the subendothelial space. Within this space, monocytes differentiate into macrophages and scavenge lipid deposited from the circulation, becoming foam cells in the process [3, 20-22]. Notably, most of these foam cells are initially derived from preexisting intimal-resident myeloid progenitors rather than recently recruited blood monocytes [23]. In addition, the inflammatory cells activate medial SMCs and stem cells, prompting adventitial stem cells to proliferate and migrate into the intima, where they may differentiate and also obtain some properties of myofibroblasts and macrophages [3, 20-22, 24, 25]. Disease proceeds as the abnormal vascular wall processes prompt macrophages, together with leukocytes, activated ECs, and SMCs, to secrete increasing amounts of inflammatory cytokines to recruit more inflammatory cells from the circulation and resident adventitial tissues. This forms a cycle of inflammatory responses in local atherosclerotic lesions [3, 4, 26-28]. All these events lead to the development of fatty streaks, formation of neointima, and thickening of arterial walls seen at the early stages of atherosclerosis [3, 26]. The extracellular matrix, too, may play a role in lipid retention [29]. As these atherosclerotic lesions continue to grow and narrow the lumen, arteries may attempt to compensate by gradual dilation; however, this compensation reaches its limit beyond a certain size of atherosclerotic lesion.

Advanced atherosclerotic plaques have developed a fibrous cap that sequesters the underlying inflammatory mixture, which includes foam cells and extracellular lipid droplets, infiltrated T cells, macrophages, and mast cells, and necrotic tissue [3, 26]. The cap itself is mainly comprised of SMCs and collagen matrix, which can be degraded and ruptured by metalloproteases released by macrophages and mast cells. Stability of plaques is thus defined by thickness of the fibrous cap. Severe thrombosis may occur upon fibrous cap rupture, leading to acute coronary artery disease (myocardial infarction) and stroke [3, 26].

Several groups provide direct evidence that smooth muscle myosin heavy chain $(SM\text{-}MHC)^+$ SMCs are a major contributor to neointimal thickening and atherosclerotic lesions, using transgenic mice with tamoxifen-regulated CreER under the control of a SM-MHC promoter (SM-MHC-CreER) [22, 30-33]. Interestingly, some studies suggest that SMCs in human atherosclerotic lesions are monoclonal [34, 35], implying heterogeneity of the SMC population. By using multi-colored lineage tracing in $ApoE^{-/-}$/SM-MHC-CreER/Rosa26-Confetti transgenic mice, a recent study demonstrates that only a small number of SMCs proliferate and contribute to atherosclerotic plaques [36]. This is consistent with our single-cell analysis of SMCs showing that only a small subpopulation of SMCs is capable of proliferation and differentiation (unpublished data). However it is worth noting that, in addition to medial SMCs, other non-SMCs such as stem cells and ECs also contribute to the SMCs of neointima and atherosclerotic lesions [22, 33, 37, 38],

while lesional macrophage-like cells can also be derived from SMCs [39], suggesting alternative mechanisms may also account for vascular disease development.

Endothelial to mesenchymal transition (EndoMT) is one possible mechanism. Some studies utilized Tie2-Cre mice for lineage tracing ECs and found that ECs contribute to pulmonary artery neointimal formation by differentiating into cells positive for smooth muscle α-actin (α-SMA) [40, 41]. However, other researchers found a very low frequency, in contrast, of EndoMT in the neointima [38]. Similarly, using Tie2-Cre mice to trace ECs in carotid artery neointimal formation, we found that although ECs contributed to neointimal formation, they still maintained endothelial identities and expressed CD31 but no or low α-SMA expression [37]. This discrepancy requires further investigation with different animal models and tissue locations, and still leaves open the possibility of additional mechanisms for neointimal pathogenesis.

Stem cells in vascular remodeling

In addition to vascular SMCs and ECs, vascular stem and progenitor cells have been isolated from the circulation and from different layers of the artery wall, and have been implicated in vascular disease development. Key examples found in or around the vasculature are summarized in Table 1. The list is organized based on differentiation potential and tissue(s) of origin, and is discussed in detail below.

Table 1. Vascular stem cells and progenitors

Location	Markers	Species/Tissue	Cell	Differentiation	*In vivo* function	Year
Adventitia	Stro1$^+$, CD105$^+$, CD73$^+$, CD44$^+$, CD90$^+$, CD29$^+$, Oct4$^+$, Sox2$^+$ [92, 93]	Human internal thoracic artery	Vascular wall-resident multipotent stem cells	Adipocyte, chondrocyte, osteocyte, SMC	Neovascularization, (Putative) neointima formation and tumor vascularization	2011, 2013
Adventitia	CD34$^+$, vWF$^-$, CD31$^-$, Sox2$^+$ [94]	Human saphenous vein	Saphenous vein-derived progenitor	Myocyte , osteoblast, adipocytes, neuron-like cell	Neovascularization	2011
Adventitia	Sca-1$^+$ [99, 100, 193]	Mouse aortic root	Adventitia progenitors	SMC, EC	Atherosclerotic lesion	2004, 2008, 2012
Adventitia	Sca-1$^+$, CD45$^+$ [28]	Mouse aorta	Macrophage progenitors	Macrophages	Inflammatory response	2014
Adventitia	Sca-1$^+$, CD34$^+$ [33]	Mouse aortic root, carotid arteries, descending aorta, femoral arteries	Vascular, myeloid progenitors	Mature SMCs, resident Macrophages, Endothelial-like cells	(Putative) Maintenance of resident vascular progenitor cell population	2016
Adventitia	Gli1$^+$, Sca1$^+$, CD34$^+$, PDGFRβ$^+$[118]	Mouse arteries	Adventitial progenitors	SMCs, osteoblast-like cells	Neointima, calcification	2016
Adventitia and media	Sox10$^+$, Sox17$^+$, CD29$^+$, CD44$^+$, S100β$^+$, NFM$^+$ [25, 194]	Human, rat and mouse arteries and veins; normal and diseased vessels	MVSC	SMC, osteoblast, chondrocyte, adipocyte, neural lineages	Neointima, proliferative SMC, osteochondrogenic	2012
Media	CD29$^+$, CD44$^+$ 3G5$^+$, SMA$^+$ [83, 84]	Bovine and human thoracic aorta	CVC/MSC	SMC, osteoblast, chondrocyte	Not reported (N/R)	2002, 2010
Media	Sca-1$^+$, c-kit$^{-/low}$ Lin$^-$, CD34$^{-/low}$ [85]	Mouse thoracic and abdominal arteries	Side population	SMC, EC	N/R	2006
Media	CD44$^+$, CD56$^+$, CD90$^+$, CD105$^+$, CD34$^-$ and CD45$^-$ [87]	Porcine aorta	Pericyte-like, MSC-like vascular progenitors	Adipocyte, Osteocyte, Chondrocyte	N/R	2014
Intima	CD13$^+$, CD29$^+$, CD44$^+$,CD54$^+$, CD90$^+$ [98]	Human saphenous vein-internal surface	Vein MSC	Osteoblasts, chondrocytes, adipocytes	N/R	2005
Around microvessel	N/R [195, 196]	Bovine retina	Pericyte	Osteoblast, chondrocyte, adipocyte	Chondrogenic and adipogenic in diffusion chambers	1990, 2004
Around microvessel	NG2$^+$, alkaline phosphatase$^+$ or CD146$^+$, NG2$^+$, and PDGFR-β$^+$ [197, 198]	Human skeletal muscle, pancreas, adipose tissue, and placenta	Pericyte/ peri-vascular MSCs	Skeletal muscle, Osteoblast, chondrocyte, adipocyte	Muscle regeneration, ectopic bone formation	2007, 2008
N/R	CD34$^+$, Tie-2$^+$, NG2$^+$, nestin$^+$, PDGFR-α$^+$, PDGFR-β$^+$ [112]	Rat aorta	Pericyte progenitor	Pericyte	N/R	2005
N/R	Oct-4$^+$, Stro-1$^+$, Sca-1$^+$, Notch-1$^+$, CD44$^+$, CD90$^+$, CD105$^+$, CD73$^+$, CD29$^+$, CD166$^+$ [14]	Human aortic arches, thoracic and femoral arteries	MSC	SMC, chondrocyte, adipocyte	N/R	2010

Bone marrow-derived progenitor or stem cells

Bone marrow cells were reported to differentiate into SMCs in neointima and atherosclerotic lesions in the early 2000s [42-45]. These findings, however, remain controversial, as later studies in vascular transplant and injury models countered by arguing that bone marrow-derived cells did not in fact differentiate into neointimal SMCs, although they did participate in the inflammatory response [46-48]. A mouse wire injury model, for instance, found that some bone marrow cells were recruited to the neointima and expressed α-SMA, but never became positive for mature SMC marker SM-MHC. Rather, these bone marrow cells expressed markers of monocytes and macrophages [48].

Other bone marrow-derived cells – specifically, certain EPCs – have also been identified as important for endothelial regeneration. It should be noted that the term "endothelial progenitor cell" has been applied to many different cell types, and defining what precisely it means to be an EPC is a source of controversy. Classification traditionally is divided into two methods: antigen classification, and culture-based classification. Both have been used to identify vascular-relevant EPCs.

Using the first method, cell-surface antigens are examined typically with flow cytometry to quantify relevant populations. Putative EPCs were first isolated by Asahara *et al.* (1997) from human peripheral blood by flow cytometry using surface markers CD34 and vascular endothelial growth factor receptor 2 (VEGFR-2, also known as kinase insert domain receptor, KDR, or fetal liver kinase 1, Flk1), both of which are characteristically expressed by ECs [49]. These circulating cells could contribute to neoangiogenesis postnatally by homing to angiogenic sites and acquiring characteristics of endothelium. Thereafter, other groups reported that EPCs contribute to endothelial regeneration in rodent models after various arterial injuries including vein graft atherosclerosis and mechanical injury [50-52], as well as in human diabetic wound healing [53].

Studies further showed that EPCs are in fact a heterogeneous population comprised of different subpopulations with different cell surface markers. In addition to CD34 and VEGFR-2, in an attempt to distinguish between immature and mature endothelial cells, investigators also commonly use markers like CD133 (also known as AC133), which is lost during endothelial maturation [54]. For example, Peichev et al. (2000) identified a unique subpopulation of EPCs ($CD34^+/VEGFR\text{-}2^+/AC133^+$) in human fetal liver and peripheral blood [55]; another subpopulation of $Flk1^+/AC133^+/CD34^-/VE\text{-}cadherin^-$ cells were also identified as EPCs in human bone marrow [56]. Despite the advantages of having specific markers for lineage tracing and drawing ties between disparate populations, one can see here too how antigen-based definitions may still be somewhat nonspecific in phenotype. The more antigen markers utilized, the more specific the definition, but also the fewer the cells identified – particularly considering the inherently probabilistic nature of antigen carriage for given cell types.

In the second method of classification, cells are isolated based on *in vitro* culture. Given the difficulties of finding specific surface markers for EPCs, some research groups isolated EPCs by single-cell colony-formation assay (SCCFA) based on the high self-renewal and proliferation potential of stem cells. Some studies subdivided EPCs based on their time of appearance in culture into populations which, interestingly, have different differentiation potential: early EPCs cannot differentiate into ECs, but only differentiate into macrophages and contribute to angiogenesis through paracrine factors, and thus were named as myeloid angiogenic cells (MACs); and late EPCs can differentiate into ECs and contribute to *de novo* blood vessel formation, and were dubbed endothelial colony forming cells (ECFCs) [57-61].

In addition to circulation-derived EPCs, EPCs with similar properties have been derived based on colony-formation assay from the vascular endothelium of large human blood vessels, placenta, and adipose tissue [62-64]. Mouse ECFCs have also been isolated from endothelial culture by surface markers $lin^-CD31^+CD105^+Sca1^+c\text{-}Kit^+$, with c-Kit expression found to be critical for the clonal expansion of these ECFCs [65].

Beyond the nature of EPC classification, their functions, too, remain controversial. The concept of bone marrow-derived EPCs playing a fundamental role in the mechanism of vascular repair and regeneration has acquired many proponents as we described, though it remains hotly debated [66]. Pre-clinical animal studies showed that transplanted human EPCs formed microvessels and promoted vascular regeneration *in vivo* [49, 55, 56, 67, 68]. In mouse models of vascular graft transplantation, for instance, bone marrow cells contributed to the regenerated ECs of the grafts [50, 69, 70]. Nevertheless, another study countered that bone marrow-derived EPCs do not contribute to vascular endothelium in mouse models of bone marrow transplantation, tumor formation, and a parabiotic system [71].

A role for bone marrow-derived EPCs in atherogenesis similarly has been inferred, but accumulation of solid evidence in this role is mixed

and still work in progress [52]. In an ApoE$^{-/-}$ mouse model, bone marrow-derived Sca-1^{+}/CD34^{+}/Flk-1^{+}/CD133^{+} EPCs were found in the lesion-prone area of endothelium, possibly for repairing the injured endothelium [72]. However, other studies have said that, although there may exist a population of bone marrow-derived EPCs, ECs derived from the vascular bed are instead responsible for the EC replacement and regeneration seen in transplant arteriosclerosis [73].

In the clinical context, the role of EPCs remains unclear. Large-scale clinical studies suggested that high levels of EPCs were associated with reduced risk of cardiovascular diseases [74, 75] and improved outcomes after acute ischemic stroke [76-78] (versus poorer stroke outcomes if blood EPCs failed to increase [79]), and that vascular trauma, acute coronary diseases, and stroke induced elevated level of EPCs [76, 80, 81], presumably for purposes of vascular repair and maintenance. However, some also found no clear correlation between EPC level and endothelial function [82].

To date, much ambiguity and controversy remains in regards to the existence of true EPCs that can differentiate into ECs, their marker expression, location, and contribution to endothelial regeneration. It is possible that EPCs are a rare but dynamic population that respond to specific stimuli such as severe endothelial injury of large arteries or vascular transplantation [50, 69, 70], but not to tumor growth, which involves microvessels [71].

Medial stem cells

Stem and progenitor cells resident to vasculature have been identified across the different vessel wall layers. Similar to the bone marrow-derived progenitor cells, isolation has relied on antigen selection or culture-based characterization. Although those derived from the adventitia are better characterized and supported – evidence which will be elaborated momentarily – a few groups of stem cells have also been characterized in the media.

A population of calcifying vascular cells (CVCs) was first isolated from human atherosclerotic lesions in the arterial medial layer by Boström *et al*. (1993) and Tintut *et al*. (2003) and found to differentiate into SMC, osteogenic, and chondrogenic lineages [83, 84]. CVCs were harvested by tissue explant culture and were identified as expressing CD29 and CD44, two non-specific mesenchymal cell markers (adhesion receptors). However, no specific transcriptional markers were identified.

Later, in 2006, Sainz *et al*. isolated a small population of Sca-1^{+}, c-kit $^{(-/low)}$, Lin^{-}, CD34$^{-/low}$ cells from the media layer (around 6±0.8% prevalence in tunica media) of healthy murine thoracic and abdominal aortas [85]. They used a Hoechst DNA binding dye method to identify non-tissue-specific stem/progenitor cells based on their ability to expel the dye via the transmembrane transporter ATP-binding cassette transporter subfamily G member 2 (ABCG2). These cells gave rise to ECs (as determined by VE-cadherin, CD31, and von Willebrand factor expression) and SMCs (determined by α-SMA, calponin, and SM-MHC expression) when cultured with vascular endothelial growth factor (VEGF) and transforming growth factor β1 (TGF-β1)/platelet-derived growth factor BB (PDGF-BB) respectively, similar to Flk-1^{+} mesoangioblasts found in the embryonic dorsal aorta, and also produced (VE-cadherin^{+} and α-SMA^{+}) vascular-like branching structures of cells [85, 86].

Another population of vascular progenitors were isolated by Zaniboni, *et al.* from the media by internal digestion of porcine aortas with collagenase [87]. These cells were described as similar to both MSCs and pericytes. Like MSCs, they had elongated, spindle-shaped, fibroblast-like morphology, and met minimum MSC criteria [88] for CD90 and CD105 positivity while lacking expression of CD34 and CD45. They also expressed additional MSC markers CD44 and CD56 and displayed classic MSC differentiation potential into adipocytes, chondrocytes, and osteocytes. At the same time, in behavior considered distinctive of pericytes, in coculture with human umbilical vein endothelial cells they were able to form network-like structures [87].

MSCs themselves have also been implicated in atherosclerosis [89]. MSCs expressing Oct-4, Stro-1, Sca-1, and Notch-1, for instance, were identified in the wall of a range of vessel segments such as the aortic arch, and thoracic and femoral arteries. These multipotent cells exhibited adipogenic, chondrogenic, and leiomyogenic potential [14, 15].

Our group, too, has identified a population of multipotent vascular stem cells (MVSCs) in the arterial medial and adventitial layers that could significantly contribute to the population of traditionally defined "proliferative and synthetic SMCs" in SMC culture and in neointima [25, 37]. Upon vascular injury (e.g., denudation injury), Sox10^{+} MVSCs are activated, become proliferative, and migrated from both medial and adventitial layers to contribute to neointima formation [25, 37]. In addition, some Sox10^{-} cells became Sox10^{+}, suggesting Sox10 may be a marker of activated cells (Fig. 1). In wound healing and scar formation, MVSC-like Sox10^{+} cells (which are also found in soft tissues around blood vessels and throughout the body) can differentiate into both myofibroblasts and SMCs [24].

Following the implantation of polymer vascular grafts for instance, these cells, rather than SMCs, are recruited to the outer surface of the grafts and gradually differentiate into SMCs [70], recapitulating some aspect of vascular development.

Of special note is that vessel-derived stem/progenitor cells as well as MSCs isolated from ApoE$^{-/-}$ mice respond to the inflammatory environment and undergo calcification in the form of significantly greater osteogenesis and chondrogenesis [90]. MVSCs can also differentiate mesenchymally into osteogenic, chondrogenic, and adipogenic cells *in vitro* [25] and *in vivo* (unpublished observation), suggesting a possible role for them in vascular fat accumulation and calcification. As CVCs, in contrast, can differentiate into osteogenic and chondrogenic cells but not adipogenic cells *in vitro*, it is possible that CVCs are derived from MVSCs that have partially differentiated. Because almost all VSCs share some characteristics of MSCs, it is also possible that MSCs are derived from one or multiple subpopulations of VSCs.

Adventitial stem cells

The adventitia is the outermost layer of a blood vessel and is composed of a collagen-rich extracellular matrix embedded with a mixture of cells. The complexity of cellular composition reflects the pivotal role of the adventitia in vascular remodeling. Indeed, of the three blood vessel layers, evidence for vascular stem/progenitor cell enrichment in the adventitia, specifically along its border with the media, is the most abundant and robust. Its significance makes physiological and anatomical sense. Proximity to the vasa vasorum, which connect to the peripheral circulation, enable vessel wall communication with otherwise removed stem cell niches including the aforementioned bone marrow [14, 15], and the pivotal role of vasa vasorum density, structural integrity, and expansion in atheroma development and complications is well documented [91].

In human arteries, in addition to the Sox10^{+} MVSCs we described in the previous section [25], a population of vascular wall-resident multipotent stem cells (VW-MPSCs) were isolated from the adventitia by Klein, *et al.* [92]. They expressed certain MSC surface markers (including Stro1, CD105, CD73, CD44, CD90 and CD29) and positivity for stem cell-associated transcription factors Oct4 and Sox2, and demonstrated lack of contaminating mature EC or EPCs and hematopoietic stem cells (HPCs) by negativity for CD31, CD34, CD45, CD68, CD11b, and CD19. These VW-MPSCs also demonstrated adipocyte, chondrocyte, and osteocyte differentiation in culture conditions. *In vivo* transplantation with human umbilical vein endothelial cells (HUVECs) into immunodeficient mice via Matrigel resulted in new vessel formation covered with VW-MPSC-derived pericyte- and smooth muscle-like cells, an effect enhanced by VEGF, FGF-2, and TGFβ1 stimulation [92]. These authors more recently identified that HOX genes may epigenetically regulate VW-MPSC differentiation into SMCs, potentially contributing to neointimal formation and tumor vascularization [93].

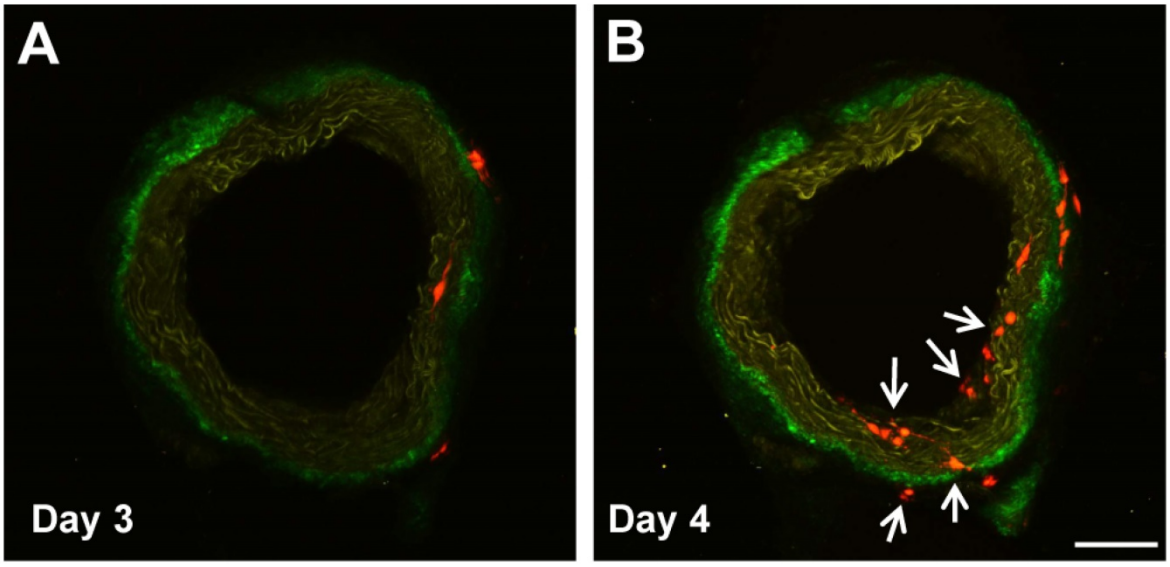

Figure 1. Sox10^{+} MVSCs in aorta ring *ex vivo* culture. Aorta rings of Sox10-Cre/Rosa-RFP mice were cultured *ex vivo*, and imaged by two-photon microscopy. Arrows indicate the emerging Sox10^{+} cells. Scale bar, 100 μm.

Progenitors have also been derived from human veins, dubbed "saphenous vein-derived progenitor cells" (SVPs) for their specific location of origin. Assessing endothelial markers CD34, CD31, and von Willebrand factor (vWF) in these cells showed $CD34^+$, $CD31^-$, vWF^-. These highly proliferative cells were found to be localized around adventitial *vasa vasorum*, and expressed pericyte/mesenchymal antigens as well as stem cell marker Sox2. In an ischemic hindlimb model in immunodeficient mice, intramuscular injection of SVPs improved neovascularization and blood flow recovery, and the cells established N-cadherin-mediated physical contact with the capillary endothelium by day 14 post-transplantation [94]. These therapeutic benefits of vein-derived adventitial stem cells have been replicated in other studies using mouse models of ischemia, with one beginning to look towards manufacturing these cells for human angina therapy [95-97]. Spindle shaped MSCs ($CD13^+$, $CD29^+$, $CD44^+$, $CD54^+$) have also been isolated from human varicose saphenous vein intima. Displaying a similar gene expression profile to bone marrow-derived MSCs, these could differentiate into osteoblasts, chondrocytes, and adipocytes [98].

In rodents, another important progenitor population, $Sca\text{-}1^+$ stem cells, has been described in the adventitia along the medial border. This population also expresses other stem cell markers including c-kit, CD34, and Flk1 and was first identified by Hu *et al.* in the aortic roots of $ApoE^{-/-}$ mice [99]. They had demonstrated capacity to differentiate into SMCs *in vivo*, with LacZ-labeled $Sca\text{-}1^+$ cells found in vein graft atherosclerotic lesions after transplantation in the adventitial space, implying the migration of $Sca\text{-}1^+$ cells from the adventitia to the neointima [99]. Years later, the same group illustrated the multipotency of the cells by demonstrating in a decellularized vessel graft mouse model the cells' *in vitro* differentiation into SMCs (with PDGF) and ECs (with VEGF) [100]. Implications to reduce neointimal thickness by applying VEGF to the adventitial layer, promoting stem cell differentiation into ECs rather than SMCs, were made clear as well [100].

Other studies have since further implicated $Sca\text{-}1^+$ stem cells in atherosclerosis and adventitial remodeling [28, 101, 102]. The later stages of atherosclerosis, for instance, mainly involve resident proliferating macrophages rather than those differentiated from bone marrow monocytes [27]. These local resident proliferating macrophages were found to be derived from a subpopulation of $Sca\text{-}1^+$ stem cells, resident macrophage progenitors, that also expressed CD45 [28]. In aging, $Sca1^+$ adventitial cells enriched for monocyte/macrophage markers and CD45 were shown to be depleted by 3-fold in mature versus young mice, raising the question of whether age-related vascular degeneration may be due to such effects on progenitors in the vascular wall [103].

Recently, Majesky *et al.* used two *in vivo* SMC lineage-tracing approaches and showed that some $Sca1^+$ vascular adventitial progenitors ($CD34^+$) are derived from differentiated SMCs, potentially thereby contributing to maintenance of the resident vascular progenitor cell population [33]. In an earlier study, Shankman *et al.* had suggested that SMCs could de-differentiate into progenitor-like cells capable of differentiating into MSC- and macrophage-like cells [32]. Interestingly, in both cases, KLF4 was identified as a key modulator of cell phenotypic changes. This intriguing relationship between SMCs and VSCs (or VSC-like cells) warrants further investigation.

Overall, although a human ortholog of Sca-1 has yet to be identified, study of pathways and mechanisms surrounding these cells have been of great value, and results suggest that locally manipulating microenvironment is a possible angle for treating atherosclerotic disease [104].

Pericytes

Pericytes play important roles in regulating microvascular stability and dynamics [105]. They were first described over a century ago, and defined as another type of vascular mural cell that surround microvessels, forming an incomplete envelope around ECs and found within the microvascular basement membrane [106]. Pericyte-like cells have also been reported in the inner intima (mostly subendothelium) in human arteries of all sizes [107]. Several markers have been used to identify pericytes, including NG2 [108], CD146 [109, 110], PDGFRβ, and α-SMA [111].

In recent years, accumulating studies have discovered important roles for pericytes in development and diseases. Pericyte-like cells were identified in atherosclerotic lesions and thought to be one of the sources of atherosclerotic cells [83, 112], which may come from the vasa vasorum, a specialized microvessel inside large vessel walls [91]. Cells histologically characterized as "true pericytes" were also found to comprise a second net-like subendothelial tissue layer, which combines with the endothelium to form the intimal barrier in healthy human and bovine microvasculature. In contrast with the endothelium, these pericytes were highly prothrombotic when exposed to serum and display overshooting growth behavior in endothelium-denuded vascular areas, making them potential key players in atherosclerosis, thrombosis, and thrombotic side-effects of venous coronary bypass grafting [92].

In the porcine aortic media, novel vascular progenitor cells with pericyte- and MSC-like properties were also found capable of differentiating into osteocytes, chondrocytes, and adipocytes [87]. Pericytes around microvessels in skeletal muscle are another type of myogenic progenitor cell distinct from satellite cells [113, 114].

Pericytes in multiple organs have been reported to have properties of MSCs [111]. Moreover, pericytes can differentiate into myofibroblasts and are another important cellular source of organ fibrosis [115-117]. It is likely that pericytes include subpopulations of stem cells or progenitors. In our recent work, we found $Sox10^+$ stem cells in the stroma of subcutaneous connective tissues which had the same properties as MVSCs in large vessels [24, 25]. These $Sox10^+$ stem cells are precursors of pericytes and fibroblasts, as described in the previous section, and contribute to both fibrosis and microvessel formation during tissue repair and regeneration [24]. $Gli1^+$ stem cells had similarly wide distribution as the $Sox10^+$ stem cells and were found in the perivascular space and also adventitial layer of large arteries. They could differentiate into myofibroblasts contributing to organ fibrosis, and neointimal SMCs contributing to atherosclerotic lesions and arterial calcification [115, 118].

Therapeutically, two separate studies examined the benefit of pericyte transplantation in mouse models of myocardial infarction. They found that pericytes from both saphenous vein [119] and skeletal muscle [120] attenuated left ventricular dilation, improved cardiac contractility and ejection fraction, reduced myocardial fibrosis and scarring, and improved neovascularization and angiogenesis. Saphenous vein-derived pericytes also reduced cardiomyocyte apoptosis, attenuated vascular permeability, and improved myocardial blood flow [119], while the skeletal muscle-derived pericytes significantly diminished host inflammatory cell infiltration at the infarct site as well [120]. Both studies attributed benefits to cellular interactions and paracrine effects [119, 120].

Dellavalle, *et al.* demonstrated the skeletal muscle-regenerating properties of both normal human pericytes and dystrophin-reprogrammed human Duchenne patient pericytes when transplanted into mouse models of muscular dystrophy [113]. In small-diameter tissue-engineered vascular grafts (TEVGs), exogenously seeded pericytes improved maintenance of patency after TEVG implantation into the aorta of rats (100% at 8 weeks, versus 38% unseeded controls) [121]. An endogenous approach has met with similar success, where promoting the differentiation of $Sca\text{-}1^+$ stem/progenitor cells into the endothelial lineage has reduced neointimal thickness by up to 80% [100]. Altogether, these findings highlight stem cells as important players and potentially significant therapeutic targets in vascular remodeling, and underscore the multifactorial complexity of vascular disease pathogenesis.

Microenvironment of vascular cells

The microenvironment plays important roles in regulating vascular cell function and the stem cell renewal and fate decision, and includes both biochemical factors (e.g., growth factors, cytokines) and biophysical factors (e.g., extracellular matrix, stiffness, flow shear stress and mechanical stretch).

Inflammatory cytokines, in addition to adhesion molecules, govern recruitment of relevant immune cells to the arterial wall in atherosclerosis. Beyond these traditional roles in regulating cell function and homeostasis, though, and notably for our discussion here, in recent years cytokines have also been found to regulate stem cell recruitment and activation during vascular remodeling [122, 123]. Cytokines like stromal cell-derived factor 1α (SDF-1α), for example, has been shown to recruit bone marrow EPCs to form microvessels in hindlimb ischemic angiogenesis [124, 125] and to promote adventitial $Sca1^+$ stem cells to migrate through vein graft walls and differentiate into neointimal SMCs [126]. In advanced atherosclerotic plaques, it is also believed that SDF-1α recruits SMC progenitor cells from bone marrow to the fibrotic cap [127]. Another cytokine, tumor necrosis factor-α (TNF-α), induces adventitial $Sca1^+$ stem cells to differentiate into ECs, while suppressing SMC gene activation [128]. Growth factors like VEGF and PDGF-BB/TGF-β1 can stimulate adventitial and medial stem cells to differentiate into ECs and SMCs, respectively [85, 100].

Among the biophysical factors found important for vascular cells, local disturbed flow is a major factor that induces EC dysfunction in the branches and curvatures of the arterial tree [129]. Disturbed flow shear stress can induce a series of intracellular signaling pathways in ECs and activate proliferative and inflammatory gene expression, initiating neointimal formation and atherosclerosis even in newborns [129, 130].

The extracellular matrix (ECM) is also important in regulating vascular dynamics. Subendothelial matrix proteoglycans are thought to contribute to lipid retention in the early stages of atherosclerosis [29]. ECM stiffness and embedded growth factors are critical in regulating cell functions. Our previous work has showed that stiff surfaces, together with TGFβ, promoted MSC differentiation into SMCs *in*

vitro [131]. Collagen IV, too, has been reported to be critical in promoting embryonic stem cell differentiation into Sca-1$^+$ stem cells, and to act together with aforementioned cytokines and growth factors to promote differentiation [132, 133]. Mechanical stretch and microtopography can regulate SMC differentiation and function as well [134, 135].

To date, the niche of VSCs has not been well defined. Although we know connection to the peripheral circulation via the *vasa vasorum* enables vessel niche communication with other stem cell niches like the bone marrow, how VSCs are activated by such communication, inflammatory signals, and local microenvironmental changes remains to be investigated.

Clinical implications

As our understanding of the importance and mechanism of stem and progenitor cell involvement in human vascular remodeling has evolved, two therapeutic angles have arisen: 1) influencing endogenous VSC behavior to prevent initiation and progression of disease, and 2) exogenous stem cell delivery to promote disease reversal and healing of tissue injury. The application of more immature stem cells with greater differentiation potential such as embryonic and induced pluripotent stem cells to cardiovascular disease (including myocardial infarction, vascular regeneration in coronary and peripheral artery disease) has been reviewed elsewhere [136-138]. Adult stem cells such as those we have discussed pose multiple advantages in their accessibility (e.g., the stromal vascular fraction of adipose aspirates contain human blood vessel fragments; coronary bypass surgery makes pieces of aorta or segments of internal thoracic artery, radial artery, and saphenous vein readily available), decreased risk of uncontrolled differentiation (e.g., teratomas), and immune-privileged nature (in the case of MSCs and pericytes) that enables allogeneic use as well [139].

That said, clinical trials and therapies utilizing such VSCs are still sadly lacking. No human clinical trials to date have examined application of pericytes or resident VSCs for vascular disease. MSCs and EPCs, perhaps because of the broadness of their definition, have accumulated a more substantial body of clinically relevant evidence. The majority of clinical trials for atherosclerosis and diseases for which it is the primary cause – such as angina, myocardial ischemia, and ischemic stroke, all diseases primarily of the macrovasculature – utilize MSCs and EPCs instead. These trials focus, too, more on stem cell/progenitors for disease treatment rather than disease prevention. Limited evidence for underlying mechanisms suggests stem cell angiogenic roles play a large part in measurable therapeutic benefit; evidence for a therapeutic role in neointimal regression, in contrast, is lacking [140, 141]. It should be noted that MSCs and EPCs have also been utilized therapeutically to promote angiogenesis in diseases of the *micro*vasculature such as diabetic ischemia-induced chronic wounds [53, 142] and peripheral occlusive disease [140, 141, 143], but we focus on *macro*vascular plaque-related diseases here instead.

Bone marrow-derived EPCs

In 2013, a phase III trial for refractory angina locally transplanted (G-CSF-stimulated) autologous blood cells positive for the EPC marker CD34 via percutaneous intramyocardial injection. The trial showed preliminary results consistent with those of earlier phase studies [144], although with higher placebo effects than previously detected, and animal studies lead us to believe benefit is derived from cell contribution to myocardial neoangiogenesis, and possible differentiation into cardiomyocytes and ECs [145-147]. If completed, it would have provided the requisite information for regulatory approval of the first cellular therapeutic for a cardiovascular indication [148]. Results may merit an expanded examination of therapeutic EPC transplantation, perhaps in combination with other vasculogenic mediators and scaffolds to improve EPC survival and function.

Other clinical trials have also attempted direct exogenous transplantation of adult bone-marrow-derived stem cells, but for myocardial ischemia (MI) and ischemic stroke patients. Several have found such intracoronary transplantation improves regional systolic function recovery and infarct size reduction in MI patients [149, 150], and a number of recent meta-analyses have confirmed improvements in not only left ventricular contractility after therapy [151-153] but also decreased mortality, acute MI recurrence, and readmission for heart failure [150, 152]. Still, effects of transplantation on infarct volume and remodeling are contradictory and inconclusive [150, 152-156]. BM cells, rather than incorporating, may prompt ischemic tissues to secrete paracrine signals (e.g., angiogenic factors); these signals in conjunction with transdifferentiation potential may underlie functional recovery [149, 156-158].

In stroke, promising results in experimental models [159] prompted clinical trials of intra-arterial or intravenous transplantation of autologous bone marrow mononuclear cells (including CD34$^+$ progenitors). A phase I/II clinical trial in middle

cerebral artery stroke patients transplanted 5-9 days after stroke found that changes in serum levels of GM-CSF, PDGF-BB, and MMP-2 associated with better functional outcomes were induced; however, varied impact on functional outcomes themselves was not measured [160]. Another phase II randomized control trial (RCT) found that cell therapy was safe, but had no beneficial effect on stroke outcome [161]. The first trial to explore dose-dependent efficacy of intra-arterial transplantation of bone marrow mononuclear cells in moderate-to-severe acute ischemic stroke patients is currently ongoing (IBIS trial, prospective phase II RCT) [162]. Despite promising animal studies, which suggest BM cell-based treatments can benefit endogenous neurorestoration by promoting contralesional pyramidal axon sprouting and preservation, increasing neurotrophic factor secretion, and possible synergistic effects between microvascular angiogenesis and neurogenesis, demonstrable long-term clinical therapeutic benefit of cell therapies for stroke is still being determined [141].

Secondary stimulation of endogenous progenitors has also been attempted. Granulocyte colony-stimulating factor (G-CSF) is one agent that can stimulate the bone marrow to release EPCs, in addition to release of granulocytes and hematopoietic stem cells [18]. Multiple clinical trials, encouraged by prior positive results in various animals [163], sought to assess its utility in upregulating endogenous EPC release in patients with ischemic heart disease. Results, however, have been mixed: although one study found an improvement of severe ischemia in severe MI patients [164] and a meta-analysis of seven RCTs including 364 acute MI patients found improvement of left ventricular ejection fraction (LVEF) [165], others (including an RCT and a meta-analysis of ten clinical trials including 445 patients) concluded no impact on infarct size, LV function, or coronary restenosis [166-168]. Interestingly, physical exercise, strongly established by many large-scale epidemiological studies as being robustly associated with decreased cardiovascular mortality and potent primary and secondary CVD prevention [169-173], has been found to mobilize EPCs from the bone marrow and is thought to exert its benefits mechanistically via the maintenance of an intact endothelial layer [174].

Using G-CSF in stroke patients has been less studied. A phase IIb RCT concluded in 2012 that G-CSF successfully and safely increased $CD34^+$ cells by 9.5-fold relative to placebo, with a trend of reducing ischemic lesion volume [175]. Further study, though, is necessary.

Bone marrow-derived MSCs

The majority of completed clinical trials (as reported on clinicaltrials.gov) involving MSC transplantation for vascular disease focuses on treatment of myocardial ischemia, finding that treatment is tolerable and safe with improvements seen in metrics such as LVEF [176-178] and global EF [179], LV end-systolic [176, 178, 179] and diastolic volumes [178], and functional walk and cardiac tests [176] and global symptom scores [177]. A phase I/II clinical trial for patients with severe stable coronary artery disease and refractory angina transplanted autologous bone marrow-derived MSCs into their viable myocardium, and found similarly promising results. The trial showed sustained safety three years post-transplantation, significant clinical improvements in symptomatic and functional metrics, as well as reduced hospital admissions for CV disease [180].

Delivery route of MSCs, furthermore, was found by meta-analysis of six clinical trials involving 334 MI patients to shape efficacy of treatment. Greatest improvement in LVEF was seen if transendocardial injection and intravenous infusion, rather than intracoronary infusion, were used to deliver MSCs [181].

In 2015 an observational clinical study for coronary atherosclerosis examined outcomes of plasmonic resonance therapy using silica-gold nanoparticles that had been incubated with allogeneic mesenchymal $CD73^+$ $CD105^+$ stem-progenitor cells. Results showed highly safe, significant plaque regression relative to stenting controls (reduction of total atheroma volume up to $60mm^3$, or 37.8% of plaque burden, relative to current maximal success of conventional drugs of $6\text{-}14mm^3$) and late lumen enlargement without arterial remodeling [182].

Overall, although animal and preliminary clinical studies have revealed much promise, there remains much to be done in understanding the mechanism of VSC therapeutic benefits in order to appropriately target them for effective therapy.

Future directions and perspectives

Strong evidence has accumulated to demonstrate the involvement of various stem and progenitor cells in vascular regeneration and disease, including atherosclerotic neointimal formation. These stem cells display a nonuniform distribution both across the vessel wall as well as across different vascular territories, a distribution perhaps contributing to explanations of why different vascular segments may have variable susceptibility to vascular disease despite similar hemodynamics and environment [183]. Different populations of vascular cells,

including SMCs, ECs, inflammatory cells (including macrophage and dendritic cell progenitors), and stem cells, may interact with and be subject to regulation by each other and by the local microenvironment during neointimal thickening. Recent studies show exosomes, nanometer lipid bilayer signaling particles secreted by cells with important roles in many physiological and pathological processes [184-187], have a hand in this regulation by mediating vascular calcification as found in atherosclerosis [188], atheroprotective communication between ECs and SMCs [189], and anti-inflammatory effects of MSCs [187]. Exosomes could thus be therapeutic targets of interest as well [190].

Identifying proper cellular targets (e.g., using screening methods such as RNA-sequencing and epigenetic profiling to characterize VSCs, along with other techniques such as laser microdissection and immunofluorescence to identify key VSC markers) and understanding the underlying regulatory mechanisms will facilitate the development of successful therapies for vascular disease. Given their differentiation potential into SMCs and ECs, these stem cells could also be good cellular sources for fabricating vascular grafts or otherwise promoting vascular regeneration.

Far as the field has come, several critical questions remain to be addressed. First, given the diversity of stem cells discovered by different research groups, confirming whether these cells are distinct populations and determining their relationship with proliferative/synthetic SMCs will be necessary. It will be helpful to obtain consensus on specific panels of markers to define different stem cell populations. Examining to what degree the difference in their marker expression profiles may be a result of different culture conditions *in vitro*, too, will be of importance.

Second, the niche of VSCs needs to be further characterized to define the macro and microenvironmental factors that maintain VSCs in a quiescent versus activated state, and how such factors promote healthy survival.

Third, stem cell fate needs to be determined in long-term *in vivo* experiments. However, stem cells may become activated and differentiated quickly at the early phase of neointimal thickening *in vivo*, which makes capture of the phenotype by immunohistology difficult. Genetic lineage tracing techniques would address this problem, if obstacles of selection of good markers and of availability of transgenic animal models can be surmounted. Such techniques could also address the relative contributions of different cell types, and multi-color reporter mice could be used to investigate heterogeneity within the same population.

Fourth, the behavior of VSCs under various pathological conditions should be elucidated. Stem cell activation and differentiation are regulated by various microenvironmental factors. Changes in biochemical and biophysical factors in a disease state and the effects of these factors, individually or in combination, may have profound effects on stem cell functions. Conversely, taking creative inspiration from current successful therapies for atherosclerosis and brainstorming approaches for cellular therapies to target their same mechanisms could yield therapies with fewer side-effects and more targeted results. For instance, any conversation on atherosclerosis would be incomplete without mention of statins, the current mainstay of treatment [191, 192]. Research has shown that, independent of cholesterol reduction, statins may exert their beneficial effects via EPC mobilization. This may be a promising direction for future therapies [52]. Similarly, piggybacking on the putative plaque-stabilizing mechanism of statins by use of the chemokine SDF-1 to recruit bone marrow-derived SM progenitor cells to the fibrous cap has yielded increases in cap thickness without altering artery diameter in mice [127]. This finding may prove useful for unstable atherosclerosis if further studies in large animals and humans continue to yield promising results.

Fifth, especially with sourcing of vascular wall MSCs becoming increasingly feasible [17], there is great promise in cell therapies if details on differences in identity and manufacturing based on specific vascular and cell source can be fleshed out. Despite their mechanistic significance, EPCs and other progenitors without immune-privilege, in contrast with MSCs and pericytes which do, may pose a challenge in clinical application if the goal is exogenous transplantation [139]. Endogenous recruitment and processes may be more feasible for these other progenitors. Although stem cell transplantation has been proven to be safe and benefit tissue regeneration, the mechanisms of benefit, too, are unclear at present. Overall, clinical trials certainly remain of value – as phenomena in humans are ultimately distinct from those in animals – but it is clear that such applications are yet in the early stages. The mixed results clearly indicate that an improved understanding of underlying mechanisms is necessary not only for effective design of therapeutic translation and study, but also for interpretation of results. Ongoing risk and safety assessment will continue to be necessary in parallel.

Finally, besides delivery of exogenous stem cells for therapies, the potential of endogenous recruitment or of using stem cells as novel targets of therapies needs to be further investigated *in vitro* and *in vivo*. *In*

vitro isolated VSCs can be used for drug screening. A well-defined culture model, such as co-culture with SMCs, mechanical loading, and 3D culture that mimics the *in vivo* microenvironment, would be valuable. Blood vessel tissue *ex vivo* culture is better than cell culture as it mimics the niche of cell-cell interactions and native extracellular matrix, which may be useful when combined with tissue clarity techniques and transgenic animal models. All these new tools and technologies will continue to facilitate further discoveries in vascular stem cell biology, enabling development of diagnostic and therapeutic strategies with unprecedented efficacy and capability to combat vascular disease and promote regeneration.

Abbreviations

CVD: cardiovascular disease; EC: endothelial cell; EPC: endothelial progenitor cell; SMC: smooth muscle cell; VSC: vascular stem cell; MSC: mesenchymal stem cell; MVSC: multipotent vascular stem cell; CVC: calcifying vascular cells; α-SMA: smooth muscle α-actin; SM-MHC: smooth muscle myosin heavy chain.

Acknowledgements

This work was supported by grants from the National Institutes of Health (HL117213 and HL121450 to S.L.) and the Medical Scientist Training Program at UCLA (NIH T32 GM008042 to L.L.).

Competing Interests

The authors have declared that no competing interest exists.

References

1. Shanthi M, Pekka P, Bo N. Global atlas on cardiovascular disease prevention and control. Geneva: World Health Organization; 2011.
2. Benjamin EJ, Blaha MJ, Chiuve SE, Cushman M, Das SR, Deo R, et al. Heart Disease and Stroke Statistics-2017 Update: A Report From the American Heart Association. Circulation. 2017; 135: e146-e603.
3. Ross R. Atherosclerosis — an inflammatory disease. N Engl J Med. 1999; 340: 115-26.
4. Libby P, Hansson GK. Inflammation and immunity in diseases of the arterial tree: players and layers. Circ Res. 2015; 116: 307-11.
5. Li S, Sengupta D, Chien S. Vascular tissue engineering: from in vitro to in situ. Wiley Interdiscip Rev Syst Biol Med. 2014; 6: 61-76.
6. Seifu DG, Purnama A, Mequanint K, Mantovani D. Small-diameter vascular tissue engineering. Nat Rev Cardiol. 2013; 10: 410-21.
7. Chiu J-J, Chien S. Effects of disturbed flow on vascular endothelium: pathophysiological basis and clinical perspectives. Physiol Rev. 2011; 91: 327-87.
8. Yoder MC. Is endothelium the origin of endothelial progenitor cells? Arterioscler Thromb Vasc Biol. 2010; 30: 1094-103.
9. Bautch VL. Stem cells and the vasculature. Nat Med. 2011; 17: 1437-43.
10. Hu Y, Xu Q. Adventitial biology: differentiation and function. Arterioscler Thromb Vasc Biol. 2011; 31: 1523-9.
11. Stenmark KR, Yeager ME, El Kasmi KC, Nozik-Grayck E, Gerasimovskaya EV, Li M, et al. The adventitia: essential regulator of vascular wall structure and function. Annu Rev Physiol. 2013; 75: 23-47.
12. Galkina E, Kadl A, Sanders J, Varughese D, Sarembock IJ, Ley K. Lymphocyte recruitment into the aortic wall before and during development of atherosclerosis is partially L-selectin dependent. J Exp Med. 2006; 203: 1273-82.
13. Houtkamp MA, de Boer OJ, van der Loos CM, van der Wal AC, Becker AE. Adventitial infiltrates associated with advanced atherosclerotic plaques: structural organization suggests generation of local humoral immune responses. J Pathol. 2001; 193: 263-9.
14. Pasquinelli G, Pacilli A, Alviano F, Foroni L, Ricci F, Valente S, et al. Multidistrict human mesenchymal vascular cells: pluripotency and stemness characteristics. Cytotherapy. 2010; 12: 275-87.
15. Psaltis PJ, Harbuzariu A, Delacroix S, Holroyd EW, Simari RD. Resident vascular progenitor cells - diverse origins, phenotype and function. J Cardiovasc Transl Res. 2011; 4: 161-76.
16. Zengin E, Chalajour F, Gehling UM, Ito WD, Treede H, Lauke H, et al. Vascular wall resident progenitor cells: a source for postnatal vasculogenesis. Development. 2006; 133: 1543-51.
17. Pasquinelli G, Tazzari PL, Vaselli C, Foroni L, Buzzi M, Storci G, et al. Thoracic aortas from multiorgan donors are suitable for obtaining resident angiogenic mesenchymal stromal cells. Stem Cells. 2007; 25: 1627-34.
18. Shi X, Zhang W, Yin L, Chilian WM, Krieger J, Zhang P. Vascular precursor cells in tissue injury repair. Transl Res. 2017; 184: 77-100.
19. Kirton JP, Xu Q. Endothelial precursors in vascular repair. Microvasc Res. 2010; 79: 193-9.
20. Allahverdian S, Chehroudi AC, McManus BM, Abraham T, Francis GA. Contribution of intimal smooth muscle cells to cholesterol accumulation and macrophage-like cells in human atherosclerosis. Circulation. 2014; 129: 1551-9.
21. Feil S, Fehrenbacher B, Lukowski R, Essmann F, Schulze-Osthoff K, Schaller M, et al. Transdifferentiation of vascular smooth muscle cells to macrophage-like cells during atherogenesis. Circ Res. 2014; 115: 662-7.
22. Albarran-Juarez J, Kaur H, Grimm M, Offermanns S, Wettschureck N. Lineage tracing of cells involved in atherosclerosis. Atherosclerosis. 2016; 251: 445-53.
23. Cybulsky MI, Cheong C, Robbins CS. Macrophages and Dendritic Cells: Partners in Atherogenesis. Circ Res. 2016; 118: 637-52.
24. Wang D, Wang A, Wu F, Qiu X, Li Y, Chu J, et al. Sox10+ adult stem cells contribute to biomaterial encapsulation and microvascularization. Sci Rep. 2017; 7: 40295.
25. Tang Z, Wang A, Yuan F, Yan Z, Liu B, Chu JS, et al. Differentiation of multipotent vascular stem cells contributes to vascular diseases. Nat Commun. 2012; 3: 875.
26. Hansson GK. Inflammation, atherosclerosis, and coronary artery disease. N Engl J Med. 2005; 352: 1685-95.
27. Robbins CS, Hilgendorf I, Weber GF, Theurl I, Iwamoto Y, Figueiredo JL, et al. Local proliferation dominates lesional macrophage accumulation in atherosclerosis. Nat Med. 2013; 19: 1166-72.
28. Psaltis PJ, Puranik AS, Spoon DB, Chue CD, Hoffman SJ, Witt TA, et al. Characterization of a resident population of adventitial macrophage progenitor cells in postnatal vasculature. Circ Res. 2014; 115: 364-75.
29. Skalen K, Gustafsson M, Rydberg EK, Hulten LM, Wiklund O, Innerarity TL, et al. Subendothelial retention of atherogenic lipoproteins in early atherosclerosis. Nature. 2002; 417: 750-4.
30. Nemenoff RA, Horita H, Ostriker AC, Furgeson SB, Simpson PA, VanPutten V, et al. SDF-1α induction in mature smooth muscle cells by inactivation of PTEN is a critical mediator of exacerbated injury-induced neointima formation. Arterioscler Thromb Vasc Biol. 2011; 31: 1300-8.
31. Herring BP, Hoggatt AM, Burlak C, Offermanns S. Previously differentiated medial vascular smooth muscle cells contribute to neointima formation following vascular injury. Vasc Cell. 2014; 6: 21.
32. Shankman LS, Gomez D, Cherepanova OA, Salmon M, Alencar GF, Haskins RM, et al. KLF4-dependent phenotypic modulation of smooth muscle cells has a key role in atherosclerotic plaque pathogenesis. Nat Med. 2015; 21: 628-37.
33. Majesky MW, Horita H, Ostriker A, Lu S, Regan JN, Bagchi AK, et al. Differentiated Smooth Muscle Cells Generate a Subpopulation of Resident Vascular Progenitor Cells in the Adventitia Regulated by KLF4. Circ Res. 2016.
34. Benditt EP, Benditt JM. Evidence for a monoclonal origin of human atherosclerotic plaques. Proc Natl Acad Sci U S A. 1973; 70: 1753-6.
35. Schwartz SM, Murry CE. Proliferation and the monoclonal origins of atherosclerotic lesions. Annu Rev Med. 1998; 49: 437-60.
36. Chappell J, Harman JL, Narasimhan VM, Yu H, Foote K, Simons BD, et al. Extensive Proliferation of a Subset of Differentiated, yet Plastic, Medial Vascular Smooth Muscle Cells Contributes to Neointimal Formation in Mouse Injury and Atherosclerosis Models. Circ Res. 2016; 119: 1313-23.
37. Yuan F, Wang D, Xu K, Wang J, Zhang Z, Yang L, et al. Contribution of Vascular Cells to Neointimal Formation. PLOS One. 2017; 12: e0168914.
38. Yang P, Hong MS, Fu C, Schmit BM, Su Y, Berceli SA, et al. Preexisting smooth muscle cells contribute to neointimal cell repopulation at an incidence varying widely among individual lesions. Surgery. 2016; 159: 602-12.
39. Tabas I, Bornfeldt KE. Macrophage Phenotype and Function in Different Stages of Atherosclerosis. Circ Res. 2016; 118: 653-67.
40. Qiao L, Nishimura T, Shi L, Sessions D, Thrasher A, Trudell JR, et al. Endothelial fate mapping in mice with pulmonary hypertension. Circulation. 2014; 129: 692-703.
41. Arciniegas E, Frid MG, Douglas IS, Stenmark KR. Perspectives on endothelial-to-mesenchymal transition: potential contribution to vascular remodeling in chronic pulmonary hypertension. Am J Physiol Lung Cell Mol Physiol. 2007; 293: L1-L8.
42. Hillebrands JL, Klatter FA, van den Hurk BM, Popa ER, Nieuwenhuis P, Rozing J. Origin of neointimal endothelium and alpha-actin-positive smooth muscle cells in transplant arteriosclerosis. J Clin Invest. 2001; 107: 1411-22.
43. Han CI, Campbell GR, Campbell JH. Circulating bone marrow cells can contribute to neointimal formation. J Vasc Res. 2001; 38: 113-9.

44. Caplice NM, Bunch TJ, Stalboerger PG, Wang S, Simper D, Miller DV, et al. Smooth muscle cells in human coronary atherosclerosis can originate from cells administered at marrow transplantation. Proc Natl Acad Sci U S A. 2003; 100: 4754-9.
45. Sata M, Saiura A, Kunisato A, Tojo A, Okada S, Tokuhisa T, et al. Hematopoietic stem cells differentiate into vascular cells that participate in the pathogenesis of atherosclerosis. Nat Med. 2002; 8: 403-9.
46. Hu Y, Davison F, Ludewig B, Erdel M, Mayr M, Url M, et al. Smooth muscle cells in transplant atherosclerotic lesions are originated from recipients, but not bone marrow progenitor cells. Circulation. 2002; 106: 1834-9.
47. Hu Y, Mayr M, Metzler B, Erdel M, Davison F, Xu Q. Both donor and recipient origins of smooth muscle cells in vein graft atherosclerotic lesions. Circ Res. 2002; 91: e13-20.
48. Iwata H, Manabe I, Fujiu K, Yamamoto T, Takeda N, Eguchi K, et al. Bone marrow-derived cells contribute to vascular inflammation but do not differentiate into smooth muscle cell lineages. Circulation. 2010; 122: 2048-57.
49. Asahara T, Murohara T, Sullivan A, Silver M, van der Zee R, Li T, et al. Isolation of putative progenitor endothelial cells for angiogenesis. Science. 1997; 275: 964-6.
50. Xu Q, Zhang Z, Davison F, Hu Y. Circulating progenitor cells regenerate endothelium of vein graft atherosclerosis, which is diminished in ApoE-deficient mice. Circ Res. 2003; 93: e76-86.
51. Werner N, Priller J, Laufs U, Endres M, Bohm M, Dirnagl U, et al. Bone marrow-derived progenitor cells modulate vascular reendothelialization and neointimal formation: effect of 3-hydroxy-3-methylglutaryl coenzyme a reductase inhibition. Arterioscler Thromb Vasc Biol. 2002; 22: 1567-72.
52. Walter DH, Rittig K, Bahlmann FH, Kirchmair R, Silver M, Murayama T, et al. Statin therapy accelerates reendothelialization: a novel effect involving mobilization and incorporation of bone marrow-derived endothelial progenitor cells. Circulation. 2002; 105: 3017-24.
53. Tanaka R, Masuda H, Kato S, Imagawa K, Kanabuchi K, Nakashioya C, et al. Autologous G-CSF-mobilized peripheral blood CD34+ cell therapy for diabetic patients with chronic nonhealing ulcer. Cell Transplant. 2014; 23: 167-79.
54. Sirker Alexander A, Astroulakis Zoe MJ, Hill Jonathan M. Vascular progenitor cells and translational research: the role of endothelial and smooth muscle progenitor cells in endogenous arterial remodelling in the adult. Clin Sci. 2009; 116: 283-99.
55. Peichev M, Naiyer AJ, Pereira D, Zhu Z, Lane WJ, Williams M, et al. Expression of VEGFR-2 and AC133 by circulating human CD34+ cells identifies a population of functional endothelial precursors. Blood. 2000; 95: 952-8.
56. Reyes M, Dudek A, Jahagirdar B, Koodie L, Marker PH, Verfaillie CM. Origin of endothelial progenitors in human postnatal bone marrow. J Clin Invest. 2002; 109: 337-46.
57. Ingram DA, Mead LE, Tanaka H, Meade V, Fenoglio A, Mortell K, et al. Identification of a novel hierarchy of endothelial progenitor cells using human peripheral and umbilical cord blood. Blood. 2004; 104: 2752-60.
58. Yoder MC, Mead LE, Prater D, Krier TR, Mroueh KN, Li F, et al. Redefining endothelial progenitor cells via clonal analysis and hematopoietic stem/progenitor cell principals. Blood. 2007; 109: 1801-9.
59. Yoder MC. Defining human endothelial progenitor cells. J Thromb Haemost. 2009; 7: 49-52.
60. Medina RJ, O'Neill CL, O'Doherty TM, Knott H, Guduric-Fuchs J, Gardiner TA, et al. Myeloid angiogenic cells act as alternative M2 macrophages and modulate angiogenesis through interleukin-8. Mol Med. 2011; 17: 1045-55.
61. Medina RJ, Barber CL, Sabatier F, Dignat-George F, Melero-Martin JM, Khosrotehrani K, et al. Endothelial Progenitors: A Consensus Statement on Nomenclature. Stem Cells Transl Med. 2017; 6: 1316-20.
62. Ingram DA, Mead LE, Moore DB, Woodard W, Fenoglio A, Yoder MC. Vessel wall-derived endothelial cells rapidly proliferate because they contain a complete hierarchy of endothelial progenitor cells. Blood. 2005; 105: 2783-6.
63. Patel J, Seppanen E, Chong MSK, Yeo JSL, Teo EYL, Chan JKY, et al. Prospective surface marker-based isolation and expansion of fetal endothelial colony-forming cells from human term placenta. Stem Cells Transl Med. 2013; 2: 839-47.
64. Lin R-Z, Moreno-Luna R, Muñoz-Hernandez R, Li D, Jaminet S-CS, Greene AK, et al. Human white adipose tissue vasculature contains endothelial colony-forming cells with robust in vivo vasculogenic potential. Angiogenesis. 2013; 16: 735-44.
65. Fang S, Wei J, Pentinmikko N, Leinonen H, Salven P. Generation of functional blood vessels from a single c-kit+ adult vascular endothelial stem cell. PLoS Biol. 2012; 10: e1001407.
66. Hagensen MK, Shim J, Thim T, Falk E, Bentzon JF. Circulating endothelial progenitor cells do not contribute to plaque endothelium in murine atherosclerosis. Circulation. 2010; 121: 898-905.
67. Yoon C-H, Hur J, Park K-W, Kim J-H, Lee C-S, Oh I-Y, et al. Synergistic neovascularization by mixed transplantation of early endothelial progenitor cells and late outgrowth endothelial cells: the role of angiogenic cytokines and matrix metalloproteinases. Circulation. 2005; 112: 1618-27.
68. Dubois C, Liu X, Claus P, Marsboom G, Pokreisz P, Vandenwijngaert S, et al. Differential effects of progenitor cell populations on left ventricular remodeling and myocardial neovascularization after myocardial infarction. J Am Coll Cardiol. 2010; 55: 2232-43.
69. Hu Y, Davison F, Zhang Z, Xu Q. Endothelial replacement and angiogenesis in arteriosclerotic lesions of allografts are contributed by circulating progenitor cells. Circulation. 2003; 108: 3122-7.
70. Yu J, Wang A, Tang Z, Henry J, Li-Ping Lee B, Zhu Y, et al. The effect of stromal cell-derived factor-1α/heparin coating of biodegradable vascular grafts on the recruitment of both endothelial and smooth muscle progenitor cells for accelerated regeneration. Biomaterials. 2012; 33: 8062-74.
71. Purhonen S, Palm J, Rossi D, Kaskenpää N, Rajantie I, Ylä-Herttuala S, et al. Bone marrow-derived circulating endothelial precursors do not contribute to vascular endothelium and are not needed for tumor growth. Proc Natl Acad Sci U S A. 2008; 105: 6620-5.
72. Foteinos G, Hu Y, Xiao Q, Metzler B, Xu Q. Rapid endothelial turnover in atherosclerosis-prone areas coincides with stem cell repair in apolipoprotein E-deficient mice. Circulation. 2008; 117: 1856-63.
73. Hillebrands J-L, Klatter FA, van Dijk WD, Rozing J. Bone marrow does not contribute substantially to endothelial-cell replacement in transplant arteriosclerosis. Nat Med. 2002; 8: 194-5.
74. Hill JM, Zalos G, Halcox JP, Schenke WH, Waclawiw MA, Quyyumi AA, et al. Circulating endothelial progenitor cells, vascular function, and cardiovascular risk. N Engl J Med. 2003; 348: 593-600.
75. Werner N, Kosiol S, Schiegl T, Ahlers P, Walenta K, Link A, et al. Circulating endothelial progenitor cells and cardiovascular outcomes. N Engl J Med. 2005; 353: 999-1007.
76. Martí-Fàbregas J, Crespo J, Delgado-Mederos R, Martínez-Ramírez S, Peña E, Marín R, et al. Endothelial progenitor cells in acute ischemic stroke. Brain Behav. 2013; 3: 649-55.
77. Sobrino T, Hurtado O, Moro MÁ, Rodríguez-Yáñez M, Castellanos M, Brea D, et al. The increase of circulating endothelial progenitor cells after acute ischemic stroke is associated with good outcome. Stroke. 2007; 38: 2759-64.
78. Bogoslovsky T, Chaudhry A, Latour L, Maric D, Luby M, Spatz M, et al. Endothelial progenitor cells correlate with lesion volume and growth in acute stroke. Neurology. 2010; 75: 2059-62.
79. Yip H-K, Chang L-T, Chang W-N, Lu C-H, Liou C-W, Lan M-Y, et al. Level and value of circulating endothelial progenitor cells in patients after acute ischemic stroke. Stroke. 2008; 39: 69-74.
80. Gill M, Dias S, Hattori K, Rivera ML, Hicklin D, Witte L, et al. Vascular trauma induces rapid but transient mobilization of VEGFR2+AC133+ endothelial precursor cells. Circ Res. 2001; 88: 167-74.
81. George J, Goldstein E, Abashidze S, Deutsch V, Shmilovich H, Finkelstein A, et al. Circulating endothelial progenitor cells in patients with unstable angina: association with systemic inflammation. Eur Heart J. 2004; 25: 1003-8.
82. Desai A, Glaser A, Liu D, Raghavachari N, Blum A, Zalos G, et al. Microarray-based characterization of a colony assay used to investigate endothelial progenitor cells and relevance to endothelial function in humans. Arterioscler Thromb Vasc Biol. 2009; 29: 121-7.
83. Bostrom K, Watson KE, Horn S, Wortham C, Herman IM, Demer LL. Bone morphogenetic protein expression in human atherosclerotic lesions. J Clin Invest. 1993; 91: 1800-9.
84. Tintut Y, Alfonso Z, Saini T, Radcliff K, Watson K, Bostrom K, et al. Multilineage potential of cells from the artery wall. Circulation. 2003; 108: 2505-10.
85. Sainz J, Al Haj Zen A, Caligiuri G, Demerens C, Urbain D, Lemitre M, et al. Isolation of "side population" progenitor cells from healthy arteries of adult mice. Arterioscler Thromb Vasc Biol. 2006; 26: 281-6.
86. Cossu G, Bianco P. Mesoangioblasts--vascular progenitors for extravascular mesodermal tissues. Curr Opin Genet Dev. 2003; 13: 537-42.
87. Zaniboni A, Bernardini C, Alessandri M, Mangano C, Zannoni A, Bianchi F, et al. Cells derived from porcine aorta tunica media show mesenchymal stromal-like cell properties in in vitro culture. Am J Physiol Cell Physiol. 2014; 306: C322-C33.
88. Lv F-J, Tuan RS, Cheung KMC, Leung VYL. Concise review: the surface markers and identity of human mesenchymal stem cells. Stem Cells. 2014; 32: 1408-19.
89. Abedin M, Tintut Y, Demer LL. Mesenchymal stem cells and the artery wall. Circ Res. 2004; 95: 671-6.
90. Leszczynska A, O'Doherty A, Farrell E, Pindjakova J, O'Brien FJ, O'Brien T, et al. Differentiation of Vascular Stem Cells Contributes to Ectopic Calcification of Atherosclerotic Plaque. Stem Cells. 2016; 34: 913-23.
91. Mulligan-Kehoe MJ, Simons M. Vasa vasorum in normal and diseased arteries. Circulation. 2014; 129: 2557-66.
92. Klein D, Weisshardt P, Kleff V, Jastrow H, Jakob HG, Ergun S. Vascular wall-resident CD44+ multipotent stem cells give rise to pericytes and smooth muscle cells and contribute to new vessel maturation. PLoS One. 2011; 6: e20540.
93. Klein D, Benchellal M, Kleff V, Jakob HG, Ergün S. Hox genes are involved in vascular wall-resident multipotent stem cell differentiation into smooth muscle cells. Sci Rep. 2013; 3: 2178.
94. Campagnolo P, Cesselli D, Al Haj Zen A, Beltrami AP, Krankel N, Katare R, et al. Human adult vena saphena contains perivascular progenitor cells endowed with clonogenic and proangiogenic potential. Circulation. 2010; 121: 1735-45.
95. Iacobazzi D, Mangialardi G, Gubernator M, Hofner M, Wielscher M, Vierlinger K, et al. Increased antioxidant defense mechanism in human adventitia-derived progenitor cells is associated with therapeutic benefit in ischemia. Antioxid Redox Signal. 2014; 21: 1591-604.

96. Gubernator M, Slater SC, Spencer HL, Spiteri I, Sottoriva A, Riu F, et al. Epigenetic profile of human adventitial progenitor cells correlates with therapeutic outcomes in a mouse model of limb ischemia. Arterioscler Thromb Vasc Biol. 2015; 35: 675-88.
97. Spencer HL, Slater SC, Rowlinson J, Morgan T, Culliford LA, Guttridge M, et al. A journey from basic stem cell discovery to clinical application: the case of adventitial progenitor cells. Regen Med. 2015; 10: 39-47.
98. Covas DT, Piccinato CE, Orellana MD, Siufi JL, Silva WA, Jr., Proto-Siqueira R, et al. Mesenchymal stem cells can be obtained from the human saphena vein. Exp Cell Res. 2005; 309: 340-4.
99. Hu Y, Zhang Z, Torsney E, Afzal AR, Davison F, Metzler B, et al. Abundant progenitor cells in the adventitia contribute to atherosclerosis of vein grafts in ApoE-deficient mice. J Clin Invest. 2004; 113: 1258-65.
100. Tsai TN, Kirton JP, Campagnolo P, Zhang L, Xiao Q, Zhang Z, et al. Contribution of stem cells to neointimal formation of decellularized vessel grafts in a novel mouse model. Am J Pathol. 2012; 181: 362-73.
101. Majesky MW, Dong XR, Hoglund V, Mahoney WM, Jr., Daum G. The adventitia: a dynamic interface containing resident progenitor cells. Arterioscler Thromb Vasc Biol. 2011; 31: 1530-9.
102. Xu Q. Stem cells and transplant arteriosclerosis. Circ Res. 2008; 102: 1011-24.
103. Psaltis PJ, Harbuzariu A, Delacroix S, Witt TA, Holroyd EW, Spoon DB, et al. Identification of a monocyte-predisposed hierarchy of hematopoietic progenitor cells in the adventitia of postnatal murine aorta. Circulation. 2012; 125: 592-603.
104. Holmes C, Stanford WL. Concise review: stem cell antigen-1: expression, function, and enigma. Stem Cells. 2007; 25: 1339-47.
105. Hirschi KK, D'Amore PA. Pericytes in the microvasculature. Cardiovasc Res. 1996; 32: 687-98.
106. Diaz-Flores L, Gutierrez R, Varela H, Rancel N, Valladares F. Microvascular pericytes: a review of their morphological and functional characteristics. Histol Histopathol. 1991; 6: 269-86.
107. Andreeva ER, Pugach IM, Gordon D, Orekhov AN. Continuous subendothelial network formed by pericyte-like cells in human vascular bed. Tissue Cell. 1998; 30: 127-35.
108. Ozerdem U, Grako KA, Dahlin-Huppe K, Monosov E, Stallcup WB. NG2 proteoglycan is expressed exclusively by mural cells during vascular morphogenesis. Dev Dyn. 2001; 222: 218-27.
109. Li Q, Yu Y, Bischoff J, Mulliken JB, Olsen BR. Differential expression of CD146 in tissues and endothelial cells derived from infantile haemangioma and normal human skin. J Pathol. 2003; 201: 296-302.
110. Middleton J, Americh L, Gayon R, Julien D, Mansat M, Mansat P, et al. A comparative study of endothelial cell markers expressed in chronically inflamed human tissues: MECA-79, Duffy antigen receptor for chemokines, von Willebrand factor, CD31, CD34, CD105 and CD146. J Pathol. 2005; 206: 260-8.
111. Crisan M, Yap S, Casteilla L, Chen C-W, Corselli M, Park TS, et al. A perivascular origin for mesenchymal stem cells in multiple human organs. Cell Stem Cell. 2008; 3: 301-13.
112. Howson KM, Aplin AC, Gelati M, Alessandri G, Parati EA, Nicosia RF. The postnatal rat aorta contains pericyte progenitor cells that form spheroidal colonies in suspension culture. Am J Physiol Cell Physiol. 2005; 289: C1396-407.
113. Dellavalle A, Sampaolesi M, Tonlorenzi R, Tagliafico E, Sacchetti B, Perani L, et al. Pericytes of human skeletal muscle are myogenic precursors distinct from satellite cells. Nat Cell Biol. 2007; 9: 255-67.
114. Mitchell KJ, Pannerec A, Cadot B, Parlakian A, Besson V, Gomes ER, et al. Identification and characterization of a non-satellite cell muscle resident progenitor during postnatal development. Nat Cell Biol. 2010; 12: 257-66.
115. Kramann R, Schneider Rebekka K, DiRocco Derek P, Machado F, Fleig S, Bondzie Philip A, et al. Perivascular Gli1+ Progenitors Are Key Contributors to Injury-Induced Organ Fibrosis. Cell Stem Cell. 2015; 16: 51-66.
116. Humphreys BD, Lin S-L, Kobayashi A, Hudson TE, Nowlin BT, Bonventre JV, et al. Fate tracing reveals the pericyte and not epithelial origin of myofibroblasts in kidney fibrosis. Am J Pathol. 2010; 176: 85-97.
117. Lin S-L, Kisseleva T, Brenner DA, Duffield JS. Pericytes and perivascular fibroblasts are the primary source of collagen-producing cells in obstructive fibrosis of the kidney. Am J Pathol. 2008; 173: 1617-27.
118. Kramann R, Goettsch C, Wongboonsin J, Iwata H, Schneider RK, Kuppe C, et al. Adventitial MSC-like Cells Are Progenitors of Vascular Smooth Muscle Cells and Drive Vascular Calcification in Chronic Kidney Disease. Cell Stem Cell. 2016; 19: 628-42.
119. Katare R, Riu F, Mitchell K, Gubernator M, Campagnolo P, Cui Y, et al. Transplantation of human pericyte progenitor cells improves the repair of infarcted heart through activation of an angiogenic program involving micro-RNA-132. Circ Res. 2011; 109: 894-906.
120. Chen CW, Okada M, Proto JD, Gao X, Sekiya N, Beckman SA, et al. Human pericytes for ischemic heart repair. Stem Cells. 2013; 31: 305-16.
121. He W, Nieponice A, Soletti L, Hong Y, Gharaibeh B, Crisan M, et al. Pericyte-based human tissue engineered vascular grafts. Biomaterials. 2010; 31: 8235-44.
122. Xie Y, Fan Y, Xu Q. Vascular Regeneration by Stem/Progenitor Cells. Arterioscler Thromb Vasc Biol. 2016; 36: e33-e40.
123. Zernecke A, Weber C. Chemokines in atherosclerosis: proceedings resumed. Arterioscler Thromb Vasc Biol. 2014; 34: 742-50.
124. Hiasa K-i, Ishibashi M, Ohtani K, Inoue S, Zhao Q, Kitamoto S, et al. Gene transfer of stromal cell-derived factor-1alpha enhances ischemic vasculogenesis and angiogenesis via vascular endothelial growth factor/endothelial nitric oxide synthase-related pathway: next-generation chemokine therapy for therapeutic neovascularization. Circulation. 2004; 109: 2454-61.
125. Friedrich EB, Walenta K, Scharlau J, Nickenig G, Werner N. CD34-/CD133+/VEGFR-2+ endothelial progenitor cell subpopulation with potent vasoregenerative capacities. Circ Res. 2006; 98: e20-5.
126. Chen Y, Wong MM, Campagnolo P, Simpson R, Winkler B, Margariti A, et al. Adventitial stem cells in vein grafts display multilineage potential that contributes to neointimal formation. Arterioscler Thromb Vasc Biol. 2013; 33: 1844-51.
127. Akhtar S, Gremse F, Kiessling F, Weber C, Schober A. CXCL12 promotes the stabilization of atherosclerotic lesions mediated by smooth muscle progenitor cells in Apoe-deficient mice. Arterioscler Thromb Vasc Biol. 2013; 33: 679-86.
128. Wong MM, Chen Y, Margariti A, Winkler B, Campagnolo P, Potter C, et al. Macrophages control vascular stem/progenitor cell plasticity through tumor necrosis factor-alpha-mediated nuclear factor-kappaB activation. Arterioscler Thromb Vasc Biol. 2014; 34: 635-43.
129. Zhou J, Li YS, Chien S. Shear stress-initiated signaling and its regulation of endothelial function. Arterioscler Thromb Vasc Biol. 2014; 34: 2191-8.
130. Hahn C, Schwartz MA. Mechanotransduction in vascular physiology and atherogenesis. Nat Rev Mol Cell Biol. 2009; 10: 53-62.
131. Park JS, Chu JS, Tsou AD, Diop R, Tang Z, Wang A, et al. The effect of matrix stiffness on the differentiation of mesenchymal stem cells in response to TGF-beta. Biomaterials. 2011; 32: 3921-30.
132. Xiao Q, Zeng L, Zhang Z, Margariti A, Ali ZA, Channon KM, et al. Sca-1+ progenitors derived from embryonic stem cells differentiate into endothelial cells capable of vascular repair after arterial injury. Arterioscler Thromb Vasc Biol. 2006; 26: 2244-51.
133. Xiao Q, Zeng L, Zhang Z, Hu Y, Xu Q. Stem cell-derived Sca-1+ progenitors differentiate into smooth muscle cells, which is mediated by collagen IV-integrin alpha1/beta1/alphav and PDGF receptor pathways. Am J Physiol Cell Physiol. 2007; 292: C342-52.
134. Li X, Chu J, Wang A, Zhu Y, Chu WK, Yang L, et al. Uniaxial mechanical strain modulates the differentiation of neural crest stem cells into smooth muscle lineage on micropatterned surfaces. PLoS One. 2011; 6: e26029.
135. Wang D, Zheng W, Xie Y, Gong P, Zhao F, Yuan B, et al. Tissue-specific mechanical and geometrical control of cell viability and actin cytoskeleton alignment. Sci Rep. 2014; 4: 6160.
136. Lalit PA, Hei DJ, Raval AN, Kamp TJ. Induced pluripotent stem cells for post-myocardial infarction repair: remarkable opportunities and challenges. Circ Res. 2014; 114: 1328-45.
137. Leeper NJ, Hunter AL, Cooke JP. Stem cell therapy for vascular regeneration: adult, embryonic, and induced pluripotent stem cells. Circulation. 2010; 122: 517-26.
138. Youssef AA, Ross EG, Bolli R, Pepine CJ, Leeper NJ, Yang PC. The Promise and Challenge of Induced Pluripotent Stem Cells for Cardiovascular Applications. JACC Basic Transl Sci. 2016; 1: 510-23.
139. Psaltis PJ, Simari RD. Vascular wall progenitor cells in health and disease. Circ Res. 2015; 116: 1392-412.
140. Rafii S, Lyden D. Therapeutic stem and progenitor cell transplantation for organ vascularization and regeneration. Nat Med. 2003; 9: 702-12.
141. Hermann DM, Chopp M. Promoting brain remodelling and plasticity for stroke recovery: therapeutic promise and potential pitfalls of clinical translation. Lancet Neurol. 2012; 11: 369-80.
142. Kirana S, Stratmann B, Prante C, Prohaska W, Koerperich H, Lammers D, et al. Autologous stem cell therapy in the treatment of limb ischaemia induced chronic tissue ulcers of diabetic foot patients. Int J Clin Pract. 2012; 66: 384-93.
143. Yang SS, Kim NR, Park KB, Do YS, Roh K, Kang KS, et al. A phase I study of human cord blood-derived mesenchymal stem cell therapy in patients with peripheral arterial occlusive disease. Int J Stem Cells. 2013; 6: 37-44.
144. Losordo DW, Henry TD, Davidson C, Sup Lee J, Costa MA, Bass T, et al. Intramyocardial, autologous CD34+ cell therapy for refractory angina. Circ Res. 2011; 109: 428-36.
145. Kawamoto A, Tkebuchava T, Yamaguchi J-I, Nishimura H, Yoon Y-S, Milliken C, et al. Intramyocardial transplantation of autologous endothelial progenitor cells for therapeutic neovascularization of myocardial ischemia. Circulation. 2003; 107: 461-8.
146. Kawamoto A, Iwasaki H, Kusano K, Murayama T, Oyamada A, Silver M, et al. CD34-positive cells exhibit increased potency and safety for therapeutic neovascularization after myocardial infarction compared with total mononuclear cells. Circulation. 2006; 114: 2163-9.
147. Iwasaki H, Kawamoto A, Ishikawa M, Oyamada A, Nakamori S, Nishimura H, et al. Dose-dependent contribution of CD34-positive cell transplantation to concurrent vasculogenesis and cardiomyogenesis for functional regenerative recovery after myocardial infarction. Circulation. 2006; 113: 1311-25.
148. Povsic TJ, Henry TD, Traverse JH, Fortuin FD, Schaer GL, Kereiakes DJ, et al. The RENEW Trial. JACC Cardiovasc Interv. 2016; 9: 1576-85.
149. Wollert KC, Meyer GP, Lotz J, Ringes-Lichtenberg S, Lippolt P, Breidenbach C, et al. Intracoronary autologous bone-marrow cell transfer after myocardial infarction: the BOOST randomised controlled clinical trial. Lancet. 2004; 364: 141-8.

150. Jeevanantham V, Butler M, Saad A, Abdel-Latif A, Zuba-Surma EK, Dawn B. Adult bone marrow cell therapy improves survival and induces long-term improvement in cardiac parameters: a systematic review and meta-analysis. Circulation. 2012; 126: 551-68.
151. Delewi R, Hirsch A, Tijssen JG, Schachinger V, Wojakowski W, Roncalli J, et al. Impact of intracoronary bone marrow cell therapy on left ventricular function in the setting of ST-segment elevation myocardial infarction: a collaborative meta-analysis. Eur Heart J. 2014; 35: 989-98.
152. Delewi R, Andriessen A, Tijssen JG, Zijlstra F, Piek JJ, Hirsch A. Impact of intracoronary cell therapy on left ventricular function in the setting of acute myocardial infarction: a meta-analysis of randomised controlled clinical trials. Heart. 2013; 99: 225-32.
153. Chen SL, Fang WW, Ye F, Liu YH, Qian J, Shan SJ, et al. Effect on left ventricular function of intracoronary transplantation of autologous bone marrow mesenchymal stem cell in patients with acute myocardial infarction. Am J Cardiol. 2004; 94: 92-5.
154. Sun L, Zhang T, Lan X, Du G. Effects of stem cell therapy on left ventricular remodeling after acute myocardial infarction: a meta-analysis. Clin Cardiol. 2010; 33: 296-302.
155. Janssens S, Dubois C, Bogaert J, Theunissen K, Deroose C, Desmet W, et al. Autologous bone marrow-derived stem-cell transfer in patients with ST-segment elevation myocardial infarction: double-blind, randomised controlled trial. Lancet. 2006; 367: 113-21.
156. Wollert KC, Meyer GP, Muller-Ehmsen J, Tschope C, Bonarjee V, Larsen AI, et al. Intracoronary autologous bone marrow cell transfer after myocardial infarction: the BOOST-2 randomised placebo-controlled clinical trial. Eur Heart J. 2017.
157. Hodgkinson CP, Bareja A, Gomez JA, Dzau VJ. Emerging Concepts in Paracrine Mechanisms in Regenerative Cardiovascular Medicine and Biology. Circ Res. 2016; 118: 95-107.
158. van Berlo JH, Molkentin JD. An emerging consensus on cardiac regeneration. Nat Med. 2014; 20: 1386-93.
159. Zhang ZG, Chopp M. Neurorestorative therapies for stroke: underlying mechanisms and translation to the clinic. Lancet Neurol. 2009; 8: 491-500.
160. Moniche F, Montaner J, Gonzalez-Marcos JR, Carmona M, Pinero P, Espigado I, et al. Intra-arterial bone marrow mononuclear cell transplantation correlates with GM-CSF, PDGF-BB, and MMP-2 serum levels in stroke patients: results from a clinical trial. Cell Transplant. 2014; 23 Suppl 1: S57-64.
161. Prasad K, Sharma A, Garg A, Mohanty S, Bhatnagar S, Johri S, et al. Intravenous autologous bone marrow mononuclear stem cell therapy for ischemic stroke: a multicentric, randomized trial. Stroke. 2014; 45: 3618-24.
162. Moniche F, Escudero I, Zapata-Arriaza E, Usero-Ruiz M, Prieto-Leon M, de la Torre J, et al. Intra-arterial bone marrow mononuclear cells (BM-MNCs) transplantation in acute ischemic stroke (IBIS trial): protocol of a phase II, randomized, dose-finding, controlled multicenter trial. Int J Stroke. 2015; 10: 1149-52.
163. Sato T, Suzuki H, Kusuyama T, Omori Y, Soda T, Tsunoda F, et al. G-CSF after myocardial infarction accelerates angiogenesis and reduces fibrosis in swine. Int J Cardiol. 2008; 127: 166-73.
164. Toyama T, Hoshizaki H, Kasama S, Yamashita E, Kawaguchi R, Adachi H, et al. Low-dose and long-term G-CSF treatment can improve severe myocardial ischemia in patients with severe coronary artery disease. J Nucl Cardiol. 2011; 18: 463-71.
165. Kang S, Yang Y, Li CJ, Gao R. Effectiveness and tolerability of administration of granulocyte colony-stimulating factor on left ventricular function in patients with myocardial infarction: a meta-analysis of randomized controlled trials. Clin Ther. 2007; 29: 2406-18.
166. Zohlnhofer D, Kastrati A, Schomig A. Stem cell mobilization by granulocyte-colony-stimulating factor in acute myocardial infarction: lessons from the REVIVAL-2 trial. Nat Clin Pract Cardiovasc Med. 2007; 4 Suppl 1: S106-9.
167. Zohlnhofer D, Ott I, Mehilli J, Schomig K, Michalk F, Ibrahim T, et al. Stem cell mobilization by granulocyte colony-stimulating factor in patients with acute myocardial infarction: a randomized controlled trial. JAMA. 2006; 295: 1003-10.
168. Zohlnhofer D, Dibra A, Koppara T, de Waha A, Ripa RS, Kastrup J, et al. Stem cell mobilization by granulocyte colony-stimulating factor for myocardial recovery after acute myocardial infarction: a meta-analysis. J Am Coll Cardiol. 2008; 51: 1429-37.
169. Lavie CJ, Thomas RJ, Squires RW, Allison TG, Milani RV. Exercise training and cardiac rehabilitation in primary and secondary prevention of coronary heart disease. Mayo Clin Proc. 2009; 84: 373-83.
170. Manson JE, Greenland P, LaCroix AZ, Stefanick ML, Mouton CP, Oberman A, et al. Walking compared with vigorous exercise for the prevention of cardiovascular events in women. N Engl J Med. 2002; 347: 716-25.
171. Manson JE, Hu FB, Rich-Edwards JW, Colditz GA, Stampfer MJ, Willett WC, et al. A prospective study of walking as compared with vigorous exercise in the prevention of coronary heart disease in women. N Engl J Med. 1999; 341: 650-8.
172. Myers J, Prakash M, Froelicher V, Do D, Partington S, Atwood JE. Exercise capacity and mortality among men referred for exercise testing. N Engl J Med. 2002; 346: 793-801.
173. Blair SN, Kampert JB, Kohl HW, 3rd, Barlow CE, Macera CA, Paffenbarger RS, Jr., et al. Influences of cardiorespiratory fitness and other precursors on cardiovascular disease and all-cause mortality in men and women. JAMA. 1996; 276: 205-10.
174. Lenk K, Uhlemann M, Schuler G, Adams V. Role of endothelial progenitor cells in the beneficial effects of physical exercise on atherosclerosis and coronary artery disease. J Appl Physiol. 2011; 111: 321-8.
175. England TJ, Abaei M, Auer DP, Lowe J, Jones DR, Sare G, et al. Granulocyte-colony stimulating factor for mobilizing bone marrow stem cells in subacute stroke: the stem cell trial of recovery enhancement after stroke 2 randomized controlled trial. Stroke. 2012; 43: 405-11.
176. Guijarro D, Lebrin M, Lairez O, Bourin P, Piriou N, Pozzo J, et al. Intramyocardial transplantation of mesenchymal stromal cells for chronic myocardial ischemia and impaired left ventricular function: Results of the MESAMI 1 pilot trial. Int J Cardiol. 2016; 209: 258-65.
177. Hare JM, Traverse JH, Henry TD, Dib N, Strumpf RK, Schulman SP, et al. A randomized, double-blind, placebo-controlled, dose-escalation study of intravenous adult human mesenchymal stem cells (prochymal) after acute myocardial infarction. J Am Coll Cardiol. 2009; 54: 2277-86.
178. Gao LR, Chen Y, Zhang NK, Yang XL, Liu HL, Wang ZG, et al. Intracoronary infusion of Wharton's jelly-derived mesenchymal stem cells in acute myocardial infarction: double-blind, randomized controlled trial. BMC Med. 2015; 13: 162.
179. Britten MB, Abolmaali ND, Assmus B, Lehmann R, Honold J, Schmitt J, et al. Infarct remodeling after intracoronary progenitor cell treatment in patients with acute myocardial infarction (TOPCARE-AMI): mechanistic insights from serial contrast-enhanced magnetic resonance imaging. Circulation. 2003; 108: 2212-8.
180. Mathiasen AB, Haack-Sorensen M, Jorgensen E, Kastrup J. Autotransplantation of mesenchymal stromal cells from bone-marrow to heart in patients with severe stable coronary artery disease and refractory angina--final 3-year follow-up. Int J Cardiol. 2013; 170: 246-51.
181. Kanelidis AJ, Premer C, Lopez J, Balkan W, Hare JM. Route of Delivery Modulates the Efficacy of Mesenchymal Stem Cell Therapy for Myocardial Infarction: A Meta-Analysis of Preclinical Studies and Clinical Trials. Circ Res. 2017; 120: 1139-50.
182. Kharlamov AN, Tyurnina AE, Veselova VS, Kovtun OP, Shur VY, Gabinsky JL. Silica-gold nanoparticles for atheroprotective management of plaques: results of the NANOM-FIM trial. Nanoscale. 2015; 7: 8003-15.
183. Haimovici H, Maier N. Fate of aortic homografts in canine atherosclerosis. 3. Study of fresh abdominal and thoracic aortic implants into thoracic aorta: role of tissue susceptibility in atherogenesis. Arch Surg. 1964; 89: 961-9.
184. Thery C, Zitvogel L, Amigorena S. Exosomes: composition, biogenesis and function. Nat Rev Immunol. 2002; 2: 569-79.
185. Robbins PD, Morelli AE. Regulation of immune responses by extracellular vesicles. Nat Rev Immunol. 2014; 14: 195-208.
186. Kilchert C, Wittmann S, Vasiljeva L. The regulation and functions of the nuclear RNA exosome complex. Nat Rev Mol Cell Biol. 2016; 17: 227-39.
187. Ibrahim A, Marbán E. Exosomes: Fundamental Biology and Roles in Cardiovascular Physiology. Annu Rev Physiol. 2016; 78: 67-83.
188. Boulanger CM, Loyer X, Rautou P-E, Amabile N. Extracellular vesicles in coronary artery disease. Nat Rev Cardiol. 2017; 14: 259-72.
189. Hergenreider E, Heydt S, Treguer K, Boettger T, Horrevoets AJG, Zeiher AM, et al. Atheroprotective communication between endothelial cells and smooth muscle cells through miRNAs. Nat Cell Biol. 2012; 14: 249-56.
190. El Andaloussi S, Mager I, Breakefield XO, Wood MJA. Extracellular vesicles: biology and emerging therapeutic opportunities. Nat Rev Drug Discov. 2013; 12: 347-57.
191. Amarenco P, Labreuche J, Lavallee P, Touboul PJ. Statins in stroke prevention and carotid atherosclerosis: systematic review and up-to-date meta-analysis. Stroke. 2004; 35: 2902-9.
192. Amarenco P, Bogousslavsky J, Callahan A, 3rd, Goldstein LB, Hennerici M, Rudolph AE, et al. High-dose atorvastatin after stroke or transient ischemic attack. N Engl J Med. 2006; 355: 549-59.
193. Passman JN, Dong XR, Wu SP, Maguire CT, Hogan KA, Bautch VL, et al. A sonic hedgehog signaling domain in the arterial adventitia supports resident Sca1+ smooth muscle progenitor cells. Proc Natl Acad Sci U S A. 2008; 105: 9349-54.
194. Tang Z, Wang A, Wang D, Li S. Smooth Muscle Cells: To Be or Not To Be? Response to Nguyen et al. Circ Res. 2012.
195. Farrington-Rock C, Crofts NJ, Doherty MJ, Ashton BA, Griffin-Jones C, Canfield AE. Chondrogenic and adipogenic potential of microvascular pericytes. Circulation. 2004; 110: 2226-32.
196. Schor AM, Allen TD, Canfield AE, Sloan P, Schor SL. Pericytes derived from the retinal microvasculature undergo calcification in vitro. J Cell Sci. 1990; 97 (Pt 3): 449-61.
197. Dellavalle A, Sampaolesi M, Tonlorenzi R, Tagliafico E, Sacchetti B, Perani L, et al. Pericytes of human skeletal muscle are myogenic precursors distinct from satellite cells. Nat Cell Biol. 2007; 9: 255-67.
198. Crisan M, Yap S, Casteilla L, Chen CW, Corselli M, Park TS, et al. A perivascular origin for mesenchymal stem cells in multiple human organs. Cell Stem Cell. 2008; 3: 301-13.